

Portland State University

**PDXScholar**

---

Dissertations and Theses

Dissertations and Theses

---

1991

# Modification of the $Ca^{2+}$ Release Channel from Sarcoplasmic Reticulum of Skeletal Muscle

Hui Xiong

*Portland State University*

Follow this and additional works at: [https://pdxscholar.library.pdx.edu/open\\_access\\_etds](https://pdxscholar.library.pdx.edu/open_access_etds)

**Let us know how access to this document benefits you.**

---

## Recommended Citation

Xiong, Hui, "Modification of the  $Ca^{2+}$  Release Channel from Sarcoplasmic Reticulum of Skeletal Muscle" (1991). *Dissertations and Theses*. Paper 1304.

<https://doi.org/10.15760/etd.1303>

This Dissertation is brought to you for free and open access. It has been accepted for inclusion in Dissertations and Theses by an authorized administrator of PDXScholar. Please contact us if we can make this document more accessible: [pdxscholar@pdx.edu](mailto:pdxscholar@pdx.edu).

MODIFICATION OF THE  $\text{Ca}^{2+}$  RELEASE CHANNEL FROM SARCOPLASMIC  
RETICULUM OF SKELETAL MUSCLE

by  
HUI XIONG

A dissertation submitted in partial fulfillment of the  
requirements for the degree of

DOCTOR OF PHILOSOPHY  
IN  
ENVIRONMENTAL SCIENCES AND RESOURCES:  
PHYSICS

Portland State University  
1991

TO THE OFFICE OF GRADUATE STUDIES:

The members of the Committee approve the dissertation of  
Hui Xiong presented October 31, 1991.

[REDACTED]  
Jonathan J. Abramson, Chair

[REDACTED]  
Pavel K. Smejtek

[REDACTED]  
Arnold D. Pickar

[REDACTED]  
David H. Peyton

[REDACTED]  
Robert L. Millette

[REDACTED]  
Stanley S. Hillman

APPROVED:

[REDACTED]  
John G. Rueter Jr., Director, Environmental Sciences and  
Resources Program

[REDACTED]  
C. William Savery, Interim Vice Provost for Graduate  
Studies and Research

AN ABSTRACT OF THE DISSERTATION OF Hui Xiong for the Doctor of  
Philosophy in Environmental Science and Resources: Physics  
presented October 31, 1991.

Title: Modification of the  $\text{Ca}^{2+}$  Release Channel from  
Sarcoplasmic Reticulum of Skeletal Muscle.

APPROVED BY THE MEMBERS OF THE DISSERTATION COMMITTEE:

[REDACTED]  
Jonathan J. Abramson, Chair

[REDACTED]  
Pavel K. Smejtek

[REDACTED]  
Arnold D. Pickar

[REDACTED]  
David H. Peyton

[REDACTED]  
Robert L. Millette

[REDACTED]  
Stanley S. Hillman

Muscle contraction and relaxation are controlled by the  
intracellular free  $\text{Ca}^{2+}$  concentration. The sarcoplasmic  
reticulum (SR) is an intracellular membrane system which

regulates this internal free  $\text{Ca}^{2+}$  concentration. Responding to an electrical excitation of the cell surface membrane, the SR releases  $\text{Ca}^{2+}$  through a specific  $\text{Ca}^{2+}$  release channel, thus elevating the  $\text{Ca}^{2+}$  concentration inside muscle cell and causing the muscle to contract. Subsequent sequestration of  $\text{Ca}^{2+}$  by the SR  $\text{Ca}^{2+}$  pumps restores the resting state of the muscle cell. This research focuses on the  $\text{Ca}^{2+}$  release channel from skeletal muscle SR. The planar lipid bilayer technique was used to study the channel at the single channel level.

The SR  $\text{Ca}^{2+}$  release channel was identified and isolated via its interaction with specific sulfhydryl oxidizing agents. This protein of a molecular mass of 106 kDa was then incorporated into a planar lipid bilayer membrane (BLM). In an asymmetrical  $\text{Ca}^{2+}$  solution, the channel protein demonstrates a single channel conductance of  $107 \pm 13$  pS and a permeability ratio of  $\text{Ca}^{2+}$  versus  $\text{Tris}^+$  of  $7.4 \pm 3.3$ . In a symmetrical 250 mM NaCl solution, the channel protein displays a large single channel conductance of  $400 \pm 20$  pS, and a weak voltage-dependence. The channel is activated by millimolar ATP and inhibited by micromolar ruthenium red. Nanomolar concentrations of ryanodine modify the channel by changing it from a rapidly gating full conductance state to a long-lived subconductance state. These results demonstrate that the isolated 106 kDa protein channel has properties similar to those observed following fusion of SR vesicles to a BLM.

The bilayer system was also used to examine the effect of  $\text{Ag}^+$  on the SR  $\text{Ca}^{2+}$  release channel.  $\text{Ag}^+$  ( $0.2\text{--}1.0\ \mu\text{M}$ ) activates the SR  $\text{Ca}^{2+}$  release channel. Activation by  $\text{Ag}^+$  does not require the presence of  $\text{Ca}^{2+}$ ,  $\text{Mg}^{2+}$ , or ATP.  $\text{Ag}^+$  activates the channel by increasing the open probability  $P_0$ .  $\text{Ag}^+$  activation is always followed by a spontaneous inactivation. The channel is still sensitive to ruthenium red inhibition after exposure to  $\text{Ag}^+$ .

Isolated SR vesicles were fused to a BLM to study the effect of the photooxidizing dye, rose bengal, on the gating characteristics of the reconstituted SR  $\text{Ca}^{2+}$  release channel. Rose bengal activates the  $\text{Ca}^{2+}$  release channel in the presence of light by increasing the channel open probability and leaving the single channel conductance unchanged. This photoactivation is independent of the myoplasmic  $\text{Ca}^{2+}$  concentration, and can be achieved from either side of the membrane. In addition, the effect is inhibited by addition of  $10\text{--}20\ \mu\text{M}$  ruthenium red. When modified to its subconducting state by ryanodine, subsequent addition of rose bengal reactivates the channel to a rapidly fluctuating full conducting state.

These studies carried out at the single channel level utilizing the planar lipid bilayer technique have not only enhanced our understanding of the  $\text{Ca}^{2+}$  release mechanism of skeletal muscle SR, but also provided information about the

toxic effects on biological membrane systems caused by heavy metals and oxidizing agents.

## ACKNOWLEDGEMENTS

I would like to express my sincere appreciation to the individuals who have offered friendship and assistance during my study in this country and have made this dissertation possible. My advisor, Dr. Jon Abramson, has not only introduced me to the world of scientific research and guided me through the making of this thesis, but has also provided me with untiring encouragement and support during the course of this project. His integrity, his kindness, and his enthusiastic pursuit of truth has set an example of how to lead one's life. My thanks to the Physics Department and the Environmental Sciences Program for providing me the opportunity to study in this country by sponsoring my research. In addition, I would like to thank the members of my advisory committee (Drs. Pavel Smejtek and Arnold Pickar from Physics, Dr. David Peyton from Chemistry, and Drs. Robert Millette and Stanley Hillman from Biology) for their advice, suggestions and precious time which they committed in addition to their research endeavors and heavy academic duties. I would also like to thank Mrs. Dawn Dressler, Dr. Joel Nissen, Dr. Joe Walters, and all the current faculty, staff, and students of the Physics Department. Special thanks to Dr. Pavel Smejtek for providing equipment, lab space and constant



comments on my project. I am especially grateful to all the co-workers in this lab: Ed Buck whose technical assistance and friendship helped me a great deal, Keith Scott who prepared the purified protein for my experiments, Terry Favero whose friendship and jokes I'll miss, Jon Trimm, Joe Cronin, Jan Stuart, Scott Milne, Tony Zable, and Margot Leonard. It is their presence, friendship, and assistance which made my study here a precious memory. I would also like to thank Garo Arakelian, Rudi Zupan, and Brian McLoughlin of the Science Support Shop. Finally, I would like to thank my family in China, my American family here, the Kents, and my Chinese friends here. Above all, I thank my husband Jian Huang for his unconditional support and encouragement. To my husband and my parents, this dissertation is dedicated.

## TABLE OF CONTENTS

	PAGE
ACKNOWLEDGEMENTS. . . . .	.iii
LIST OF TABLES. . . . .	viii
LIST OF FIGURES . . . . .	ix
TABLE OF ABBREVIATIONS. . . . .	.xii
CHAPTER	
I INTRODUCTION . . . . .	1
Muscle and Contraction . . . . .	1
Sarcoplasmic Reticulum . . . . .	7
Major Proteins of SR the Membrane System Monovalent Channel Present in the SR	
Hypotheses of EC Coupling . . . . .	12
Preparations for Studying EC Coupling Proposed Theories Describing EC Coupling	
Calcium Channels . . . . .	24
The Ca <sup>2+</sup> Channel of T-tubule The Ca <sup>2+</sup> Release Channel of SR	
Overview of Dissertation . . . . .	28
Reconstitution and Characterization of SR 106 kDa Protein Ag <sup>+</sup> Modification of SR Ca <sup>2+</sup> Release Channel Photooxidation of SR Ca <sup>2+</sup> Release Channel	

II	METHODS . . . . .	32
	Isolation of SR Vesicles . . . . .	32
	Isolation of 106 kDa Protein . . . . .	33
	Synthesis of SPDP-Biotin Conjugate	
	Covalent Labeling of SR Protein with Biotin	
	Isolation of Biotin-Labeled SR Proteins by Biotin-Avidin Chromatography	
	Planar Lipid Bilayer Technique . . . . .	35
	Bilayer Chambers	
	Formation of Bilayer Membranes	
	Reconstitution of the Native SR $\text{Ca}^{2+}$ Release Channel	
	Reconstitution of Purified 106 kDa Protein	
	Signal Acquisition and Analysis	
III	RECONSTITUTION AND CHARACTERIZATION OF THE 106 KDA $\text{Ca}^{2+}$ RELEASE CHANNEL . . . . .	45
	Summary . . . . .	45
	Introduction . . . . .	45
	Results . . . . .	48
	Discussion . . . . .	60
IV	SILVER MODIFICATION OF THE SR CALCIUM RELEASE CHANNEL . . . . .	66
	Summary . . . . .	66
	Introduction . . . . .	67
	Results . . . . .	70
	Discussion . . . . .	78
V	PHOTOOXIDATION OF THE SR CALCIUM RELEASE CHANNEL . . . . .	87
	Summary . . . . .	87
	Introduction . . . . .	88

	vii
Results . . . . .	93
Discussion . . . . .	108
VI CONCLUSION . . . . .	.112
REFERENCES . . . . .	115
APPENDIX. . . . .	.127

## LIST OF TABLES

TABLE		PAGE
I	Free ionic concentrations and equilibrium potentials for mammalian skeletal muscle . .	6
II	Modulators of $\text{Ca}^{2+}$ release from isolated SR vesicles of skeletal muscle . . . . .	16
III	Different types of $\text{Ca}^{2+}$ channels . . . . .	25
IV	The properties of the native SR $\text{Ca}^{2+}$ release channel, the 106 kDa channel, and the 400 kDa channel in the standard asymmetrical $\text{Ca}^{2+}$ solution . . . . .	62

## LIST OF FIGURES

FIGURE		PAGE
1.	The internal membrane system of a skeletal muscle fiber . . . . .	4
2.	Electrical and mechanical responses of a single frog twitch muscle fiber to an electrical stimulus. . . . .	7
3.	A planar lipid bilayer setup. . . . .	36
4.	Fusion of a SR vesicle to a lipid bilayer. .	40
5.	Structure of reactive disulfide compounds and reactions of SPDP. . . . .	47
6.	Reconstituted 106 kDa protein in the standard $\text{Ca}^{2+}$ solution. . . . .	51
7.	Reconstituted 106 kDa protein shows monovalent cation conductance. . . . .	52
8.	Reconstituted 106 kDa protein shows monovalent cation conductance. . . . .	54
9.	The properties of monovalent conductance of the 106 kDa channel. . . . .	55
10.	The native SR $\text{Ca}^{2+}$ release channel conducts monovalent cations. . . . .	56
11.	Subconducting states of the reconstituted 106 kDa protein. . . . .	57
12.	ATP and ruthenium red modification of the reconstituted 106 kDa channel. . . . .	59
13.	Ryanodine modification of the reconstituted 106 kDa channel. . . . .	61
14.	$\text{Ag}^+$ dependence of $\text{Ca}^{2+}$ release rate of isolated SR vesicles. . . . .	69

15.	The current-voltage curve of a typical native SR $\text{Ca}^{2+}$ channel in a 500 mM to 100 mM CsCl gradient. . . . .	71
16.	$\text{Ag}^+$ modification of a native SR $\text{Ca}^{2+}$ release channel under physiological conditions. . . . .	73
17.	$\text{Ag}^+$ modification of the SR $\text{Ca}^{2+}$ channel in the absence of $\text{MgCl}_2$ . . . . .	75
18.	$\text{Ag}^+$ modification of SR $\text{Ca}^{2+}$ release channel at a low $\text{Ca}^{2+}$ concentration. . . . .	76
19.	Ruthenium red inhibition of the SR $\text{Ca}^{2+}$ channel after $\text{Ag}^+$ modification. . . . .	77
20.	$\text{Ag}^+$ modification of the $\text{Ca}^{2+}$ channel from the luminal face of the SR. . . . .	79
21.	The effect of high concentration of $\text{Ag}^+$ on the SR $\text{Ca}^{2+}$ channel. . . . .	80
22.	The effect of $\text{Ag}^+$ on the purified 106 kDa SR $\text{Ca}^{2+}$ release channel. . . . .	81
23.	The structure of rose bengal as C-2', C-6 potassium salt. . . . .	89
24.	Rose bengal induced $\text{Ca}^{2+}$ efflux from actively loaded SR vesicles. . . . .	91
25.	Rose bengal activation and ruthenium red inhibition of the SR $\text{Ca}^{2+}$ release channel. . . . .	94
26.	Current-voltage curve of a single $\text{Ca}^{2+}$ channel in the absence and presence of 0.5 $\mu\text{M}$ rose bengal with illumination. . . . .	96
27.	Open lifetime analysis of a SR $\text{Ca}^{2+}$ release channel upon photooxidation. . . . .	97
28.	Closed lifetime analysis of a SR $\text{Ca}^{2+}$ release channel upon photooxidation. . . . .	98
29.	Light dependence of the rose bengal effect. . . . .	100
30.	Rose bengal activation of SR $\text{Ca}^{2+}$ release channel at low $\text{Ca}^{2+}$ concentration. . . . .	101

31.	Rose bengal activation of channel activity is side independent. . . . .	102
32.	Ryanodine modification of the $\text{Ca}^{2+}$ release channel is reversed by rose bengal. . .	103
33.	Light dependent displacement of [ $^3\text{H}$ ]-ryanodine from its binding sites by rose bengal. .	105
34.	Rose bengal activation of the purified $\text{Ca}^{2+}$ release channel and subsequent modification by ryanodine. . . . .	106
35.	Rose bengal activation of ryanodine modified 106 kDa $\text{Ca}^{2+}$ release channel. . . . .	107



# TABLE OF ABBREVIATIONS

2,2'-DTDP	2,2'-dithiodipyridine
4,4'-DTDP	4,4'-dithiodipyridine
AMP-PCP	$\beta$ , $\gamma$ -methyleneadenosine 5'-triphosphate
ATP	adenosine 5'triphosphate
CHAPS	3-[(3-cholamidopropyl)dimethylammonio]-1-propanesulfonate
DHP	dihydropyridine
DTT	dithiothreitol
EFA	ethoxyformic anhydride
EGTA	[ethylenebis(oxyethylenenitrilo)] tetraacetic acid
HEPES	4-(2-hydroxyethyl)-1-piperazineethanesulfonic acid
IP <sub>3</sub>	inositol 1,4,5-triphosphate
PC	phosphatidyl choline
PE	phosphatidylethanolamine
PIPES	1,4-piperazinediethanolsulfonic acid
PS	phosphatidyl serine
pS	picosiemans
SPDP	N-succinimidyl 3(2-pyridyldithio)propionate
SR	sarcoplasimic reticulum
Tris	tris[hydroxymethyl]aminomethane

## CHAPTER I

### INTRODUCTION

In muscle cells, the chemical energy from the hydrolysis of ATP is transformed into the mechanical energy of contraction. Muscle contraction and relaxation are regulated by the cytoplasmic (myoplasmic) free  $\text{Ca}^{2+}$  concentrations. The sarcoplasmic reticulum (SR) of striated muscle cells is a highly specialized intracellular membrane system which controls intracellular  $\text{Ca}^{2+}$  concentration of muscle cells. This function is carried out mainly by two transport proteins in the SR membrane. The  $\text{Ca}^{2+}$  pump transports  $\text{Ca}^{2+}$  against electrochemical gradient into the lumen of the SR to maintain the low myoplasmic  $\text{Ca}^{2+}$  level of resting muscle cells. The  $\text{Ca}^{2+}$  release channel releases  $\text{Ca}^{2+}$  stored in SR and elevates the myoplasmic  $\text{Ca}^{2+}$  concentration. This research is focused on understanding the mechanism of  $\text{Ca}^{2+}$  release from SR.

### MUSCLE AND CONTRACTION

Vertebrate muscle cells are generally grouped into two categories, striated and smooth. Striated muscle makes up the tissue of the heart and skeletal muscles. The skeletal muscle cells are multinucleate and referred to as muscle fibers. In heart and smooth muscle, the cells are called myocytes. The

response time of muscle contraction has a wide range in the different types of muscle, ranging from milliseconds in fast-twitch skeletal muscle to seconds in smooth muscle. The highly ordered structure of skeletal muscle cells has received the most attention and has led to the formulation of the sliding-filament model for muscular contraction.

Skeletal muscle fibers are 10 to 100  $\mu\text{m}$  thick and up to a few centimeters on length. These fibers are multinucleate cells formed by the fusion of numbers of elongated uninucleate cells called myoblasts. Each cell is surrounded by an electrically excitable membrane known as the sarcolemma. Most of the interior of the fibre consists of the protein filaments termed myofibrils, which constitute the contractile apparatus. Along the axis of contraction, myofibrils are divided into repeating units about 2.5  $\mu\text{m}$  in length which are termed sarcomeres. The intracellular fluid bathing the myofibrils is termed sarcoplasm (myoplasm) and contains an elaborate system of intracellular membranes, the sarcoplasmic reticulum, as well as mitochondria, lipid droplets, and glycogen granules. The sarcoplasmic reticulum (SR) is an enclosed membrane system wrapping around the surface of myofibrils. It has a central role in controlling the myoplasmic  $\text{Ca}^{2+}$  concentration.

The SR is broadly divided into two morphologically and functionally distinct regions: the junctional SR (also called the terminal cisternae), and the longitudinal SR (Peachey, 1965; Peachey et al. 1983). The junctional SR (JSR) are

closely packed next to the transverse tubule (T-tubule) membrane, which is a continuous invagination of the sarcolemma extended into the interior of muscle cells (Figure 1). The association of one T tubule and two apposed terminal cisternae forms the triadic junction. The longitudinal SR (LSR) connect with two terminal cisternae, forming SR compartments. Bridging the 12 to 14 nm gap between the junctional SR and the T-tubule membranes are regularly spaced structures termed feet (Franzini-Armstrong, 1975; 1980). The triad junction is involved in transmission of the excitatory stimulus from the surface membrane to the SR, causing  $\text{Ca}^{2+}$  release. How signal transmission occurs at the triad junction is one of the major unsolved problems of muscle biology.

In skeletal muscle, the signal for  $\text{Ca}^{2+}$  release is initiated at the neuro-muscular junction. This electrical signal, termed the action potential, spreads over the sarcolemma and down to the T-tubule as a depolarization of the membrane. Depolarization of the T-tubule membrane, by an unknown mechanism, causes an extremely rapid release of  $\text{Ca}^{2+}$  from the SR. The elevated myoplasmic  $\text{Ca}^{2+}$  concentration, in turn, triggers muscle contraction. Subsequently  $\text{Ca}^{2+}$  uptake by the SR  $\text{Ca}^{2+}$  pumps ( $\text{Ca}^{2+}$ - $\text{Mg}^{2+}$  ATPase) decreases the intracellular  $\text{Ca}^{2+}$  concentration and causes relaxation. The process linking depolarization of the T-tubule and  $\text{Ca}^{2+}$  release from SR is referred to as excitation-contraction coupling (EC coupling). The mechanism of EC coupling has been

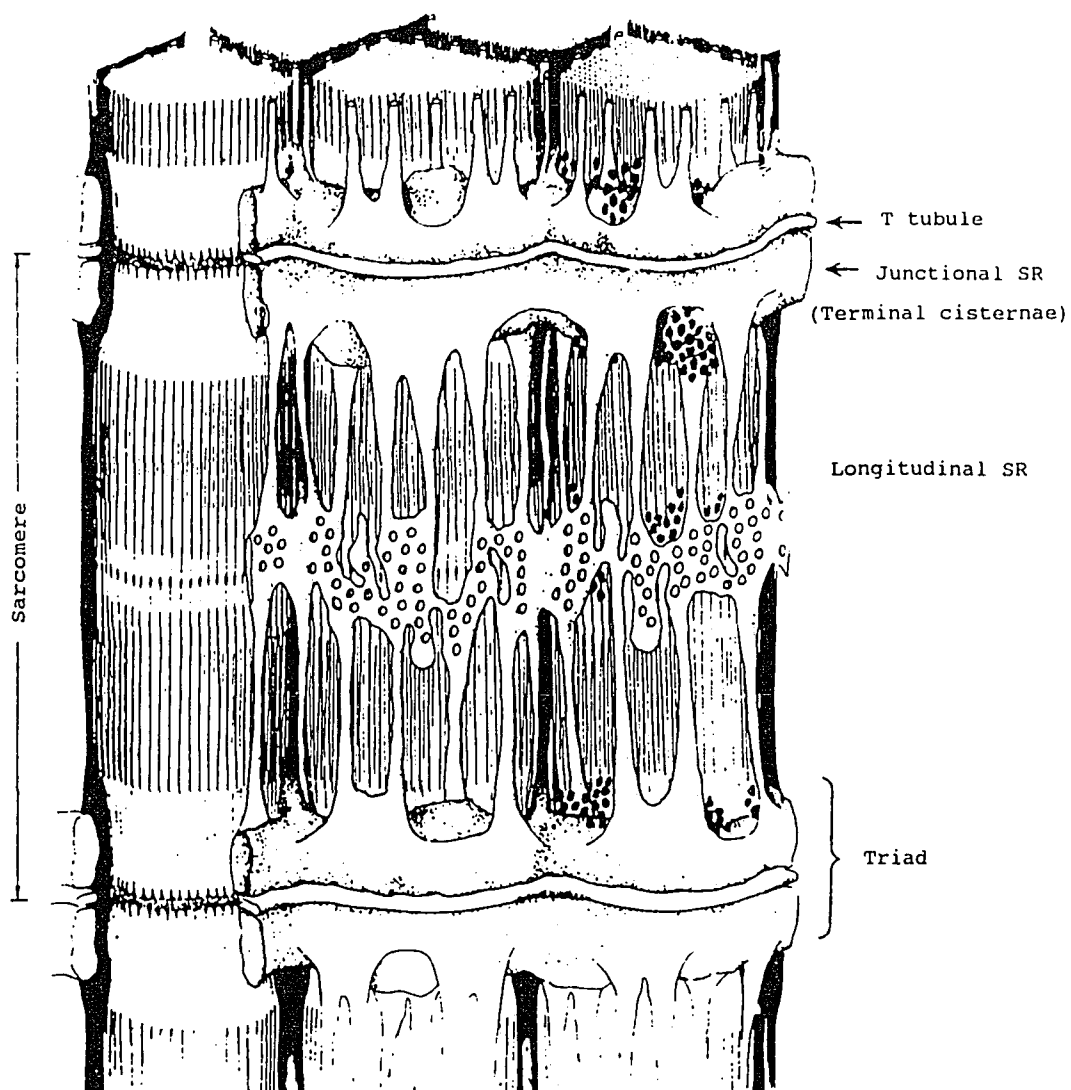


Figure 1. The internal membrane system of a skeletal muscle fiber. Reproduced from Peachey, 1965.

extensively investigated over the last three decades. Although the exact mechanism is still unknown, remarkable progress has been made in characterizing the molecular machinery involved in EC coupling.

The molecular mechanism of reactions of contractile proteins has been worked out (Ebashi, 1975). Each myofibril contains tightly packed protein myofilaments, the thick and thin filaments. The thick filaments are made up of myosin. The thin filaments consist of two strands of fibrous actin with myosin binding sites at regular intervals and two smaller proteins, troponin, and tropomyosin. Under resting conditions the myoplasmic free  $\text{Ca}^{2+}$  concentration is low ( $0.1 \mu\text{M}$ ); the interaction of actin and myosin is blocked by the troponin-tropomyosin complex. When SR releases its stored  $\text{Ca}^{2+}$  in response to a neural stimulation, the elevated intracellular free  $\text{Ca}^{2+}$  level unblocks the troponin-tropomyosin complex and the interaction between actin and myosin occurs. The mechanism of action of  $\text{Ca}^{2+}$  on the contractile system is to remove an inhibition that has been exerted on actin molecules by troponin-tropomyosin complex in the absence of  $\text{Ca}^{2+}$ . Thus,  $\text{Ca}^{2+}$  is the essential mediator of physiological contraction of muscle cells, and, in skeletal muscle, this  $\text{Ca}^{2+}$  is almost exclusively from the SR.

Table I lists the concentrations of ions when mammalian skeletal muscle is in a resting state (Hill, 1984). The resting potential ( $-90 \text{ mV}$  inside the cell) of muscle cells is

TABLE I

FREE IONIC CONCENTRATIONS AND EQUILIBRIUM POTENTIALS FOR  
MAMMALIAN SKELETAL MUSCLE<sup>a</sup>

Ion	Extracellular concentration (mM)	Intracellular concentration (mM)	Equilibrium potential <sup>b</sup> (mV)
Na <sup>+</sup>	145	12	+67
K <sup>+</sup>	4	155	-98
Ca <sup>2+</sup>	1.5	<10 <sup>-7</sup> M	>+128
Cl <sup>-</sup>	123	4.2 <sup>c</sup>	-90 <sup>c</sup>

<sup>a</sup>Reproduced from Hille, 1984

<sup>b</sup>Calculated from  $E_x = \frac{RT}{F} \ln \frac{[X]_o}{[X]_i}$

<sup>c</sup>Calculated assuming a -90 mV resting potential for the muscle membrane and that Cl<sup>-</sup> ions are at equilibrium at rest.

due to the high K<sup>+</sup> permeability of the sarcolemma. The action potential of muscle cells is resulted from a transient increase in Na<sup>+</sup> permeability of the sarcolemma. Figure 2 illustrates the time course of the muscle action potential and the twitch contraction of a single fiber following an electrical stimulation. The action potential is almost completely finished in less than 4 ms. The first signs of mechanical activity are detectable only 1 or 2 ms after the peak of the action potential (Hodgkin and Horowicz, 1957). Ca<sup>2+</sup> release from SR begins a few milliseconds after the rising phase of the action potential, and is essentially complete before the development of tension. In the very fast toadfish swim bladder muscle, the whole cycle of release and reuptake of Ca<sup>2+</sup> is accomplished within 3-5 ms (Martonosi, 1984). Each cycle of Ca<sup>2+</sup> release and accumulation results in

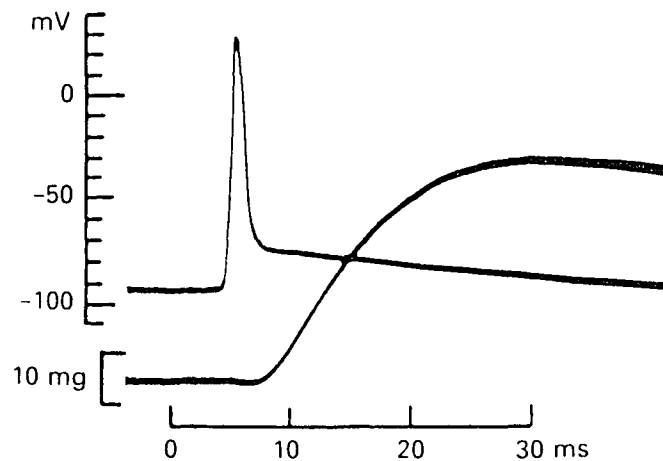


**Figure 2.** Electrical and mechanical responses of a single frog twitch muscle fiber to an electrical stimulus. The upper trace shows the action potential, recorded with an intracellular microelectrode, and the lower trace the isometric tension, recorded with a sensitive force transducer. Temperature 20°C. Reproduced from Hodgkin and Horowicz, 1957.

a brief period of tension production called a twitch. The  $\text{Ca}^{2+}$  release and accumulation cycles can be repeated below a certain frequency termed the fusion frequency. Above the fusion frequency, characteristic for different types of fibers, the  $\text{Ca}^{2+}$  concentration in the myoplasmic space stays relatively high, the contractile apparatus is in a state of constant activation, and the contraction becomes a tetanus. The amount of  $\text{Ca}^{2+}$  released by a single action potential is about 30% of the amount of  $\text{Ca}^{2+}$  present in the SR in the resting state (Somlyo et al., 1981)

#### SARCOPLASMIC RETICULUM

The SR of muscle cells is a smooth-surfaced endoplasmic reticulum. During cell differentiation the SR is formed from



the rough-surfaced endoplasmic reticulum and develops simultaneously with the formation of the myofibrils and T tubules. Early SR forms irregular associations with the developing T-tubules, and later takes on the mature form of triads (Luff and Atwood, 1971; Kelly, 1980).

Autoradiographic evidence suggests that the  $\text{Ca}^{2+}$  release takes place primarily at the terminal cisternae part of SR (Winegrad, 1968; 1970). On the other hand, the LSR contains the  $\text{Ca}^{2+}$  pump as its principal component and its major function is sequestering  $\text{Ca}^{2+}$  into the SR during the relaxation phase of the contraction cycle.

#### Major Proteins of the SR Membrane System

$\text{Ca}^{2+}$  pump protein. The  $\text{Ca}^{2+}$  pump ( $\text{Ca}^{2+}$ - $\text{Mg}^{2+}$  ATPase) accounts for approximately 60 to 70% of the total SR protein and is evenly distributed throughout LSR. It was first purified with high ATPase activity from rabbit skeletal muscle SR in 1970 (MacLennan). The purified pump possesses all of the properties of its native state. When reconstituted into phospholipid vesicles it transports  $\text{Ca}^{2+}$  against a concentration gradient (Racker, 1972). The  $\text{Ca}^{2+}$  pump actively transports two moles of  $\text{Ca}^{2+}$  into the SR lumen for each mole of ATP hydrolyzed. The concentration of the  $\text{Ca}^{2+}$  pump of the SR is correlated with the rate of relaxation of a specific muscle type (Martonosi, 1984). The pump consists of a single polypeptide chain of 105,000 daltons (105 kDa).

Ca<sup>2+</sup> binding protein. Calsequestrin is the second major protein constituent of the SR. It was first isolated in 1971 and has a molecular mass of 63,000 daltons (MacLennan and Wong, 1971). It is a Ca<sup>2+</sup> binding protein with high capacity (43 mol Ca<sup>2+</sup> / mol) and low affinity ( $K_D = 1$  mM) for Ca<sup>2+</sup> (Reviewed by MacLennan et al., 1983). It appears that calsequestrin is responsible for Ca<sup>2+</sup> storage in the SR. Meissner (1970) proposed that the calsequestrin was located in the lumen of the terminal cisternae, based on his studies with LSR and HSR vesicles. He suggested that the electron-dense material within the HSR vesicles was calsequestrin and/or the 53 kDa glycoprotein. Using immunofluorescence stain, the localization of calsequestrin to the terminal cisternae has been proven (Jorgensen et al., 1983).

Ca<sup>2+</sup> release protein--Ca<sup>2+</sup> release channel. The Ca<sup>2+</sup> release channel is a minor protein component of the SR. Before its purification, the channel was studied mostly at the level of isolated membrane vesicles. The development of the planar lipid bilayer fusion technique made it possible to characterize the SR Ca<sup>2+</sup> release channel at the single channel level.

Ion channels are extremely efficient enzymes with turnover numbers approaching  $10^9$  sec<sup>-1</sup>. The high rate of ion translocation across membrane means that individual channels conduct currents in the range of picoamperes. In the late 1970s and early 1980s, electrophysiological and biophysical

techniques were developed which have sufficient resolution to record currents through a single ion channel. The patch clamp technique permits single channel currents to be observed in the native cell membranes. Two German scientists, Bert Sakmann and Erwin Neher, won this year's Nobel Prize in medicine for their important roles in developing this technique. On the other hand, the planar lipid bilayer technique allows recording of single ion channels of T-tubules, SR, and other intracellular organelles which are inaccessible to glass microelectrodes required for patch clamping.

The fusion method of Miller and Racker (1976) was used to incorporate the SR  $\text{Ca}^{2+}$  channel into planar lipid bilayer. Current fluctuations through a single  $\text{Ca}^{2+}$  release channel of SR was first recorded in 1985 (Smith et al.). This channel has characteristics different from  $\text{Ca}^{2+}$  channels isolated from other cell membranes (as described in the next section). The unit conductance of the channel is large. In a solution of 53 mM  $\text{Ca}^{2+}$ /125 mM Tris<sup>+</sup> (the standard asymmetrical  $\text{Ca}^{2+}$  solution), the single channel conductance is 100 pS. The permeability ratio ( $P_{\text{Ca}}/P_{\text{Tris}}$ ) is 11.4. Unlike other types of  $\text{Ca}^{2+}$  channels, the SR  $\text{Ca}^{2+}$  channel does not inactivate. The SR  $\text{Ca}^{2+}$  channel is modulated by known effectors of  $\text{Ca}^{2+}$  release from skinned fibers and isolated SR vesicles. Myoplasmic  $\text{Ca}^{2+}$ , in the range of 2-950  $\mu\text{M}$  activates the channel by increasing its open probability ( $P_0$ ), without affecting channel open lifetime.

Millimolar ATP also activates the channel activity. Submillimolar  $Mg^{2+}$  or micromolar ruthenium red inhibits the channel.

#### Monovalent Channels Present in the SR

The permeability of SR to other ions has been studied to understand the parameters involved in the regulation of the physiological SR  $Ca^{2+}$  release mechanism. Light scattering measurements of SR vesicles showed the membrane is permeable to small uncharged molecules (Selser et al. 1976, Kometani and Kasai, 1978). This may allow for an exchange of metabolic intermediates between the SR lumen and the myoplasm. Radioisotope flux measurements demonstrated that the SR vesicles are highly permeable to monovalent cations and anions (reviewed by Meissner, 1986). These findings suggested the existence of other cation and anion channels in the SR membrane.

K<sup>+</sup> channel. The existence of monovalent ion channels in the SR were confirmed by the planar lipid bilayer technique. In mammalian skeletal SR preparations, a K<sup>+</sup> channel and a Cl<sup>-</sup> channel have been studied (Miller et al., 1984; Rousseau et al., 1988). Miller and Racker (1976) successfully developed a technique for fusing SR vesicles into an artificial membrane and studying the characteristics of channel proteins of the SR membrane. Vesicles were added to the aqueous solution bathing an planar phospholipid bilayer, and the increase of bilayer conductance was monitored. In searching for the SR

$\text{Ca}^{2+}$  channel, a  $\text{K}^+$  channel was found (Miller, 1978). The SR  $\text{K}^+$  channel has a unit conductance of 120 pS (in 100 mM  $\text{K}^+$ ), and a slow (seconds) kinetics. The channel is selective for  $\text{K}^+$  over  $\text{Cl}^-$  and for  $\text{K}^+$  over  $\text{Ca}^{2+}$ . In symmetrical 1 M solutions, the single channel conductance (in pS) falls in the order:  $\text{K}^+(214) > \text{NH}_4^+(157) > \text{Rb}^+(125) > \text{Na}^+(72) > \text{Li}^+(8) > \text{Cs}^+(0)$ .

$\text{Cl}^-$  channel. The behavior of single  $\text{Cl}^-$  channels of SR was also examined by fusing isolated SR vesicles into planar lipid bilayers bathed in choline chloride solution (Rousseau et al., 1988). The channel exhibited a full open state with a unit conductance of 65 pS (in 100 mM  $\text{Cl}^-$ ).  $\text{Cl}^-$  channel activity was not affected by variations of  $\text{Ca}^{2+}$  concentration on either side of the membrane. Neither millimolar ATP or millimolar  $\text{Mg}^{2+}$  affects the channel activity. Open probability of the channel is 60%-95% for membrane potentials ranging from -60 to +60 mV.

The role of these monovalent channels may be to minimize osmotic and potential changes during  $\text{Ca}^{2+}$  uptake and release. Rapid movement of monovalent ions would prevent the development of a retarding membrane potential during electrogenic  $\text{Ca}^{2+}$  release and uptake by the SR.

#### HYPOTHESES OF EC COUPLING

##### Preparations for Studying EC Coupling

The mechanism of coupling between depolarization of the T-tubule membrane and  $\text{Ca}^{2+}$  release from the SR (EC coupling)

has been under extensive investigation over the last three decades. Physiological and biochemical information has been obtained from studies on various preparations.

Isolated muscle fiber. Isolated intact muscle fibers have been used to study the temporal sequence in muscle excitation. The  $\text{Ca}^{2+}$  transients (the change of myoplasmic free  $\text{Ca}^{2+}$  concentration during contraction cycle) can be monitored by measuring tension development or by observing  $\text{Ca}^{2+}$ -sensitive dyes microinjected into the fiber (Baylor, 1983; Blinks et al., 1982). A new generation of  $\text{Ca}^{2+}$ -sensitive dyes such as quin-2 and fura-2 have facilitated such studies (Baylor and Hollingworth, 1988). In a more electrophysiological approach, intracellular  $\text{Ca}^{2+}$  fluxes have been studied in cut fiber segments under voltage clamp conditions. With this method, the potential of the sarcolemma and T tubule can be precisely controlled and changed at will. This system also has been used to study charge movement across the surface membrane, and within the membrane. The isolated muscle fibers are complicated systems which can provide information, in addition to regulation, about temporal and spacial coordination during EC coupling. However, the results of a fiber system require very careful interpretation.

Skinned muscle fiber. Skinned fibers are fibers from which the surface membrane has been removed or made permeable, so that the SR is accessible. Properly prepared skinned fibers have functional SR systems.  $\text{Ca}^{2+}$  can be taken up by

$\text{Ca}^{2+}$  pump and the  $\text{Ca}^{2+}$  release mechanism can be studied.  $\text{Ca}^{2+}$  release from SR can be assayed by tension,  $^{45}\text{Ca}^{2+}$ , and spectrophotometric methods. In Natori-type skinned fiber (Natori, 1954; Donaldson, 1985) the sarcolemma is mechanically peeled off. The disrupted T-tubule membrane is likely to be sealed off and the voltage across the T-tubule membrane (which resembles the resting state) reestablished with the aid of active  $\text{Na}^+$  transport (Natori, 1965; Costantin and Podolsky, 1967). Depolarization of the T-tubule can be achieved by ionic substitution. These fibers appear to have an operationally coupled T-tubule and SR system. The real physiological stimulus to cause  $\text{Ca}^{2+}$  release, depolarization of the T-tubule, can still be effective in this preparation. Chemically skinned fibers are made by treatment with the detergent saponin which reacts with cholesterol (Endo and Iino, 1988). Saponin creates holes in the sarcolemma and T-tubule, which have high contents of cholesterol, yet leaves the SR membrane intact. In chemical skinning, no potential gradient can be established across the T tubule membrane. In skinned fiber systems most of the machinery of muscle function is still intact, but any change of solution in the immediate environment of SR is slow due to diffusion limits.

Isolated SR vesicles. The isolation of subcellular membrane fractions from muscle is an important step in their functional characterization. The SR membrane can be isolated in considerable quantities by differential centrifugation of

muscle homogenate (Martonosi and Feretos, 1964). Electron microscopic studies reveal the isolated SR membrane as a population of outside-out vesicles ranging from 100  $\mu\text{m}$  to 300  $\mu\text{m}$  in sizes. SR vesicles are identified by their ability to accumulate  $\text{Ca}^{2+}$  from ATP containing solutions and by their  $\text{Ca}^{2+}$ -dependent ATPase activity. SR from rabbit fast-twitch skeletal muscle has been subfractionated by density-gradient centrifugation into fractions originating from terminal cisternae (HSR) or longitudinal SR (LSR) (Meissner, 1975). The isolated SR vesicle is a simplified, controlled *in vitro* system in which the  $\text{Ca}^{2+}$  release mechanism can be studied without interference from other influences normally present within the muscle cells. It has been found that these vesicles maintain much of their structural and functional characteristics (Campbell et al., 1980). Although the isolated SR vesicle preparation is less physiological than the SR in skinned fibers, it is easier to follow  $\text{Ca}^{2+}$  movement precisely and it allows relatively easy control of the environment in which experiments are carried out.

The  $\text{Ca}^{2+}$  release mechanism in SR has been studied most extensively with isolated SR vesicles. Table II lists stimulators and inhibitors of  $\text{Ca}^{2+}$  release in isolated SR vesicles from skeletal muscle (Fleischer and Inui, 1989). These results qualitatively agree with those obtained with skinned fiber (Endo, 1985). Among these compounds,  $\text{Ca}^{2+}$ , ATP, and caffeine are commonly used as specific stimulators, while



TABLE II  
MODULATORS OF  $\text{Ca}^{2+}$  RELEASE FROM ISOLATED SR  
VESICLES OF SKELETAL MUSCLE<sup>a</sup>

Activators	Effective concentration	Inhibitors	effective concentration
$\text{Ca}^{2+}$ <sup>b</sup> ATP or ATP analogs AMP Caffeine Ryanodine <sup>b</sup> Doxorubicin <sup>b</sup> $\text{Ag}^+$ $\text{Cu}^{2+}$ /cysteine	1 $\mu\text{M}$ 1-5 mM 10 mM >0.5 mM 10-20 nM 15 $\mu\text{M}$ 0.1-15 $\mu\text{M}$ 2 $\mu\text{M}$ / 10 $\mu\text{M}$	$\text{Mg}^{2+}$ Ruthenium red Procaine Tetracaine Ryanodine Calmodulin	5 mM 15 $\mu\text{M}$ 10 mM 0.6 mM >10 $\mu\text{M}$ 0.2 $\mu\text{M}$

<sup>a</sup>Adapted from Fleisher and Inui, 1989.

<sup>b</sup>These activators inhibit the  $\text{Ca}^{2+}$  release at higher concentration.

$\text{Mg}^{2+}$  and ruthenium red are commonly used as specific inhibitors in studies of  $\text{Ca}^{2+}$  release.

Isolated triads. A fraction rich in triads (about 50%) can be prepared from rabbit fast-twitch muscle HSR by performing two sequential sucrose-gradient centrifugations (Caswell et al., 1976; Mitchell et al., 1983). Electron microscopic studies and other assays show that the purified triads consist terminal cisternae in junctional association with sealed, inside-out T tubules. The coupling of T tubules to the junctional SR can be disrupted mechanically by using a French press cell (Caswell et al., 1979) or by treatment with salt solution (Caswell and Brandt, 1981). Reassociation of triads is possible and is enhanced by potassium cacodylate or

glyceraldehyde 3-phosphate dehydrogenase (Corbett et al., 1985).

An alternative preparation rich in triads was prepared and used for  $\text{Ca}^{2+}$  release studies (Kim et al., 1983). French press treatment to dissociate the T tubules from SR eliminated depolarization-induced  $\text{Ca}^{2+}$  release from SR without affecting  $\text{Ca}^{2+}$ -induced or caffeine-induced  $\text{Ca}^{2+}$  release. These results suggest that the T-tubule associated with SR is crucial in triggering rapid depolarization-induced  $\text{Ca}^{2+}$  release from SR and that  $\text{Ca}^{2+}$  and caffeine appear to stimulate  $\text{Ca}^{2+}$  release a direct interaction with the SR (Ikemoto et al., 1984; 1985).

Isolated SR  $\text{Ca}^{2+}$  release protein. To define the molecular machinery of the  $\text{Ca}^{2+}$  release channel, it is essential to identify and isolate the channel protein. Two specific ligands have been used to label the  $\text{Ca}^{2+}$  release protein, and two proteins have been purified.

The 400 kDa protein is also called the ryanodine receptor complex. Ryanodine is a plant alkaloid known to interfere with EC coupling in cardiac and skeletal muscle. It binds specifically to SR vesicles with high affinity. The conditions for ryanodine binding are similar to those for  $\text{Ca}^{2+}$ -induced  $\text{Ca}^{2+}$  release. High affinity binding is stimulated by  $\text{Ca}^{2+}$ , adenine nucleotide and caffeine. The SR  $\text{Ca}^{2+}$  release channel is identified through its specific binding to ryanodine. The ryanodine receptor complex is purified from detergent-solubilized junctional SR as a high molecular mass

400 kDa protein (Imagawa et al., 1987; Inui et al., 1987; Lai et al., 1988). When reconstituted into a planar lipid bilayer, the purified ryanodine receptor complex is shown to behave as a large conductance divalent cation channel, with electrophysiological properties identical to the channel that is detected with the use of intact SR vesicles (Smith et al., 1988). The unit conductance is found to be 110 pS in the standard asymmetrical  $\text{Ca}^{2+}$  solution with a permeability ratio ( $P_{\text{Ca}}/P_{\text{Tms}}$ ) of 14. The channel activity of the purified receptor is activated by submicromolar  $\text{Ca}^{2+}$  and 1-2 mM ATP, and is inhibited by 1-4 mM  $\text{Mg}^{2+}$  and 30  $\mu\text{M}$  ruthenium red. Ryanodine at 7  $\mu\text{M}$  brought the channel to a long lifetime subconducting state of about 40% full unit conductance. The data suggested that the ryanodine receptor and the  $\text{Ca}^{2+}$  release channel are contained within the same protein. Electron microscopy reveals that four ryanodine receptors compose a structure indistinguishable from the feet observed at the intact transverse tubule-SR junction (Inui et al., 1987). It is also believed that four ryanodine receptors form one functional  $\text{Ca}^{2+}$  release channel. The primary structure of the ryanodine receptor has been deduced from its cDNA sequence (Takeshima et al., 1989). It is a single polypeptide chain of 565 kDa. A predicted structure suggests that the  $\text{Ca}^{2+}$  release channel resides in the C-terminal region of the receptor molecule. The remaining region of the receptor constitutes the foot that spans the junctional gap between the SR and the T-tubule.

We have identified a second protein, which has molecular mass of 106 kDa. The 106 kDa protein is identified and purified based on its interaction with sulfhydryl reagents. The detailed characterization of this protein is described in Chapter III.

#### Proposed Theories Describing EC Coupling

As a result of these studies, several hypotheses have been proposed to describe E-C coupling--the communication between the 12 to 14 nm gap of junctional SR and T-tubule membranes. These hypotheses can be divided into three categories: electrical coupling, mechanical coupling and chemical coupling.

Electrical coupling. The electrical coupling hypothesis suggests that the depolarization of T tubule causes a potential change at the SR membrane by an ionic conduction (Mathias et al., 1980) or by capacitive coupling. The depolarization of SR, in turn, opens the SR  $\text{Ca}^{2+}$  release channel. As discussed by Eisenberg (1987), the transient opening of a conductive pathway between the T-tubule and SR is highly unlikely. Also, the resting permeability of the SR to monovalent cations and anions is too high for any transport system to develop a significant membrane potential within the time scale required for EC coupling. In addition, the separation between the two membranes appears to be too large to provide efficient capacitive coupling between them (Rios and Pizarro, 1991). The other argument against this

hypothesis comes from ionic substitution studies using SR vesicle and triad preparations (Meissner and McKinley, 1976; Ikemoto et al., 1984). While ionic depolarization of isolated triads (isolated SR vesicles with sealed T-tubules attached) induces  $\text{Ca}^{2+}$  release, the same conditions fail to induce  $\text{Ca}^{2+}$  release from isolated SR vesicles. Despite the slight voltage dependence of the reconstituted single SR  $\text{Ca}^{2+}$  release channel in a bilayer membrane, the channel is not activated or inactivated by voltage across the membrane.

Mechanical coupling. Schneider and Chandler reported detection of charge movement within the T tubule membrane upon depolarization by using voltage clamped muscle fibers (1973). They suggested the existence of charge groups and dipoles in T-tubule which can move within the membrane according to trans-membrane potentials. These charged groups (voltage sensor) may be mechanically linked, via the feet proteins, to the activation mechanisms of the SR  $\text{Ca}^{2+}$  channel. The voltage sensor was imaged as a plug to sense the depolarization of T-tubule which, in turn, to open the SR  $\text{Ca}^{2+}$  channel (Chandler et al, 1976).

Using voltage clamp technique, intramembrane charge movement and SR  $\text{Ca}^{2+}$  release can be regularly recorded just prior to contraction. Low concentrations of nitrendipine (a dihydropyridine) inhibit both SR  $\text{Ca}^{2+}$  release and charge movement (Rios and Brum 1987). This indicates a possible role of the dihydropyridine receptor (DHP receptor) as a voltage

sensor. Evidence for possible mechanical coupling is the electron microscopic study (Block et al., 1988), which shows the proximity and the fixed stoichiometry between the DHP receptors of T tubule and the feet protein of SR. On the other hand, the direct binding study (Brandt et al., 1990) fail to show any direct interaction between the DHPR and the foot. The results indicate the involvement of glyceraldehyde 3-phosphate dehydrogenase, aldolase and a 95 kDa protein in the triad junction.

Chemical coupling I:  $\text{Ca}^{2+}$ -induced  $\text{Ca}^{2+}$  release. Using a skinned fiber preparation, Endo et al. (1970) and Ford et al. (1970) reported that  $\text{Ca}^{2+}$  release from the SR was facilitated by  $\text{Ca}^{2+}$  itself. Since then the  $\text{Ca}^{2+}$ -induced  $\text{Ca}^{2+}$  release (CICR) has been extensively investigated in skinned fibers (Stevenson, 1981) and isolated SR vesicles (Ohnishi, 1981; Miyamoto and Racker, 1982; Meissner, 1984).  $\text{Ca}^{2+}$ -induced  $\text{Ca}^{2+}$  release is modulated by myoplasmic  $\text{Ca}^{2+}$  concentration and stimulated by adenine nucleotides and caffeine. CICR is inhibited by ruthenium red,  $\text{Mg}^{2+}$ , and local anesthetics. Single channel studies of SR vesicle fused into planar bilayers showed similar properties (Smith, 1986). The studies of CICR greatly enhanced our understanding of the SR  $\text{Ca}^{2+}$  release channel. These studies also conclude that  $\text{Ca}^{2+}$ , at a concentration that is subthreshold for contraction, is able to trigger  $\text{Ca}^{2+}$  release from SR. It is possible that extracellular  $\text{Ca}^{2+}$  ions enter through T-tubules during

depolarization and cause  $\text{Ca}^{2+}$  release from SR. Additional fiber studies have been conducted to investigate the physiological role CICR plays in EC coupling. The main argument against the physiological role of CICR is from experiments which show that  $\text{Ca}^{2+}$  entry through surface membrane  $\text{Ca}^{2+}$  channels is not necessary to trigger contraction (McCleskey, 1985; Beatty et al., 1987). Most data is consistent with the hypothesis that  $\text{Ca}^{2+}$ -induced  $\text{Ca}^{2+}$  release amplifies an initial process of release elicited by other means (Rios et al., 1991; Endo, 1985).

Chemical coupling II: Inositol 1,4,5-triphosphate-induced  $\text{Ca}^{2+}$  release. Inositol 1,4,5-triphosphate ( $\text{IP}_3$ ) is involved in intracellular signal transduction controlling a variety of cellular functions in different cell types (Berridge, 1987).  $\text{IP}_3$  regulates intracellular  $\text{Ca}^{2+}$  in smooth muscle and nonmuscle cells.  $\text{IP}_3$  may play an important role in EC coupling of smooth muscle (Somlyo and Somlyo, 1986). Thus, it is reasonable to consider whether  $\text{IP}_3$  is a chemical messenger for EC coupling in skeletal muscle cells. The biochemical machinery for the synthesis, release, and hydrolysis of  $\text{IP}_3$  is present in the skeletal muscle. Although some laboratories failed in their attempts, Volpe et al. (1985) and Vergara et al. (1985) demonstrated that  $\text{IP}_3$  induces  $\text{Ca}^{2+}$  release from SR of skinned fiber and SR vesicles. They proposed that the depolarization of T-tubule membrane facilitates the production of  $\text{IP}_3$ , which then migrates across the junctional gap and

stimulates  $\text{Ca}^{2+}$  release from SR. It was also reported that  $\text{IP}_3$  activates SR  $\text{Ca}^{2+}$  channels reconstituted into lipid bilayers (Suarez-Isla et al, 1988). However, it is questionable that  $\text{IP}_3$  (at concentration needed) can be regulated near the SR membrane at a time scale comparable to EC coupling. Furthermore, blocker of  $\text{IP}_3$ -induced  $\text{Ca}^{2+}$  release failed to block the  $\text{Ca}^{2+}$  transient invoked by depolarization of the skeletal muscle fiber (Pape et al., 1988). In another comparative study of skeletal and smooth muscle fibers using caged  $\text{IP}_3$  (its release was precisely controlled by laser pulse photolysis), only in smooth muscle were the  $\text{IP}_3$  concentration and activation rate compatible with the *in vivo* physiological response (Walker et al., 1987).

Chemical coupling III: Sulfhydryl oxidation-induced  $\text{Ca}^{2+}$  release. In this laboratory, we have been investigating sulfhydryl oxidation induced- $\text{Ca}^{2+}$  release from SR. Heavy metals such as  $\text{Hg}^{2+}$ ,  $\text{Ag}^+$ , and  $\text{Zn}^{2+}$  were found to induce rapid  $\text{Ca}^{2+}$  release from SR vesicles. The potency of these heavy metals to induce  $\text{Ca}^{2+}$  release is similar to their relative binding affinities to sulfhydryl groups (Abramson et al., 1983). In addition, mercaptans such as cysteine were found to cause  $\text{Ca}^{2+}$  release from junctional SR in the presence of  $\text{Cu}^{2+}$  (1-2  $\mu\text{M}$ ). The  $\text{Cu}^{2+}$  plus mercaptan effect appears to be due to a  $\text{Cu}^{2+}$ -catalyzed oxidation reaction which results in the formation of a mixed disulfide bond between the exogenous mercaptan and a sulfhydryl on the release mechanism.



Reduction of the disulfide bond with dithiothreitol (DTT) reverses the effect and results in  $\text{Ca}^{2+}$  re-uptake by the SR vesicles (Trimm et al., 1986). More recently, a group of compounds called reactive disulfides (dithiopyridines) such as 2,2'-DTDP, 4,4'-DTDP, and N-succinimidyl 3-(2-pyridyldithio) propionate (SPDP) were tested and found to cause  $\text{Ca}^{2+}$  release from SR vesicles (Zaidi et al., 1989a). Dithiopyridines are known to oxidize free SH sites specifically via a thiol-disulfide exchange reaction with the stoichiometric production of thiopyridone. The increase of SR  $\text{Ca}^{2+}$  permeability caused by oxidation is reversed by reducing the mixed disulfide bond with reducing agents, such as glutathione or DTT.

#### CALCIUM CHANNELS

$\text{Ca}^{2+}$  channels are ubiquitous. They help regulate a wide range of cellular functions, including secretion, contraction, and excitability (Tsien et al., 1983; Hagiwara, 1983).  $\text{Ca}^{2+}$  channels are the most diverse group of channels. They are not as well characterized as the  $\text{Na}^+$  and  $\text{K}^+$  channels.  $\text{Ca}^{2+}$  channels can play two important roles. First, they are responsible for prolonging depolarization of cell surface membranes, because they do not inactivate as quickly as  $\text{Na}^+$  channels. Second,  $\text{Ca}^{2+}$  channels serve as pathways for the secondary messenger  $\text{Ca}^{2+}$  ions to enter cells.

$\text{Ca}^{2+}$  channels from cell membrane are loosely divided into three types according to their kinetics (activation and

TABLE III  
DIFFERENT TYPES OF  $\text{Ca}^{2+}$  CHANNELS<sup>a</sup>

	T-type	N-type	L-type
Single channel conductance	8-10 pS	13 pS	25 pS
Inactivation range	-100 mV to -60 mV	-100 mV to -40 mV	-60 mV to -10 mV
Activation range	-70 mV	-10 mV	-10 mV
Inactivation rate	20-50 ms	20-50 ms	>700 ms

<sup>a</sup>Adapted from McCleskey, 1986)

inactivation) and unit conductance (Table III) (McCleskey, 1986; Bean, 1989). T-type (also called fast, or low-threshold) channels have transient currents which inactivate completely in about 50 ms. They are activated by low voltages and have small unit conductance. In contrast, the L-type (also called slow, or high-threshold) channels have long-lasting currents. They are activated by high voltages and have relatively large unit conductance. The kinetics and conductance of N-type channels (fast but high-threshold) are intermediate between the T- and L-type channels. N-type channels are only found in neurons. In fact, all three types of  $\text{Ca}^{2+}$  channels exist in neurons (Fox et al., 1987). A peptide from a marine snail,  $\omega$ -Conotoxin, blocks high-threshold current (N- and L-type) of neurons without affecting currents of cardiac, smooth, or skeletal muscles (McCleskey et al., 1987).

T- and L-type channels are best characterized in cardiac muscle (Bean, 1989). Using  $Ba^{2+}$  as the charge carrier, macroscopic current of T- and L-type channels are readily distinguished on the basis of inactivation kinetics. T- and L-type channels can also be distinguished based on their different pharmacological properties. L-type channels are potently inhibited by dihydropyridine (DHP)  $Ca^{2+}$  channel blockers (e.g. nifedipine, and nitrendipine) and by phenylalkamine  $Ca^{2+}$  channel blockers (e.g. verapamil, and D 600). L-type channels are stimulated by the DHP  $Ca^{2+}$  channel agonist Bay K 8644. On the other hand, T-type channels are not as sensitive to these drugs as that of L-type channels. The insecticide tetramethrin completely inhibits T-type current at 100 nM without affecting L-type current (Hagiwara et al., 1988). The same T- and L-type channels are also found in smooth muscle.

In developing skeletal muscle, only T-type current exists (Beam and Knudson, 1988a; 1988b). Its presence is thought to help initiate spontaneous activity. There are two current components in adult skeletal muscle. The predominant is L-type current (also called slow  $Ca^{2+}$  current), which resembles the L-type current in cardiac muscle except with slower activation rates. Another component, only recently recognized, is T-type current (also called fast  $Ca^{2+}$  current), which is activated rapidly with a low threshold (Garcia and

Stefani, 1987). This component does not inactivate and is not sensitive to DHPs. Both slow and fast  $\text{Ca}^{2+}$  current, as in cardiac muscle, is potentiated by  $\beta$ -adrenergic agonists or internal cAMP (Arreola et al., 1987). The slow  $\text{Ca}^{2+}$  channel (also called DHP receptor) in T tubule is proposed to act as a voltage sensor for EC coupling (Rios and Brum, 1987). No special functional role for fast  $\text{Ca}^{2+}$  channel is known.

#### The $\text{Ca}^{2+}$ Channel of T-tubule

The studies of dihydropyridine (DHP)  $\text{Ca}^{2+}$  channel antagonists have revealed the existence of a DHP-binding protein in T-tubule membranes. It was purified based on its specific binding to DHPs (Borsotto et al., 1984; Curtis et al., 1984). The purified protein is composed of five subunits:  $\alpha_1$  (170 kDa),  $\alpha_2$  (150 kDa),  $\beta$  (50-55 kDa),  $\gamma$  (30-33 kDa), and  $\delta$  (19-30 kDa). The subunit (often referred to as the DHP receptor) is thought to contain the DHP binding site, the voltage sensor, and the channel pore. The primary structure of the subunit has been deduced from its complementary DNA (Tanabe et al., 1987). It has a molecular mass of 212 kDa, and it has 66% sequence in common to that of the  $\text{Na}^+$  channel.

However, Schwartz et al. (1985) showed that less than 5% of the specific DHP binding site in intact skeletal muscle are actually functional  $\text{Ca}^{2+}$  channels. This surprising fact is explained by assigning the role of voltage sensor to DHP receptors. The postulation that the DHP receptor is the

voltage sensor is greatly enforced by the study with dysgenic skeletal muscle (Tanabe et al., 1988) which genetically lacks the DHP receptor. In skeletal muscle of mice with muscular dysgenesis, both EC coupling and slow L-type  $\text{Ca}^{2+}$  current are missing. Expression of cDNA for the DHP receptor restored EC coupling in the dysgenic myotubes in primary culture.

#### The $\text{Ca}^{2+}$ Release Channel of SR

As described before, the  $\text{Ca}^{2+}$  release channel from the SR membrane has unique characteristics which are different than those of any other types of  $\text{Ca}^{2+}$  channels. This dissertation is about my research on some aspects of this channel using the planar lipid bilayer technique.

### OVERVIEW OF DISSERTATION

#### Reconstitution and Characterization of SR 106 kDa Protein

One crucial step in characterizing a membrane bound-protein is to isolate the target protein. In our collaborator, Dr. Salama's laboratory in University of Pittsburgh, a protein involved in the SR  $\text{Ca}^{2+}$  release mechanism has been purified by labeling with a sulfhydryl reagent (Zaidi et al., 1989b). The first part of my research was to reconstitute this purified 106kDa protein into planar lipid bilayers and to study its electrophysiological and biochemical characteristics. This study helped to establish the identity of this protein and its relation with the SR  $\text{Ca}^{2+}$  release process.

### Ag<sup>+</sup> Modification of SR Ca<sup>2+</sup> Release Channel

From data accumulated with Ca<sup>2+</sup> flux measurements of isolated SR vesicles, our group proposed that sulfhydryl oxidizing reagents open the SR Ca<sup>2+</sup> release channel by interacting with critical sulfhydryl groups (Abramson et al, 1983; Trimm et al., 1986). Among the sulfhydryl reagents tested, Ag<sup>+</sup> is the most potent in inducing Ca<sup>2+</sup> release from SR vesicles. Ag<sup>+</sup> induced Ca<sup>2+</sup> release is optimal at physiological free Mg<sup>2+</sup> concentration. Detailed flux measurements have shown that the initial Ca<sup>2+</sup> release rate has an interesting Ag<sup>+</sup> dependence.

To study the SR Ca<sup>2+</sup> release channel, the planar bilayer system has following advantages over the SR vesicle system: (1) a voltage can be applied across the channel; (2) ionic composition of either side of the channel can be changed; and (3) the behavior of a single channel can be observed in a long period of time (minutes) with high time resolution (milliseconds). The planar bilayer technique was applied to study how does Ag<sup>+</sup> interact with SR Ca<sup>2+</sup> release channel at the single channel level. Since heavy metals are potentially hazardous to the environment, this study contributes to a better understanding of the biological effects of heavy metals, specifically their toxic effects in muscle.

### Photooxidation of SR Ca<sup>2+</sup> Release Channel

In addition to the finding that oxidation of reactive thiols induces rapid Ca<sup>2+</sup> release from SR, modification of

amino groups have also been shown to stimulate  $\text{Ca}^{2+}$  release from passively loaded SR vesicles (Shoshan-Barmatz, 1986; 1987). Work in our laboratory has shown that photooxidation of the SR vesicles (actively or passively loaded), using rose bengal as a sensitizer, resulted in rapid  $\text{Ca}^{2+}$  release (Stuart et al., 1991). The molecular mechanism underlying rose bengal modification of the SR appears to involve modification of specific histidyl residues. In the presence of light, rose bengal appears to exert its effects by the generation of short-lived highly reactive oxygen intermediates. Production of singlet oxygen is directly measured in parallel with an increase in the  $\text{Ca}^{2+}$  permeability of the SR. Rose bengal-induced  $\text{Ca}^{2+}$  release is insensitive to  $\text{Mg}^{2+}$  or  $\text{Ca}^{2+}$ . AMP-PCP (a non-hydrolyzable analog of ATP) or ruthenium red partially inhibit rose bengal induced release. In the last part of this dissertation I examine the effect of photooxidation on the SR  $\text{Ca}^{2+}$  release channel. This study shows that photooxidation acts directly on the SR  $\text{Ca}^{2+}$  channel and further describes how it modifies the channel.

Strong oxidizing agents are becoming increasingly significant as major health hazards in the environment. For instance, ozone now seems to be one of the most troublesome pollutants. The damaging effects of ozone in living systems are known to be partly mediated through free radical reactions. Rose bengal has been used in model systems *in vitro* to study the damaging actions of reactive oxygen

intermediates on biological membranes. Studies on the interaction of reactive oxygen species with ion channel proteins will enhance our understanding of their toxic effects to biological systems.



## CHAPTER II

### METHODS

#### ISOLATION OF SR VESICLES

SR vesicles were isolated from rabbit white skeletal muscle according to the method of MacLennan (1970). Muscle was removed from the back and hind leg of a rabbit. The fat and connective tissue was trimmed off, and the muscle was put into ice-cold buffer A (120 mM NaCl, 10 mM imidazole, 100  $\mu$ M dithiothreitol, pH 7.4). The muscle was then ground in a meat grinder and homogenized in a blender in three volumes of buffer A for 15 seconds on low speed, 45 seconds on high speed. The procedure was repeated once after waiting 30 seconds. The resulting suspension was then centrifuged at 1,600 g (3,100 rpm in the large Sorvall GSA rotor) for 10 minutes. The supernatant liquid (total 1500 ml) was filtered through four layers of cheesecloth and adjusted to pH 7.4 with dry imidazole. The pelleted cell debris was discarded. The supernatant liquid was centrifuged at 10,000 g (8,000 rpm in the GSA rotor) for 15 minutes. Again, the supernatant was filtered through four layers of cheesecloth and the brown mitochondrial pellet was discarded. The supernatant liquid was ultracentrifuged at 44,000 g for 70 minutes (19,000 rpm in

the Beckman type 19 rotor). The pellet (without the brown mitochondrial ring) was scraped off, homogenized, and suspended at approximately 10 mg/ml in buffer A. This suspension was centrifuged at 7,500 g for 10 minutes (11,000 rpm in the Beckman Ti60 rotor, total volume 150 ml, or 7,500 rpm in the GSA rotor, two tubes containing 250 ml each). The large myosin pellet was discarded. The supernatant liquid was centrifuged at 78,000 g (35,000 rpm in the Ti60 for 30 minutes, or 19,000 rpm in the type 19 rotor for 70 minutes). This pellet, which constitutes our SR preparation, was suspended in appropriate buffer, and stored in small aliquots in liquid nitrogen for later use. For vesicle fusion experiments, the SR vesicles were suspended at about 1 mg/ml in 100 mM KCl, 0.7 M sucrose, 10 mM Tris-HEPES, pH 7.4. For 106 kDa protein isolation, the SR vesicles were suspended at 10-20 mg/ml in 0.9 M sucrose, 20 mM Tris-HEPES, pH 7.0. All buffers were prepared with distilled, deionized water.

#### ISOLATION OF 106 KDA PROTEIN

The 106 kDa protein was purified from isolated SR vesicles through the specific labeling by the reactive disulfide reagent N-succinimidyl 3-(2-pyridyldithio) propionate (SPDP) (Zaidi et al., 1989b). Biotin was linked to SPDP, and the resulting PDP-biotin conjugate was used to label detergent (CHAPS) solubilized SR vesicles. The labeled

proteins were detained on a avidin column, and then eluted with sulfhydryl reducing agent dithiothreitol (DTT).

#### Synthesis of SPDP-Biotin Conjugate

Equimolar concentrations (10 mM) of SPDP and biotin hydrazide were mixed in dimethyl sulfoxide (2 ml) and allowed to react in the dark at room temperature for 4 hours.

#### Covalent Labeling of SR Protein with Biotin

PDP-biotin hydrazide was used to covalently link biotin to SR proteins. SR vesicles (2 mg/ml) were allowed to react with 100  $\mu$ M PDP-biotin hydrazide in a pH 5.0 buffer (100 mM NaCl, 20 mM Tris-HEPES, 1 mM  $MgCl_2$ ) at room temperature for 5 minutes. The reaction was terminated by diluting 25-fold in a ice-cold pH 7.0 buffer (100 mM NaCl, 20 mM Tris-HEPES, 1 mM  $MgCl_2$ ). The dilution was centrifuged at 19,000 rpm (in the type 19 rotor) for 70 minutes to remove unreacted PDP-biotin hydrazide. The pellet was then washed with the pH 7.0 buffer and centrifuged again. The pellet (biotinylated SR vesicles) was resuspended at about 15 mg/ml in the pH 7.0 buffer.

#### Isolation of Biotin-Labeled SR Proteins by Biotin-Avidin Chromatography

Biotinylated SR vesicles were solubilized in 1 M NaCl, 20 mM PIPES, 1.6% CHAPS, 0.5% phosphatidylcholine, pH 7.1 at about 1 mg/ml. The solubilization was done on ice with continuous stirring for two hours in the dark. The detergent-

solubilized SR membrane was centrifuged at 49,000 rpm (in Ti50 rotor) for 20 minutes, and the pellet was discarded, and the supernatant liquid was reacted with avidin beads (avidin conjugated to beaded agarose, Molecular Probes) for two hours on ice (in the dark with continuous stirring). The avidin-conjugated beads were washed four times in wash buffer (1 M NaCl, 20 mM PIPES, 1% CHAPS, 0.5% phosphatidylcholine) to remove non-biotinylated proteins. The beads were then loaded into a small column (1 cm x 8 cm). Biotinylated proteins bound to the avidin-beads were selectively eluted with buffer containing sulfhydryl reducing agent dithiothreitol (1 M NaCl, 20 mM PIPES, 5 mM DTT, 0.3% CHAPS, 0.15% phosphatidylcholine, pH 7.1).

#### PLANAR LIPID BILAYER TECHNIQUE

In a planar bilayer system (Figure 3a), a phospholipid bilayer membrane was formed onto an aperture in a wall separating two aqueous compartments of milliliter-size dimensions. With two electrodes, each connected to the aqueous solution on one side of the membrane, a voltage was applied and the current across the membrane was measured. Under the right conditions, SR vesicles or isolated proteins added to the solution in one chamber were incorporated into the bilayer membrane and then electrical measurements could be made. The system had the following advantages: 1) the accessibility to both sides of the channel; 2) the ability to

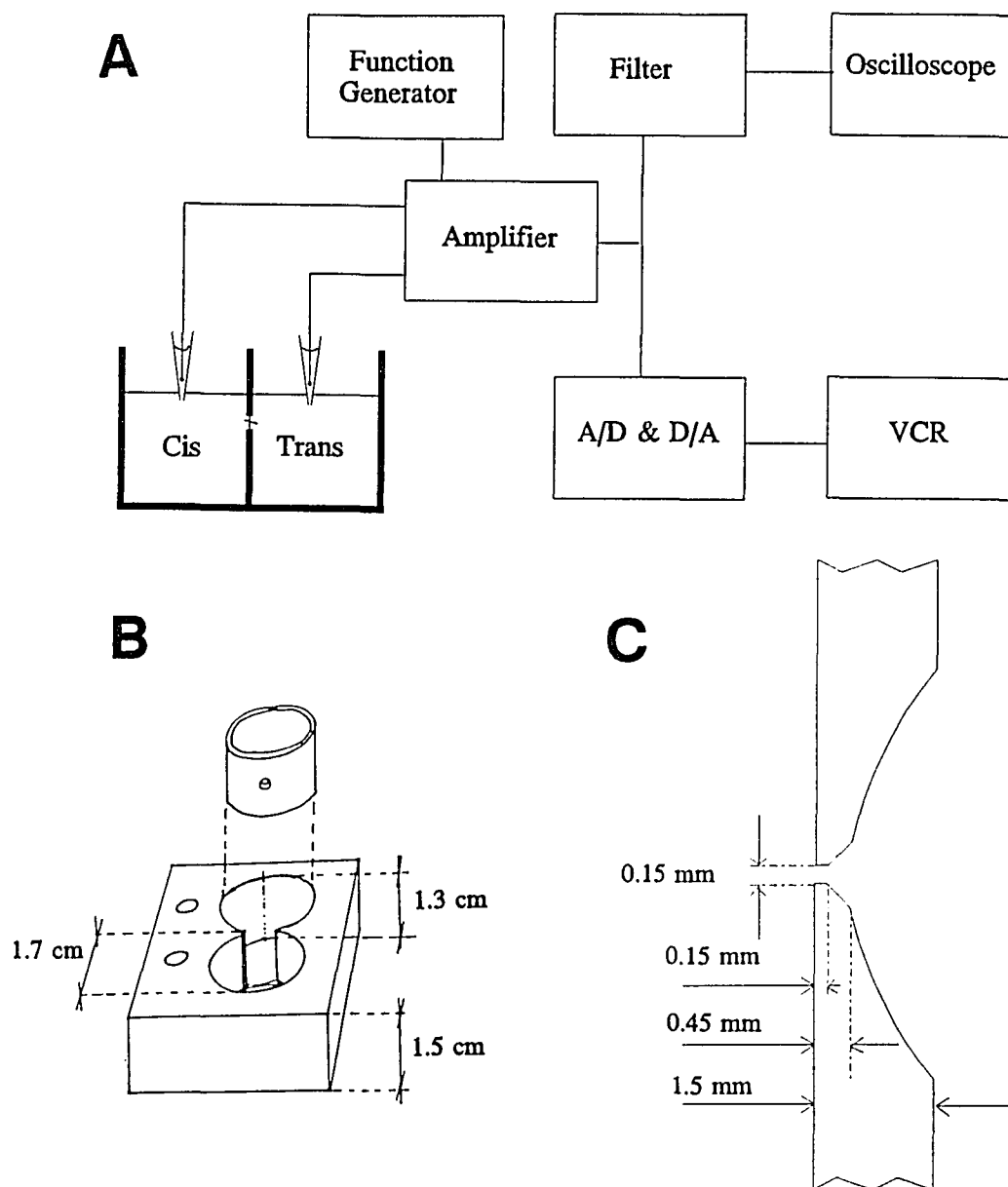


**Figure 3.** A planar lipid bilayer setup. (A) Schematic illustration of a bilayer system for single channel recording. (B) A bilayer chamber. (C) Cross-section view of a aperture for forming a lipid bilayer.

control the ionic composition on both sides of the channel; and 3) the ability to control the voltage across the channel.

### Bilayer Chambers

A bilayer chamber is shown in Figure 3b. A cylindrical polystyrene cup was fitted into a polyvinyl chloride holder. A small hole of 150  $\mu\text{m}$  diameter was drilled into a sector of the cup wall (Figure 3c). The cup was referred to as the trans chamber (1.5 ml) which was held at virtual ground; the opposite side was defined as the cis chamber (1.5 ml) to which SR vesicles or purified proteins were added.

The chambers were washed with running water to remove all salts. The chambers were then sonicated in the detergent JOY for 30 seconds to remove lipids and protein. After rinsing with running water, the chambers were sonicated in 1% HCl for 30 seconds and then washed several times with distilled, deionized water. Chambers were stored in distilled, deionized water.

### Formation of Bilayer Membranes

Phospholipid bilayers were made by the method of Mueller et al. (1962). A lipid film was formed by applying a lipid mixture to the aperture which connects two aqueous solution using a small camel hair brush. When an appropriate amount of lipid was applied, the film thinned to a bilayer spontaneously to minimize the free energy of this lipid and aqueous solution system (White, 1986). Phospholipids dissolved in chloroform

were purchased from Avanti Polar Lipids and stored at  $-20^{\circ}\text{C}$  to prevent decomposition. Lipids were freshly prepared each day by evaporating chloroform under nitrogen and dissolving the dry lipids with decane at a concentration of 50 mg lipids/ ml decane. The lipid mixture used was phosphatidylethanolamine (PE): phosphatidyl serine (PS): phosphatidyl choline (PC) = 5: 3: 2 or PE: PS = 1:1. The presence of the negatively charged lipid PS in the mixture facilitated vesicle fusion (Miller and Racker, 1976).

The formation of a bilayer was a critical step in reconstitution experiments. To achieve easy membrane formation and stable membranes, the aperture was preconditioned with lipids. For membranes to thin spontaneously, the use of excess amounts of lipid was avoided. If a bilayer was not formed after three application of lipids, the chamber was cleaned to remove lipids on the aperture. It was important to use a clean brush to paint membranes. To clean a brush, salts were first washed off with distilled, deionized water, and then it was washed once in ethanol and once in chloroform.

The thickness of the membranes was determined by monitoring the capacitance. To measure the capacitance, a triangle wave of fixed period ( $t$ ) and amplitude ( $V$ ) was applied across a membrane. The amplitude of the current across the membrane ( $i = C \cdot dV/dt$ ) was used to calculate the specific capacitance of a membrane, which should be in the range of

1  $\mu F / cm^2$  for a bilayer (Hille, 1984). The capacitance of the bilayer was constantly checked, in order to insure that the bilayer thickness remained the same throughout a reconstitution experiment. The noise level of a membrane was also a good indicator of the thickness of a membrane.

#### Reconstitution of the Native SR $Ca^{2+}$ Release Channel

The native SR  $Ca^{2+}$  release channel was reconstituted by the vesicle fusion technique. The ionic composition on both sides of the membrane was controlled to facilitate fusion. The following three conditions were generally used.

The standard asymmetrical  $Ca^{2+}$  solution. This protocol was first used by Smith et al. (1985) to characterize the native  $Ca^{2+}$  release channel. SR vesicle fusion was accomplished in a 5:1 choline chloride gradient (cis: 250 mM choline chloride, 10 mM Tris-HEPES, pH 7.4; trans: 50 mM choline chloride, 10 mM Tris-HEPES, pH 7.4). Vesicles were added to the cis chamber in the presence of 1 mM  $CaCl_2$ . Fusion events (Figure 4) were monitored as an increase of  $Cl^-$  current. After one such event, 1 mM EGTA was added to the cis chamber to prevent further fusion. Then, the cis chamber was perfused with three volumes of 125 mM Tris-250 mM HEPES, pH 7.4, and the trans chamber was perfused with three volumes of 53 mM  $Ca^{2+}$ -250 mM HEPES, pH 7.4. The cis (myoplasmic face) free  $Ca^{2+}$  concentration was controlled with a  $Ca$ -EGTA buffer. Monovalent cations such as  $K^+$ ,  $Na^+$ , and the anion  $Cl^-$  were avoided in this system to eliminate interference by SR  $K^+$



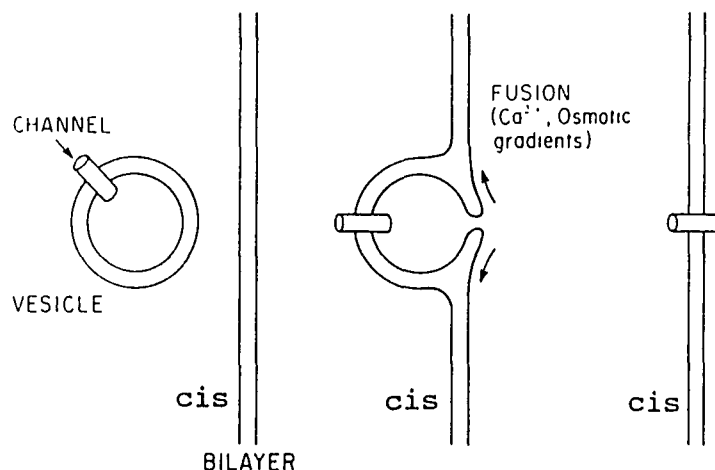


**Figure 4.** Fusion of a SR vesicle to a lipid bilayer. A vesicle is incorporated into a bilayer by the method of Miller and Racker (1976). The fusion is controlled by  $[Ca^{2+}]_{cis}$ , the presence of negatively charged lipid PS in the bilayer, and the osmotic gradient across the bilayer. The gradient across the bilayer ensures that vesicles incorporate into the bilayer with maintained orientation (outside facing cis). Adapted from White, 1986.

channels and  $Cl^-$  channels. The permeability ratio of  $Ca^{2+}$  to  $Tris^+$  was obtained by determining the reversal potential of  $Ca^{2+}$  current (see appendix).

The CsCl gradient. It was convenient to characterize the  $Ca^{2+}$  channel in the same solution in which fusion was performed. This was achieved by using a CsCl gradient (cis: 500 mM CsCl, 10 mM Tris-HEPES, pH 7.2; trans: 100 mM CsCl, 10 mM Tris-HEPES, pH 7.2). These conditions, first reported by Fill et al. (1990), avoided the  $K^+$  and  $Cl^-$  currents normally found in SR preparations.  $Cs^+$  was chosen because it was reported (Coronado et al., 1980) that SR  $K^+$  channels are almost impermeable to  $Cs^+$  ( $<3$  pS in 1 M symmetrical  $Cs^+$ ). The

high  $\text{Cs}^+$  conductance of the SR  $\text{Ca}^{2+}$  channel improved the signal to noise level. The effect of  $\text{Cl}^-$  channels was minimized by monitoring the  $\text{Ca}^{2+}$  channel activity near the reversal potential of  $\text{Cl}^-$ . The disadvantage of this method was the narrow voltage range (0 to +40 mV) at which  $\text{Ca}^{2+}$  channel activity could be monitored. SR vesicles were added to the cis chamber at a final concentration of 2-10  $\mu\text{g} / \text{ml}$  in the presence of 0.35-0.7 mM  $\text{CaCl}_2$ . Fusion events were monitored as an increase in the  $\text{Cl}^-$  current. The osmotic gradient and the millimolar cis  $\text{Ca}^{2+}$  were essential for vesicle fusion.  $\text{Cl}^-$  was also believed to be essential for fusion. After one such event, a two fold excess of EGTA (over  $\text{Ca}^{2+}$ ) was added to the cis chamber to prevent further fusion. The cis chamber was then perfused with three volumes of vesicle free solution.

Solution perfusions were performed by using a back to back double syringe arrangement. Solution was pumped into the bottom of a chamber via a small tubing and simultaneously withdraw through another tubing positioned at the top of the chamber. The solutions in the two chambers were electrically shorted with a piece of silver wire to avoid buildup of static charge and breakage of the bilayer during the solution changing process.

The symmetrical NaCl solution. A symmetrical NaCl solution (250 mM NaCl, 10 mM NaOH-HEPES, 0.5 mM  $\text{CaCl}_2$ , 0.5 mM EGTA, pH 7.4.) was used to study the monovalent conductivity of the native  $\text{Ca}^{2+}$  release channel. The SR vesicle fusion was

carried out in the presence of 0.7 mM  $\text{CaCl}_2$  and a 2:1 NaCl gradient (500 mM cis/250 mM trans) or with a symmetrical 250 mM NaCl solution. The cis chamber was then perfused with a vesicle-free solution containing 250 mM NaCl. After one fusion event, 0.7 mM EGTA was added to prevent further fusions. The interference of SR  $\text{Cl}^-$  channels was minimized by using SR vesicle preparations which contained only a few  $\text{Cl}^-$  channels per vesicle. The protocol was effective because the conductivity of SR  $\text{K}^+$  channels to  $\text{Na}^+$  is relative low ( ~ 40pS in 250 mM NaCl), and the gating of the  $\text{K}^+$  channel is much slower (on the second scale) than that of the  $\text{Ca}^{2+}$  release channel (on the millisecond scale). Generally, less than five SR  $\text{K}^+$  channels were incorporated after a single fusion event.

#### Reconstitution of Purified 106 kDa Protein

The reconstitution of purified 106 kDa channel protein into a planar lipid bilayer was carried out with two ionic conditions.

The standard asymmetrical  $\text{Ca}^{2+}$  solution. For comparison with the native SR  $\text{Ca}^{2+}$  release channel, the activity of the purified protein was monitored in the standard asymmetrical  $\text{Ca}^{2+}$  solution described above for the native channel. The incorporation of the purified protein to a bilayer was obtained in a symmetrical NaCl solution (150 mM NaCl, 10 mM Na-HEPES, 0.1 mM  $\text{CaCl}_2$ , 0.1 mM EGTA, pH 7.4) by adding 5-30  $\mu\text{l}$  of purified 106 kDa protein (at a protein concentration of about 20  $\mu\text{g}/\text{ml}$ ). A bilayer was formed after the addition

of purified protein to the vicinity of the aperture of a bilayer chamber. This often produced a bilayer with a few incorporated proteins. Breaking and reforming bilayers also seemed to assist protein incorporation. Generally these procedures were repeated until a bilayer was formed containing only one or two channel proteins. Sonication of protein prior to addition gave bilayers containing a fewer numbers of proteins. After a successful reconstitution, the solutions in both chambers were perfused to the standard asymmetrical  $\text{Ca}^{2+}$  solution.

The symmetrical NaCl solution. The lack of other SR channels in the purified protein preparation made it possible to use this convenient experimental procedure. Symmetrical NaCl solution (250 mM NaCl, 10 mM Na-HEPES, 0.1 mM  $\text{CaCl}_2$ , 0.1 mM EGTA, pH 7.4) was used in most 106 kDa protein reconstitution studies. The incorporation of purified protein into a bilayer was as described above. Compared to the standard asymmetrical  $\text{Ca}^{2+}$  solution, the use of the symmetrical NaCl solution greatly improved the success rate of reconstitution of the 106 kDa channel protein.

#### Signal Acquisition and Analysis

The planar lipid bilayer setup was enclosed in a Faraday cage so that the system was isolated from electrical noise. A vibration-isolation table was used to protect the system from physical vibrations. A D.C. stirring motor was placed directly under the bilayer chamber to achieve fast mixing of

solutions. As shown in Figure 3a, two agar bridges (1% agar in 100 mM KCl, 20 mM Tris-HEPES, pH 7.0) connected the solution of two chambers to two Ag/ AgCl electrodes. A patch clamp amplifier (List EPC-7), applied a known voltage across the bilayers. The amplifier also allowed measurement of the trans-membrane current and converted the picoampere current to a millivolt voltage reading. This signal was then passed through a 3000 Hz low pass filter inside the amplifier. Data were digitized with an VR-10 Digital Data Recorder (Instrutech) and stored on a VHS HQ video recorder. The signal was simultaneously passed through a low pass filter (Frequency Devices, model 902) and displayed on a digital storage oscilloscope (Kikusui; 20 MHz 5020A). Data stored on VCR tapes were filtered at 400-1,500 Hz and digitized at 500-4,000 Hz for later analysis on an IBM-PC using the software package pCLAMP (Axon Instruments).

## CHAPTER III

### RECONSTITUTION AND CHARACTERIZATION OF THE 106 KDA $\text{Ca}^{2+}$ RELEASE CHANNEL

#### SUMMARY

The purified 106 kDa protein was reconstituted into a planar lipid bilayer membrane and the resulting channel activity was examined. In an asymmetrical  $\text{Ca}^{2+}$  solution, the channel demonstrated a single channel conductance of  $107 \pm 13$  pS and a permeability ratio of  $\text{Ca}^{2+}$  versus  $\text{Tris}^+$  of  $7.4 \pm 3.3$ . In a symmetrical 250 mM NaCl solution, the channel displayed a large single channel conductance of  $400 \pm 20$  pS, and a weak voltage-dependence of the open probability. The channel was activated by millimolar ATP and inhibited by micromolar ruthenium red. Nanomolar concentrations of ryanodine modified the channel by changing the channel from a fast gated full conductance state to a long-lived subconducting state. Thus, the 106 kDa protein is a  $\text{Ca}^{2+}$  channel protein which has similar properties to the native SR  $\text{Ca}^{2+}$  release channel.

#### INTRODUCTION

Previous work from our laboratory strongly indicated that SH groups are involved in the SR  $\text{Ca}^{2+}$  release process

(reviewed by Abramson and Salama, 1989). A group of disulfide compounds (Figure 5a) were examined in an effort to find ideal sulfhydryl oxidizing reagents which would label and help to purify the  $\text{Ca}^{2+}$  release protein (Zaidi et al., 1989a). These reactive disulfide compounds (RDSs) with a pyridyl ring adjacent to an S-S bond, include 2,2'-dithiopyridine (2,2'-DTDP), 4-4'-dithiopyridine (4,4'-DTDP), and N-succinimidyl 3-(2-pyridyldithio)propionate (SPDP). These compounds are known specifically to oxidize free SH sites via a thiol-disulfide exchange reaction with the stoichiometric production of thiopyridone. The RDSs cause  $\text{Ca}^{2+}$  release from isolated SR vesicles at micromolar concentrations. This sulfhydryl oxidation-induced  $\text{Ca}^{2+}$  release can be reversed by addition of the reducing agents glutathione (GSH), or dithiothreitol (DTT). At micromolar concentrations, reactive disulfides displace [ $^3\text{H}$ ]ryanodine binding from SR vesicles, indicating further that the RDSs specifically interact with the  $\text{Ca}^{2+}$  release protein. It appears that the RSDs oxidize one or more sulfhydryl groups on the  $\text{Ca}^{2+}$  channel, resulting in a mixed disulfide between the release protein and the RSDs (Figure 5b).

Among the dithiopyridines causing release, SPDP is a heterobifunctional reagent. It can be covalently linked to another easily identifiable molecule which, in turn, can be attached to a column. Figure 5c shows the reaction of SPDP with biotin hydrazide to form PDP-biotin hydrazide. As

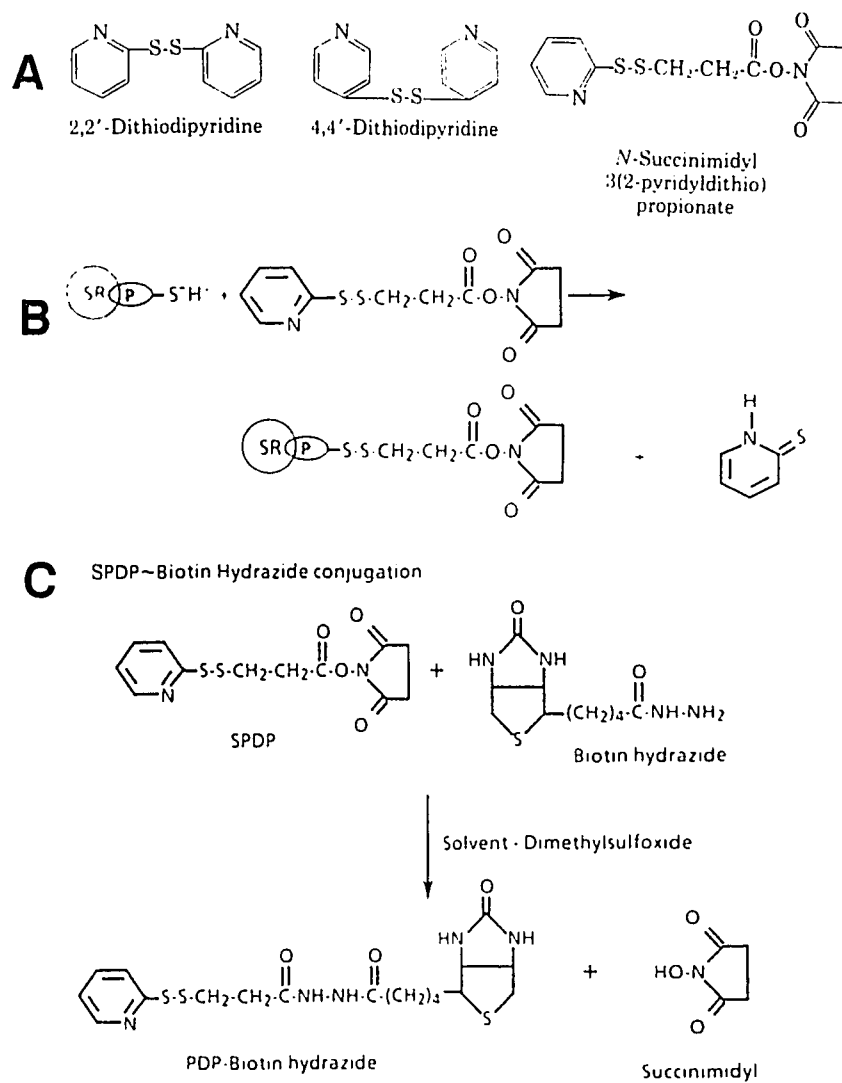


**Figure 5.** Structure of reactive disulfide compounds and reactions of SPDP. (A) Structure of three reactive disulfide compounds. (B) Thiol-disulfide exchange reaction between a free SH site on the SR and SPDP. (C) Synthesis of SPDP-biotin conjugate.



expected, PDP-biotin hydrazide was effective in causing SR  $\text{Ca}^{2+}$  release, with characteristics similar to SPDP. PDP-biotin hydrazide covalently labeled one SR protein which was identified by biotin-avidin peroxidase reaction. This was an elegant method to link covalently the channel protein with an easily identifiable probe which facilitated isolation and purification. The reactive disulfide SPDP was first used successfully in our collaborator's laboratory to label and purify a single protein from solubilized SR (Zaidi et al., 1989b). The biotinylated protein was isolated and purified by biotin-avidin chromatography. The purified protein consists of a single polypeptide of molecular mass about 106,000 dalton (106 kDa).

This chapter describes characterization of this 106 kDa protein reconstituted in planar lipid bilayers. The purified 106 kDa protein used in my early experiments was obtained from Dr. Salama's laboratory at the University of Pittsburgh. Keith Scott, a fellow student in this laboratory, kindly provided the purified 106 kDa protein for most of my experiments.

## RESULTS

The purified 106 kDa protein was first characterized in a standard asymmetrical  $\text{Ca}^{2+}$  solution. The purified 106 kDa protein was first incorporated into a bilayer in a symmetrical NaCl solution, which was then changed to an asymmetrical

calcium solution. The protein was added to the cis chamber at a final concentration of 50-500 ng/ml in the presence of CHAPS (2-20  $\mu\text{M}$ ). The bilayer bathing buffer contained symmetrical 150 mM NaCl, 10 mM NaOH / HEPES, 0.1 mM  $\text{CaCl}_2$ , 0.1 mM EGTA, pH 7.4. After the incorporation of proteins into the bilayer, the cis chamber was perfused with 125 mM Tris, 250 mM HEPES, 0.1 mM  $\text{CaCl}_2$ , 0.1 mM EGTA, pH 7.4; the trans chamber was perfused with 53 mM  $\text{Ca}(\text{OH})_2$ , 250 mM HEPES, pH 7.4. Incorporation of the 106 kDa protein into bilayer membrane was monitored through changes in the bilayer current. In the NaCl solution, about 20% of the bilayers showed discrete current fluctuation which is a characteristic feature of single channel activity. This may reflect the percentage of 106 kDa proteins which were structurally intact after purification procedure and incorporated into bilayer membranes in the native conformation. The difficulty in studying channel behavior using this procedure lay in the fact that after changing solutions to a standard  $\text{Ca}^{2+}$  containing buffer, the thickness of bilayer membranes was likely to increase, and at this point channel activity was often lost. The increased thickness of the membranes might be caused by changes in the ionic environment or the interaction between high concentration of  $\text{Ca}^{2+}$  and the lipid component of the membranes. If the protein survived the solution changing, measurements such as shown in Figure 6 were recorded. Figure 6a shows a typical current fluctuation following incorporation

of the isolated 106 kDa protein into a bilayer. The corresponding current-voltage (I-V) curve (Figure 6b) reveals a single channel conductance of  $107 \pm 13$  pS. The reversal potential is  $-27 \pm 7$  mV, yielding a permeability ratio of  $\text{Ca}^{2+}$  to  $\text{Tris}^+$  ( $P_{\text{Ca}}/P_{\text{Tris}}$ ) of  $7.4 \pm 3.3$ . As a control, the detergent CHAPS without protein was added at higher concentration ( $200 \mu\text{M}$ ) and no current fluctuations were observed.

As mentioned above, the 106 kDa protein also conducted current in a symmetrical NaCl solution. The ability of the 106 kDa protein to conduct monovalent ions was investigated. The purified 106 kDa protein was added to the cis chamber at a final concentration of 50-500 ng/ml in the presence of CHAPS ( $2-20 \mu\text{M}$ ). The bilayer bathing buffer contained symmetrical 250 mM NaCl, 10 mM NaOH / HEPES, 0.1 mM  $\text{CaCl}_2$ , 0.1 mM EGTA, pH 7.4. Figure 7 shows current fluctuation recorded at four different holding potentials. In this figure,  $\text{Na}^+$  is transported through a single 106 kDa protein molecule. The single channel current is large and the kinetics of opening and closing is fast (on the scale of ms). The channel does not spontaneously inactivate. The other feature clearly demonstrated in Figure 7 is the weak voltage dependence of the open probability ( $P_0$ ), which is smaller at positive potentials ( $P_0 = 3\%$  at +40 mV;  $P_0 = 6\%$  at +20 mV), and larger at negative potentials ( $P_0 = 24\%$  at -20 mV;  $P_0 = 38\%$  at -40 mV). This voltage asymmetry of  $P_0$  is evident in all experiments performed in symmetrical solution, where the channel can be

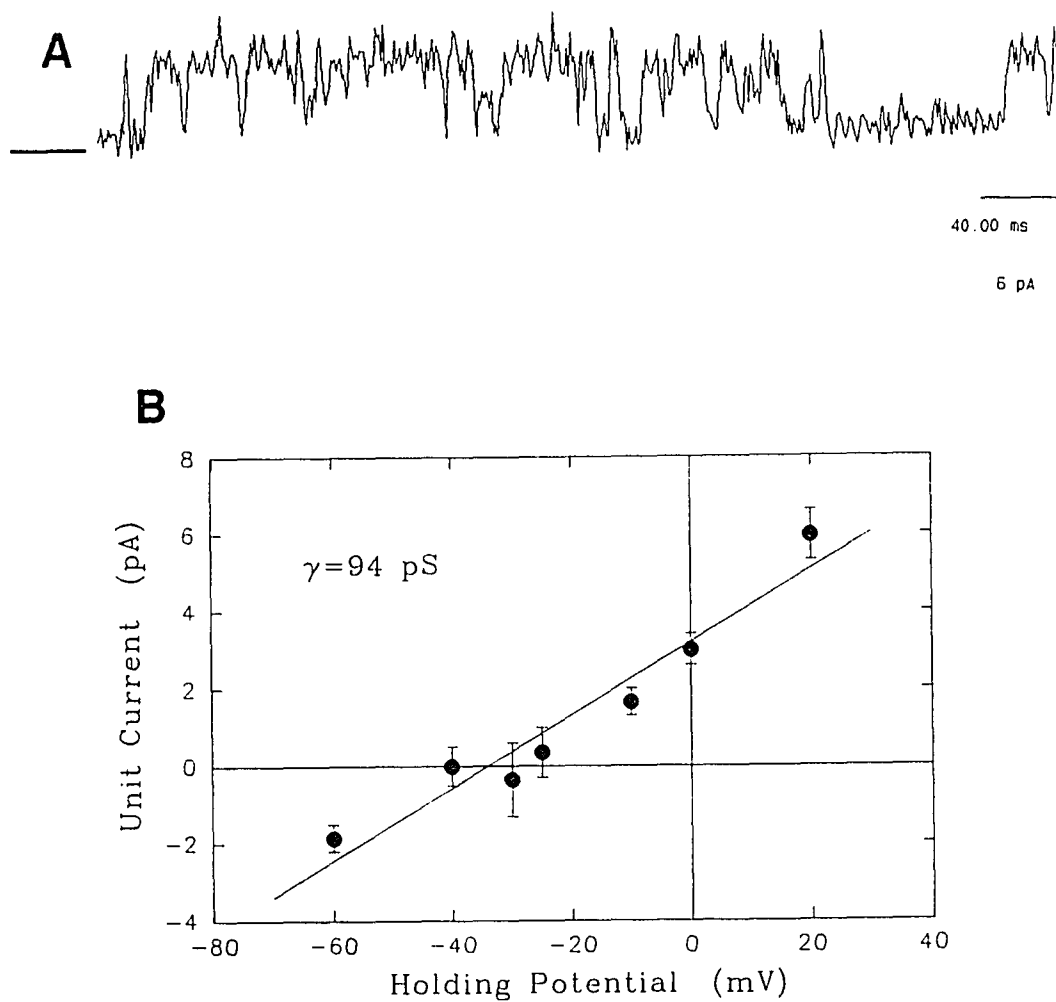


**Figure 6.** Reconstituted 106 kDa protein in the standard  $\text{Ca}^{2+}$  solution. (A)  $\text{Ca}^{2+}$  current fluctuation through the reconstituted 106 kDa channel. Holding potential (HP) is 20 mV. Number of experiments (n) is 3. The bar indicates the closed state of the channel. (B) The current-voltage curve of a single 106 kDa channel. The straight line is determined by a least square fit.

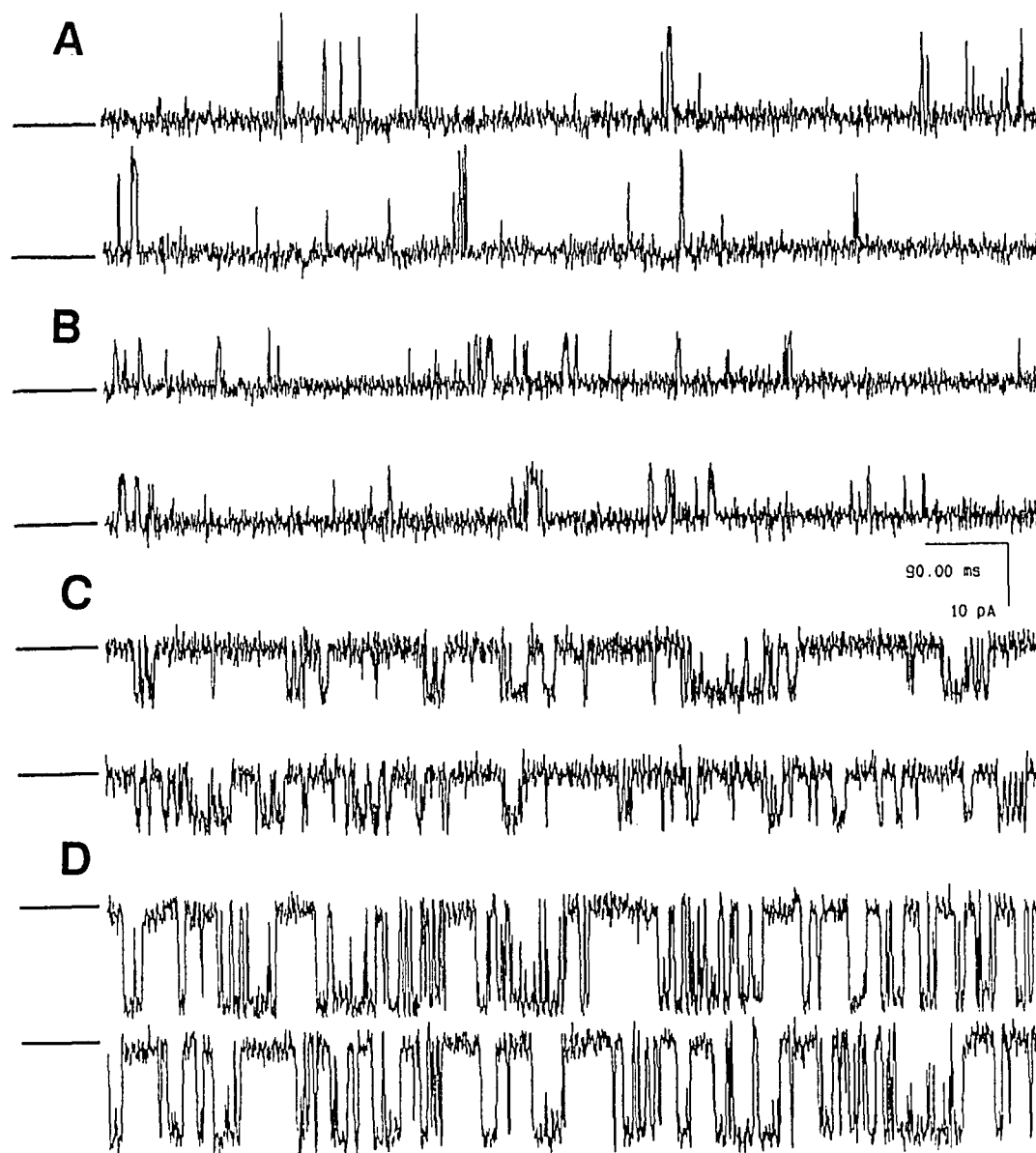
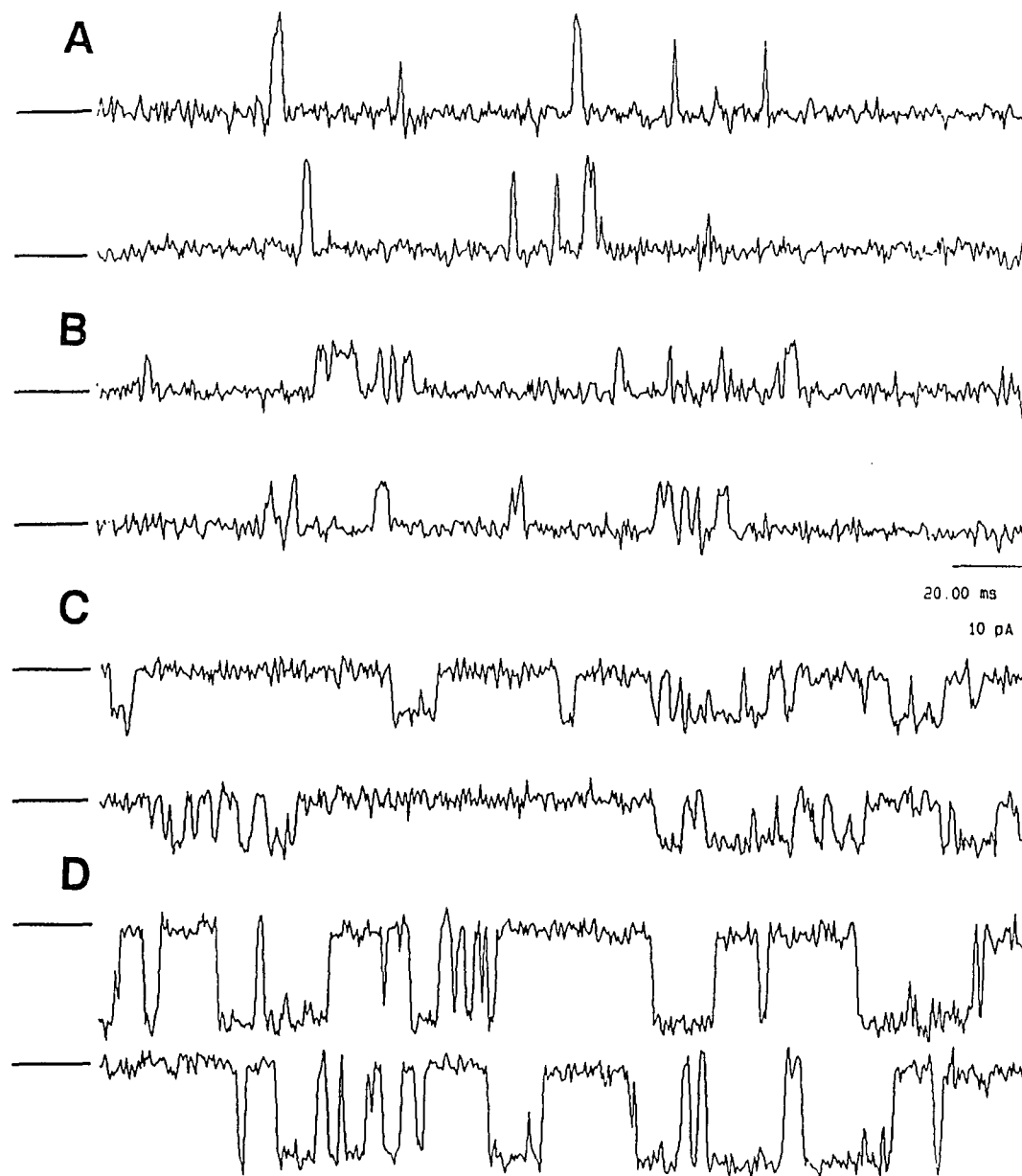


**Figure 7.** Reconstituted 106 kDa protein shows monovalent cation conductance. Purified protein was incorporated into a bilayer in symmetrical 250 mM NaCl, 10 mM NaOH/HEPES, pH 7.4. ( $n > 10$ ) The  $\text{Na}^+$  current through the 106 kDa channel was recorded under four different holding potentials. (A) HP = 40 mV,  $P_0 = 3\%$ . (B) HP = 20 mV,  $P_0 = 6\%$ . (C) HP = -20 mV,  $P_0 = 24\%$ . (D) HP = -40 mV,  $P_0 = 38\%$ . The bars indicate the closed state of the channel.

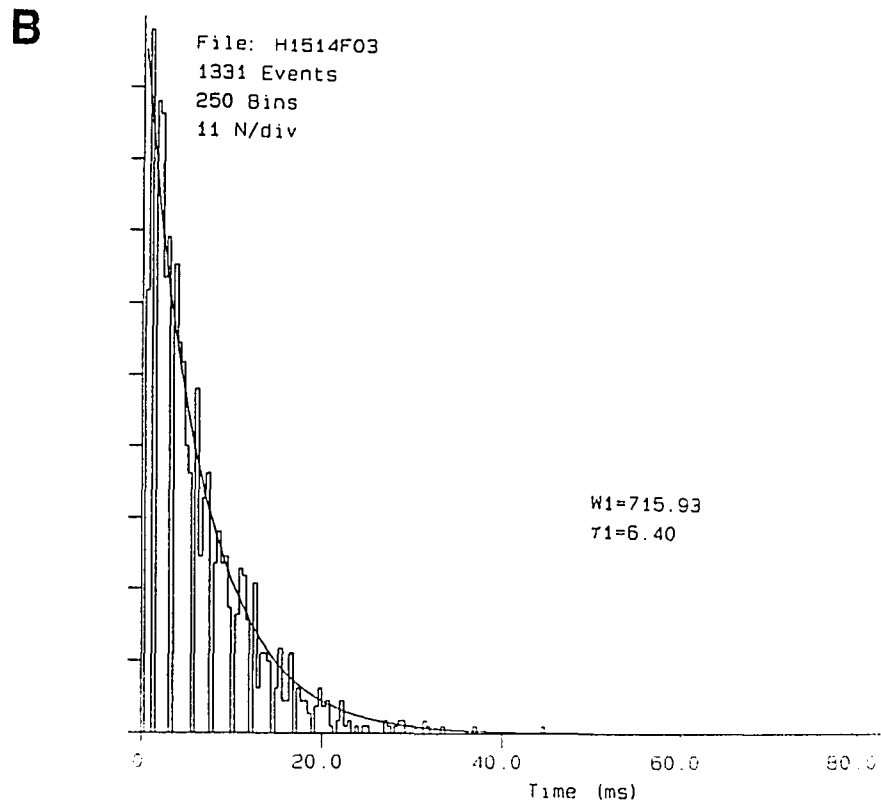
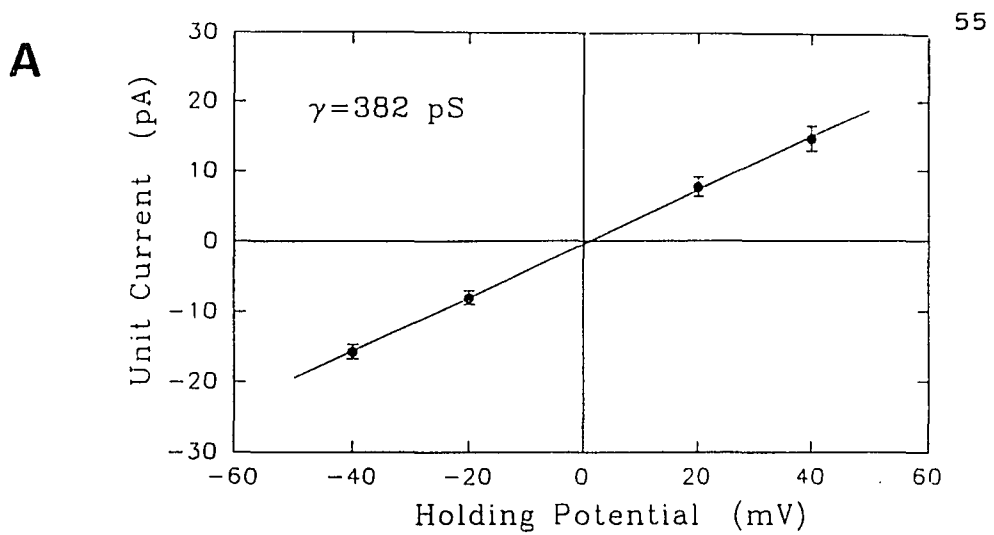
observed under a large range of holding potential. Figure 8 displays the  $\text{Na}^+$  current through the 106 kDa protein channel at a higher time resolution (data from the same experiment as Figure 7). Here, the opening and closing of the channel (the gating of the channel) can be seen clearly. The channel open lifetime can be fit to a single exponential with a mean open lifetime ranging from 1.1-6.4 ms, depending on the holding potential (Figure 9b at  $\text{HP} = -40$  mV). The corresponding I-V curve (Figure 9a) shows a single channel conductance of  $400 \pm 20$  pS.

The permeability of the native SR  $\text{Ca}^{2+}$  release channel to  $\text{Na}^+$  ions was also investigated. Figure 10 shows a SR vesicle fusion experiment performed in the same symmetric solution of 250 mM NaCl. Both the purified 106 kDa channel and the native channel (from a fusion experiment) conducts  $\text{Na}^+$  ions. The single channel conductance of the native  $\text{Ca}^{2+}$  release channel is  $405 \pm 35$  pS, which agrees with that of 106 kDa protein ( $400 \pm 20$  pS). The voltage dependence of open probability is also evident in native  $\text{Ca}^{2+}$  channel.

The other frequently observed feature of the reconstituted 106 kDa channel is the presence of subconducting states. The traces in Figure 11 show the presence of four subconducting states with a conductance of one quarter (102 pS) of the full unitary conductance ( $400 \pm 20$  pS). Note the different kinetics associated with each state. Following reconstitution, about half of the bilayer experiments showed

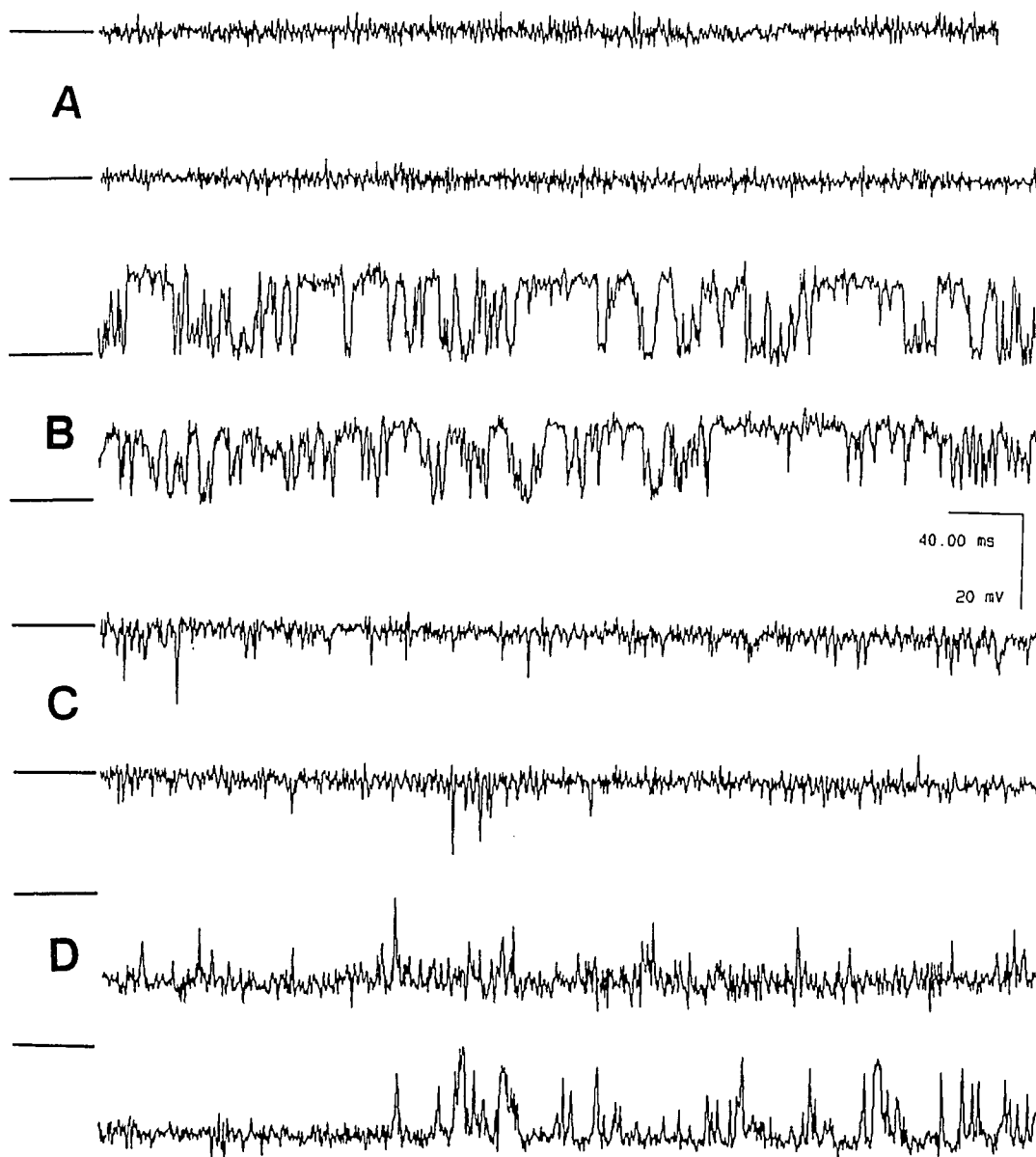


**Figure 8.** Reconstituted 106 kDa protein shows monovalent cation conductance. Purified protein was incorporated into a bilayer in symmetrical 250 mM NaCl, 10 mM NaOH/HEPES, pH 7.4. The four traces are from the same recording of Figure 7 at a shorter time scale. (A) HP = 40 mV. (B) HP = 20 mV. (C) HP = -20 mV. (D) HP = -40 mV. The bars indicate the closed state of the channel.

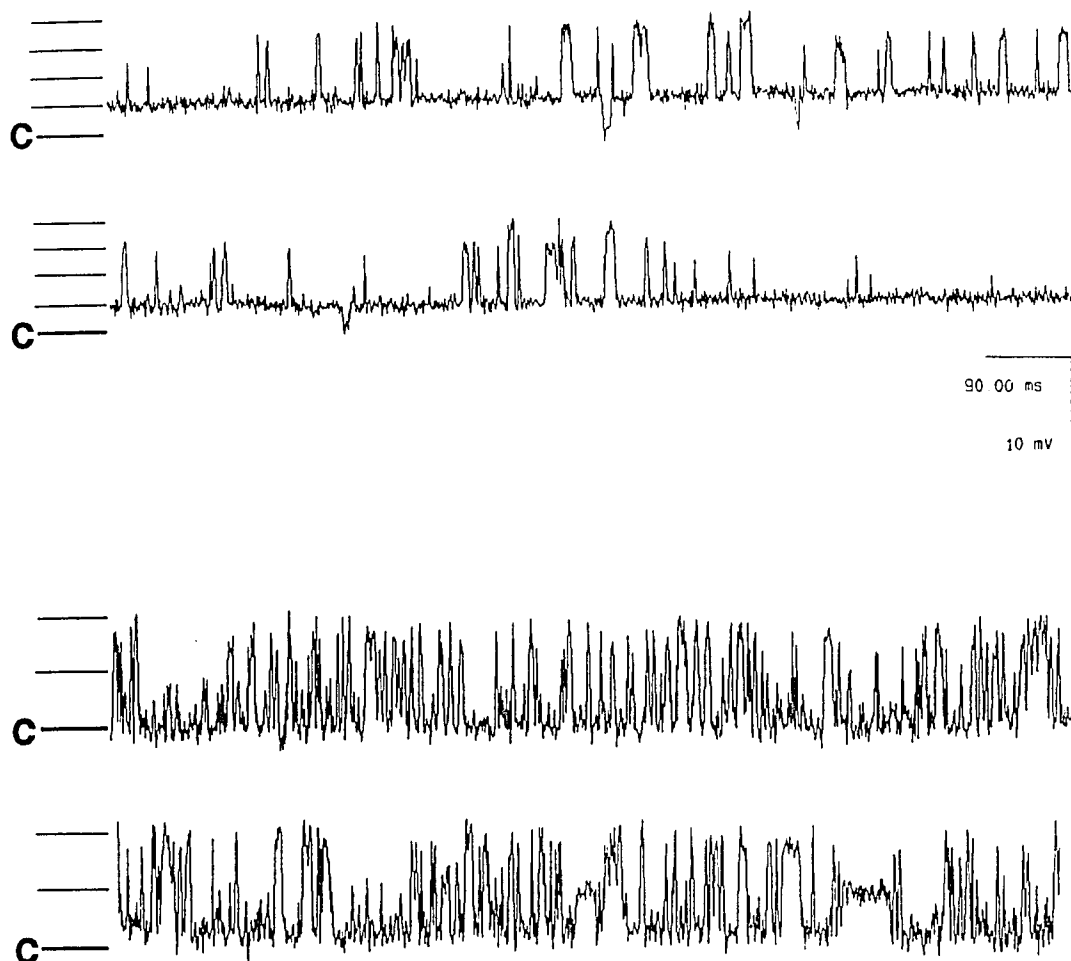


**Figure 9.** The properties of monovalent conductance of the 106 kDa channel. (A) Current-voltage curve in symmetrical NaCl solution. Data are taken from the same recording as Figure 7. (B) Open lifetime histogram of the same recording at HP=-40 mV. A single exponential fitting reveals open time constant of 6.4 ms.





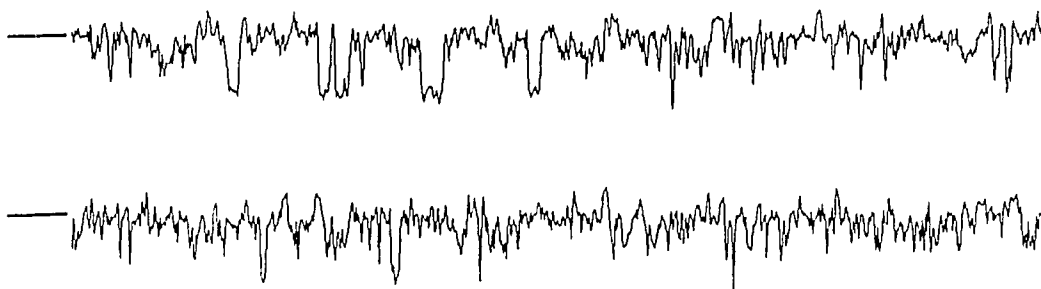
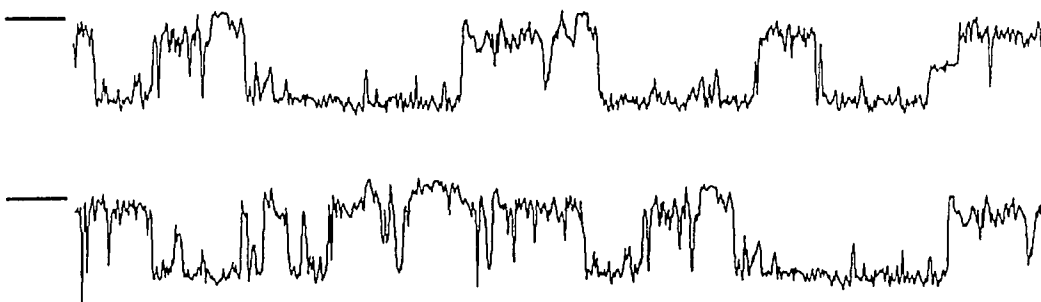
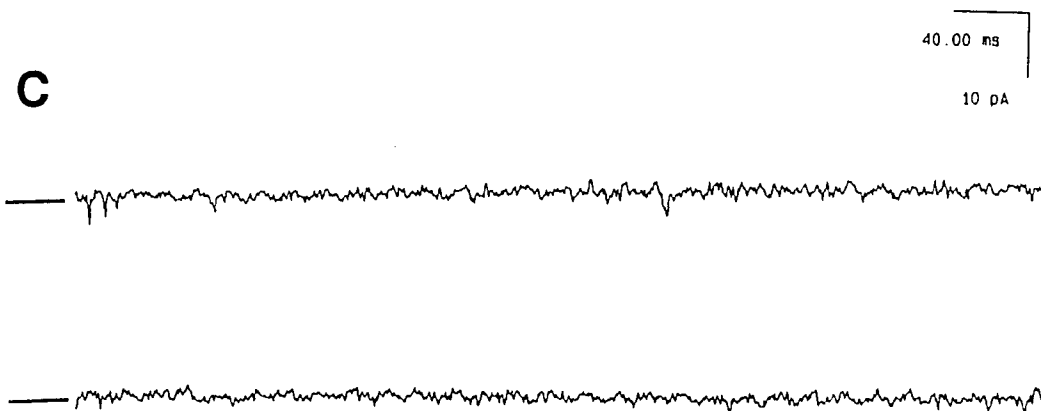
**Figure 10.** The native SR  $\text{Ca}^{2+}$  release channel conducts monovalent cations. SR vesicles were added to the cis chamber of a bilayer in symmetric solution (250 mM NaCl, 10 mM NaOH/HEPES, pH 7.4, with 0.7 mM cis  $\text{Ca}^{2+}$ ). Following vesicle fusion the cis chamber was perfused with 250 mM NaCl, 10 mM NaOH/HEPES, pH 7.4.  $[\text{Ca}^{2+}]_{\text{free}} = 10 \mu\text{M}$ . (A) HP = 40 mV,  $P_0 = 0\%$ . (C) HP = -40 mV,  $P_0 = 1\%$ . Traces c and d were made after the photoactivation of 0.3  $\mu\text{M}$  rose bengal. (B) HP = 40 mV,  $P_0 = 87\%$ . (D) HP = -40 mV,  $P_0 = 95\%$ . The bars indicate the closed state of the channel. (n=3)



**Figure 11.** Subconducting states of the reconstituted 106 kDa protein. The recordings were made in 250 mM symmetrical NaCl solution. The top three traces show quarter states. In the bottom two traces, half-conducting states are evident. The thick bars indicate the closed state of the channel, and the fine bars indicate subconducting states of the channel. HP = 40 mV.

a full conductance of about 400 pS with no or seldom occurrence of half or quarter states. These types of channels were used to study the ligand sensitivity of the 106 kDa protein. The other half of the reconstituted channels showed behavior that was not reproducible. These channels had single channel conductance other than 400 pS, very slow gating, or unstable channel activity such as changing unit conductance and unstable gating behavior. Such abnormal channel activity may have resulted from channel molecules which were damaged in the purification procedure, or from channel proteins which were not incorporated into bilayers in a normal conformation.

To establish further the identity of the 106 kDa channel, its ligand sensitivity was tested. A symmetrical NaCl solution (250 mM NaCl, 10 mM NaOH /HEPES, pH 7.4) was used in these studies to simplify the experimental procedure. Figure 12 shows current traces following the incorporation of 106 kDa protein into a bilayer in a symmetrical NaCl solution. Open events are shown as downward deflections. Addition of 1 mM ATP greatly increased the open probability of the channel, and the subsequent addition of 6  $\mu$ M ruthenium red completely inhibited the channel activity. The ligand sensitivity of the reconstituted 106 kDa channel was apparently dependent on the integrity of its structure. If the channel had normal unitary conductance and fast kinetics, there was a larger probability that experiments carried out with it would respond to the ligands added. Of all the 106 kDa channels which showed

**A****B****C**

**Figure 12.** ATP and ruthenium red modification of the reconstituted 106 kDa channel. Recordings were made in 250 mM symmetrical NaCl solution. (A) Control trace,  $P_0 = 7\%$ . (B) After addition of 1 mM ATP to both chambers,  $P_0 = 33\%$ . (C) After addition of  $6 \mu\text{M}$  ruthenium red to both chambers,  $P_0 = 0\%$ . HP =  $-40 \text{ mV}$ .  $\gamma = 375 \text{ pS}$ . The bars indicate the closed state of the channel. ( $n=4$ )

normal conductance, about 50% were sensitive to the addition of ATP, and about 30% were sensitive to the addition of ruthenium red. The reconstituted 106 kDa channel was insensitive to  $\text{Ca}^{2+}$ .

In comparison with the native SR  $\text{Ca}^{2+}$  channel reconstituted in bilayer (Rousseau et al., 1987), the 106 kDa channel had a much greater sensitivity to ryanodine. Figure 13 shows the current fluctuation of a single 106 kDa channel before and after the addition of ryanodine (also see Figure 34 in Chapter V). In trace A, the channel is in its full conducting state (420 pS) with an open probability  $P_0$  of 33%. As shown in Figure 13b, the channel passed into a subconducting state (210 pS) about one minute after addition of 20 nM ryanodine to both sides of the bilayer. The  $P_0$  of the subconducting state was close to unity.

## DISCUSSION

Reconstitution of the purified, sulfhydryl-activated 106 kDa protein into planar lipid bilayers indicated the presence of a channel with similar characteristics to the native SR  $\text{Ca}^{2+}$  release channel. The properties of the native SR  $\text{Ca}^{2+}$  channel, the 106 kDa channel, and the purified 400 kDa ryanodine receptor channel are compared in Table IV. The native  $\text{Ca}^{2+}$  channel refers to the channel obtained following fusion of SR vesicles to the bilayer. This is a detergent free preparation. The native SR  $\text{Ca}^{2+}$  channel was identified

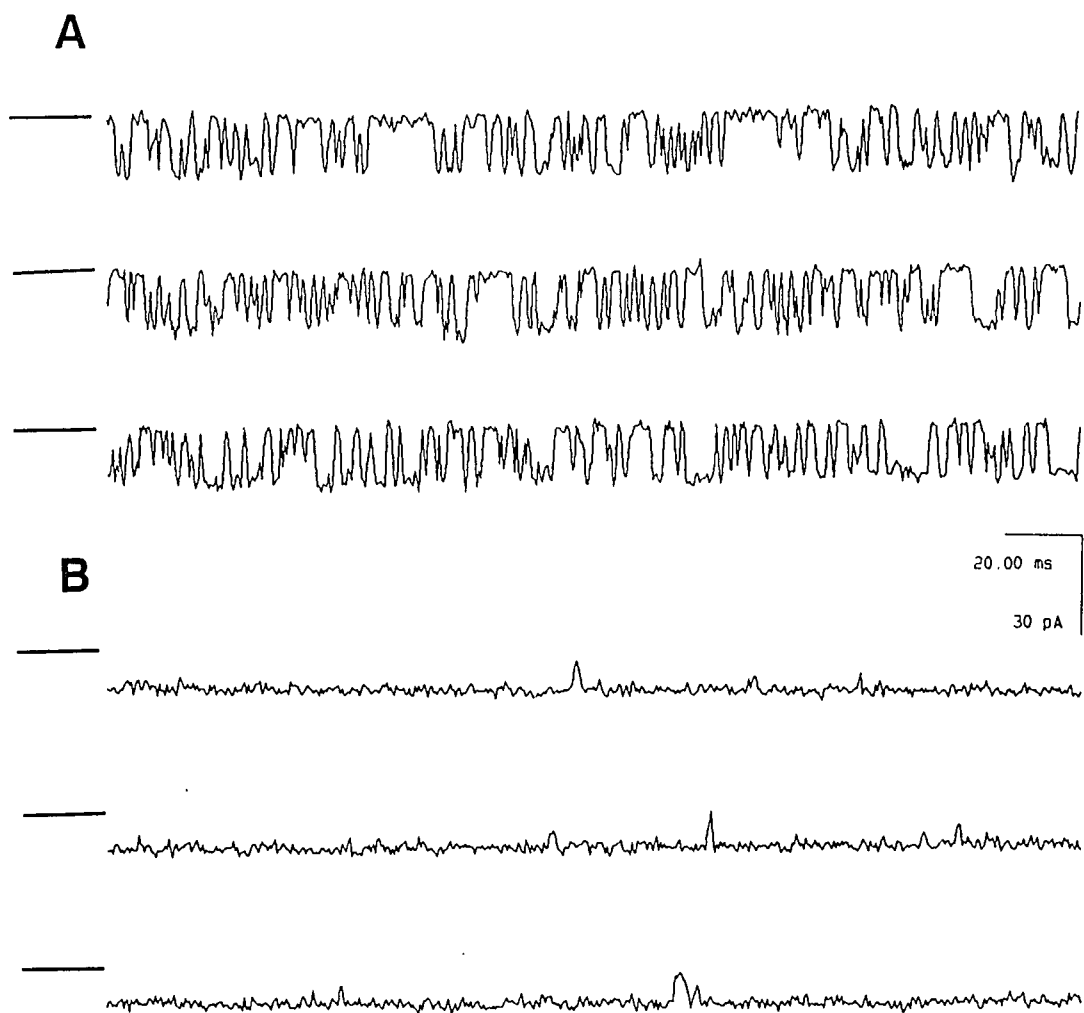


**Figure 13.** Ryanodine modification of the reconstituted 106 kDa channel. Recordings were made in 250 mM symmetrical NaCl solution. (A) Control trace,  $P_0 = 33\%$ . (B) After addition of 20 nM of ryanodine to both chambers. HP = -40 mV.  $\gamma = 420$  pS. The bars indicate the closed state of the channel. (n=4)

TABLE IV

THE PROPERTIES OF THE NATIVE SR  $\text{Ca}^{2+}$  RELEASE CHANNEL, THE 106 KDA CHANNEL, AND THE 400 KDA CHANNEL IN THE STANDARD ASYMMETRICAL  $\text{Ca}^{2+}$  SOLUTION

	Native channel	106 kDa channel	400 kDa channel
Unitary conductance (pS)	100 $\pm$ 4	107 $\pm$ 13	110 $\pm$ 10
Reversal potential (mV)	30	-27 $\pm$ 7 <sup>a</sup>	38
Permeability ratio ( $P_{\text{Ca}}/P_{\text{Tris}}$ )	8.7	7.4	14

<sup>a</sup>The sign convention is the opposite of that of the other entries shown.

on the basis of its selectivity for divalent cations, activation by adenine nucleotides and inhibition by ruthenium red. The SR  $\text{Ca}^{2+}$  channel was further distinguished from other SR channels by its high unit conductance and by the fact that it does not inactivate (Smith et al., 1986).

To establish the identity of the 106 kDa protein, reconstitution experiments of the isolated protein were carried out with the identical solutions. The protein was found to conduct  $\text{Ca}^{2+}$  current, and the unit conductance was 107  $\pm$  13 pS. The current-voltage curve gave a reversal potential of -27  $\pm$  7 mV. Using an expression derived from constant field electrodiffusion theory (Shamoo and Goldstein, 1977; Lee and Tsien, 1984; see appendix), which considers both divalent and monovalent cation permeability, the permeability ratio of  $\text{Ca}^{2+}$  to  $\text{Tris}^+$  ( $P_{\text{Ca}}/P_{\text{Tris}}$ ) was found to be 7.4  $\pm$  3.3. The result demonstrates an agreement between the 106 kDa channel and the native SR  $\text{Ca}^{2+}$  channel. The purified 400 kDa

protein also showed a similar conductance in the same solution (Smith et al., 1988).

The 106 kDa channel demonstrates large unit conductance for monovalent cations in a solution containing low  $\text{Ca}^{2+}$  concentrations ( $[\text{Ca}^{2+}] < 0.5 \text{ mM}$ ) and a high  $\text{Na}^+$  concentration (250 mM). This may reflect the fact that the SR  $\text{Ca}^{2+}$  release channel is a large pore, which has a much larger unit conductance than  $\text{Ca}^{2+}$  channels found in cell surface membranes. It would be difficult for such a large pore to differentiate between monovalent cations and  $\text{Ca}^{2+}$  ions. However, this high monovalent cation permeability should not pose problems for the channel under physiological conditions, since in the resting muscle cell, there is only a  $\text{Ca}^{2+}$  gradient across the SR membrane. No monovalent cation or anion gradient exists across the SR. Smith et al. (1988) showed a high monovalent cation permeability of the 400 kDa protein. They also showed that in symmetrical 150 mM KCl solution, the addition of 5 mM  $\text{Ca}^{2+}$  to the luminal side resulted in a 60% reduction of single channel conductance. This implied that there is a competition between  $\text{K}^+$  and  $\text{Ca}^{2+}$  for binding sites inside the 400 kDa channel pore.

Both the 106 kDa channel and the native  $\text{Ca}^{2+}$  channel show a voltage asymmetry in the channel open probability. This may reflect structural aspects of the release protein. Although the voltage sensitivity of the release channel is unlikely to play a role in EC coupling, it may, however, play a role in



the release process. It was reported that the 400 kDa protein has a similar voltage dependence at pH 7.15, but not at pH 7.4 (Ma et al., 1988).

The polycationic dye, ruthenium red is the most effective inhibitor of the  $\text{Ca}^{2+}$  release channel (Smith et al., 1985). At micromolar concentrations, it completely blocks the  $\text{Ca}^{2+}$  release channel. To establish the identity of the purified 106kDa protein, ruthenium red was also tested. Addition of 5-20  $\mu\text{M}$  ruthenium red completely closed the 106 kDa release channel. Furthermore, millimolar ATP activates the reconstituted 106 kDa channel by increasing the channel open probability.

Ryanodine exerts its effect on the native release channel by increasing the open probability and locking the channel into a subconducting open state (Rosseau and Meissner, 1987). Ryanodine had a similar effect on the purified 106 kDa release channel. Ryanodine (2-20 nM) changed the kinetics of the 106 kDa channel from a rapid fluctuating full conductance state to a open long-lifetime subconducting state. The effect could be reversed by rose bengal (see chapter V). There was no inactivation of the channel at ryanodine concentrations ranging from 10 nM to 20  $\mu\text{M}$ .

The purified protein was isolated in the presence of detergent and is in a different lipid environment than that of the native protein. It is not surprising that the properties of the purified 106 kDa are slightly different than channels

observed following fusion of SR vesicles to bilayer. Unlike the native channel, the 106 kDa protein is not sensitive to  $\text{Ca}^{2+}$  activation. Another very noticeable and frequently observed phenomenon upon the incorporation of the 106kDa protein is the appearance of multiple subconducting levels after an apparent single incorporation event. The characteristic unitary conductance of the native channel may result from simultaneous activation of several coupled sublevels present within one or more 106 kDa protein. In the case of the purified 400 kDa protein, half and quarter subconducting states were also reported (Lui et al., 1989). Combined with the electron microscopic study (Lai et al., 1988), it was concluded that the 400 kDa channel is a tetramer composed of four 400 kDa proteins.

An important issue raised by this work is the relationship between the 400 kDa ryanodine receptor complex and the 106 kDa sulfhydryl activated protein. Despite the lack of cross-reactivity between anti-106 antibodies and the 400 kDa protein, the 106 kDa protein still may be a fragment of the 400 kDa ryanodine receptor complex. The SR membrane also may have more than one  $\text{Ca}^{2+}$  release channel. Important questions remain regarding the role of the 106 kDa  $\text{Ca}^{2+}$  release channel protein. Efforts to clone and sequence the cDNA of the 106 kDa protein should enable us to determine if the 106kDa protein is a distinctly different protein than the 400 kDa foot protein.

## CHAPTER IV

### SILVER MODIFICATION OF THE SR CALCIUM RELEASE CHANNEL

#### SUMMARY

In this chapter, the effect of  $\text{Ag}^+$  on the activity of the reconstituted SR  $\text{Ca}^{2+}$  release channel from skeletal muscle was examined. Experiments were performed by using the vesicle fusion technique in a 5:1 CsCl gradient. The results showed that  $\text{Ag}^+$  ( $0.2\text{--}1.0\ \mu\text{M}$ ) activated the SR  $\text{Ca}^{2+}$  release channel. The activation by  $\text{Ag}^+$  did not require the presence of  $\text{Ca}^{2+}$ ,  $\text{Mg}^{2+}$ , or ATP.  $\text{Ag}^+$  activated the channel activity by increasing the open probability  $P_0$ . The  $\text{Ag}^+$  activation was always followed (about 10-40 seconds after activation) by a spontaneous inactivation. The channel was still sensitive to ruthenium red after exposure to  $\text{Ag}^+$ . These modifications of channel gating were also observed when  $\text{Ag}^+$  is added to the trans chamber (the luminal face of the SR). At high  $\text{Ag}^+$  concentration ( $>7\ \mu\text{M}$ ), large increases in current were observed which could only be partially inhibited by ruthenium red.  $\text{Ag}^+$  also stimulated the channel activity of the reconstituted 106 kDa protein. However, no spontaneous inactivation was observed with this purified protein.

## INTRODUCTION

The involvement of sulfhydryl groups in  $\text{Ca}^{2+}$  release from the SR was first reported in 1983 by Abramson et al. Various heavy metals cause rapid  $\text{Ca}^{2+}$  release from SR vesicles isolated from rabbit skeletal muscle. The addition of micromolar concentrations of heavy metal (e.g.,  $\text{Hg}^{2+}$ ,  $\text{Ag}^+$ ,  $\text{Cu}^{2+}$ , and  $\text{Cd}^{2+}$ ) to SR vesicles passively loaded with  $^{45}\text{Ca}^{2+}$  or actively loaded in the presence of ATP, produces a sudden increase in  $\text{Ca}^{2+}$  permeability of the SR membranes and an almost complete efflux of releasable  $\text{Ca}^{2+}$  accumulated inside the SR vesicles. At such low concentrations, heavy metals do not inhibit the ATPase activity of the SR nor do they lyse the SR. The potency of these heavy metals to induce  $\text{Ca}^{2+}$  release from SR is similar to their relative binding affinities to sulfhydryl groups. This indicates the possible involvement of sulfhydryl groups in the  $\text{Ca}^{2+}$  release mechanism.

To determine whether heavy metal-induced  $\text{Ca}^{2+}$  release is a specific interaction with the  $\text{Ca}^{2+}$  release protein or a nonspecific interaction with other components of the SR membrane, the action of  $\text{Ag}^+$ , as a sulfhydryl reagent, on isolated SR vesicles was investigated in detail (Salama and Abramson, 1984). Known inhibitors of  $\text{Ca}^{2+}$  release such as ruthenium red (micromolar), tetracaine (submillimolar), procaine (millimolar) and  $\text{Mg}^{2+}$  ( $>1$  mM) were shown to inhibit  $\text{Ag}^+$  induced  $\text{Ca}^{2+}$  release. Adenine-containing nucleotides, which had been shown to stimulate  $\text{Ca}^{2+}$  release in a  $\text{Ca}^{2+}$ -

dependent manner, were also found to stimulate  $\text{Ag}^+$  induced  $\text{Ca}^{2+}$  release. The rates of release were substantially greater (5-6 times) in SR vesicles derived from the terminal cisternae region (HSR) than in those derived from the longitudinal region (LSR). The maximum rate of efflux was observed under physiological conditions, at pH 7.0, and at 1 mM  $\text{Mg}^{2+}$ .  $\text{Ag}^+$  also caused the rapid dissociation of [ $^3\text{H}$ ]ryanodine from isolated SR vesicles (Pessah et al., 1987). The data strongly suggested that  $\text{Ag}^+$  acts at the  $\text{Ca}^{2+}$  release protein which appears to be the physiological site for  $\text{Ca}^{2+}$  release in SR. As shown in Chapter III, these studies led to the investigation the effect of sulfhydryl oxidation on the SR  $\text{Ca}^{2+}$  release channel and finally the isolation of the 106 kDa  $\text{Ca}^{2+}$  release channel.

Since  $\text{Ag}^+$  is able to induce rapid  $\text{Ca}^{2+}$  release, it is a useful probe of structure and function of the  $\text{Ca}^{2+}$  release channel. Dr. Cronin did more detailed efflux measurements and showed that the rate of  $\text{Ag}^+$  induced  $\text{Ca}^{2+}$  release was multiphasic (Figure 14). At low  $[\text{Ag}^+]$  ( $[\text{Ag}^+] < 10 \mu\text{M}$ ), rapid  $\text{Ca}^{2+}$  release was completely inhibited by ruthenium red. At slightly higher  $[\text{Ag}^+]$  ( $10 \mu\text{M} < [\text{Ag}^+] < 20 \mu\text{M}$ ),  $\text{Ag}^+$  induced  $\text{Ca}^{2+}$  release rates were greatly diminished. While at high  $[\text{Ag}^+]$  ( $[\text{Ag}^+] > 20 \mu\text{M}$ ),  $\text{Ca}^{2+}$  release rates were further stimulated, but were only partially inhibited by ruthenium red.

To understand  $\text{Ag}^+$  activation at the single channel level,  $\text{Ag}^+$  regulation of the gating of the  $\text{Ca}^{2+}$  release channel was

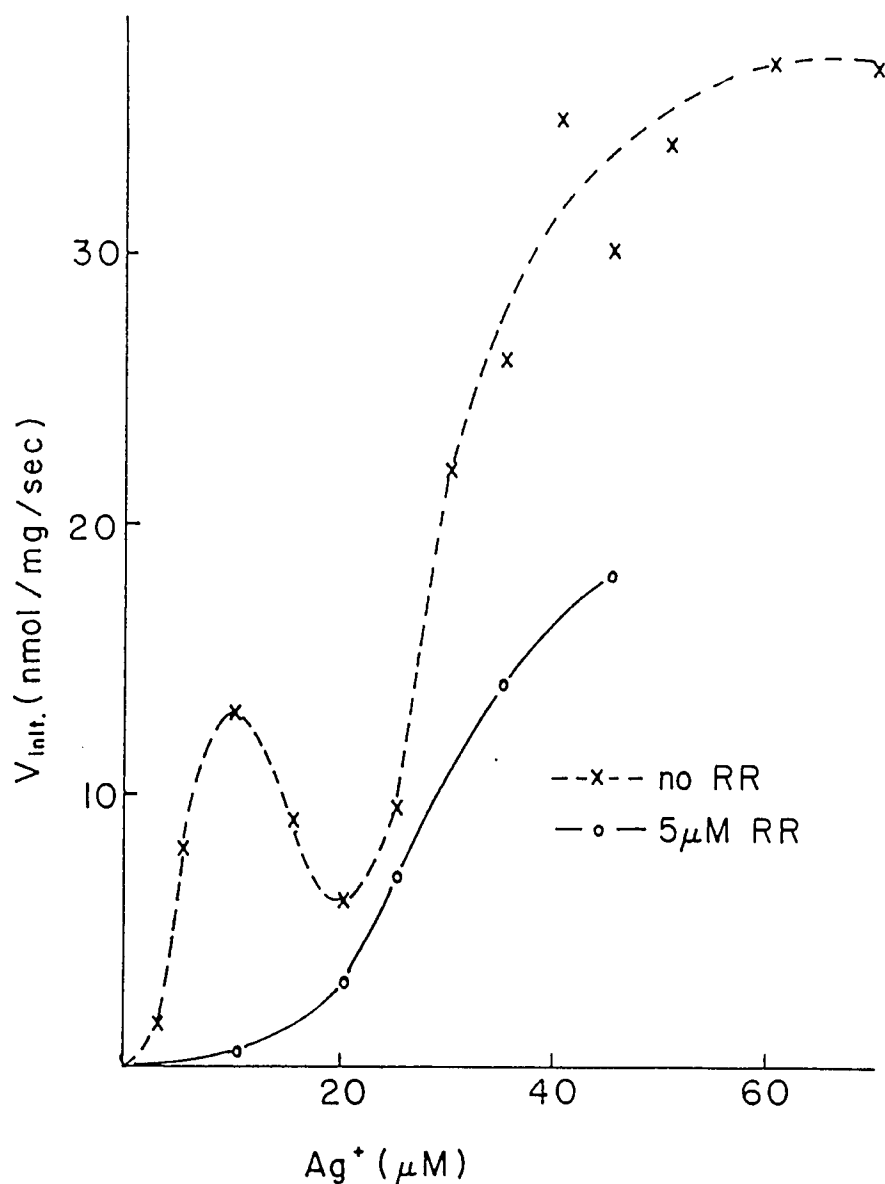


**Figure 14.**  $\text{Ag}^+$  dependence of  $\text{Ca}^{2+}$  release rate of isolated SR vesicles. Efflux measurements were carried out in 100 mM  $\text{KNO}_3$ , 20 mM HEPES, 5 mM  $\text{Mg}(\text{NO}_3)_2$ , pH 7.0. The  $\text{Ca}^{2+}$  was taken up by SR vesicles actively in the presence of 0.5 mM  $\text{Mg}^{2+}$ -ATP. After uptake was complete, either  $\text{AgNO}_3$  (x) or 5  $\mu\text{M}$  ruthenium red followed by  $\text{AgNO}_3$  (o) was added to initiate  $\text{Ca}^{2+}$  release. Extravesicular  $\text{Ca}^{2+}$  concentration was measured by a  $\text{Ca}^{2+}$  electrode. Estimation of the error for each point is  $\pm 10\%$ .

investigated with the reconstitution technique. Reconstitution of the native channels was performed in asymmetric 5:1 CsCl gradient with fused SR vesicles, and the purified 106 kDa channel was studied in a symmetric NaCl solution.

## RESULTS

Single channel recording technique was used to study the interaction of  $\text{Ag}^+$  and the SR  $\text{Ca}^{2+}$  release channel following fusion of SR vesicles to planar lipid bilayer membranes (phosphatidylethanolamine / phosphatidyl serine = 5:3). SR vesicles were added to the cis chamber of an asymmetric 5:1 CsCl gradient at a final concentration of 2-10  $\mu\text{g}/\text{ml}$ . The cis chamber contained 500 mM CsCl, 10 mM Tris-HEPES, 0.1 mM  $\text{CaCl}_2$ , 0.1 mM EGTA, pH 7.2; the trans chamber contained 100 mM CsCl, 10 mM Tris-HEPES, pH 7.2). Vesicle fusion was facilitated by addition of 0.35 mM  $\text{CaCl}_2$  to the cis chamber. A two fold excess of EGTA was added immediately after incorporation of a vesicle to the bilayer, and the solution in the cis chamber was perfused to prevent further fusion events.

Figure 15 shows a current-voltage curve of a typical native SR  $\text{Ca}^{2+}$  release channel in a 500 mM to 100 mM CsCl gradient. It reveals a single channel conductance of  $511 \pm 24$  pS and a reversal potential of  $-32 \pm 10$  mV, from which the permeability ratio ( $P_{\text{Cs}}/P_{\text{Cl}}$ ) is calculated as 11. As expected, the channels incorporated into bilayers by fusion of SR

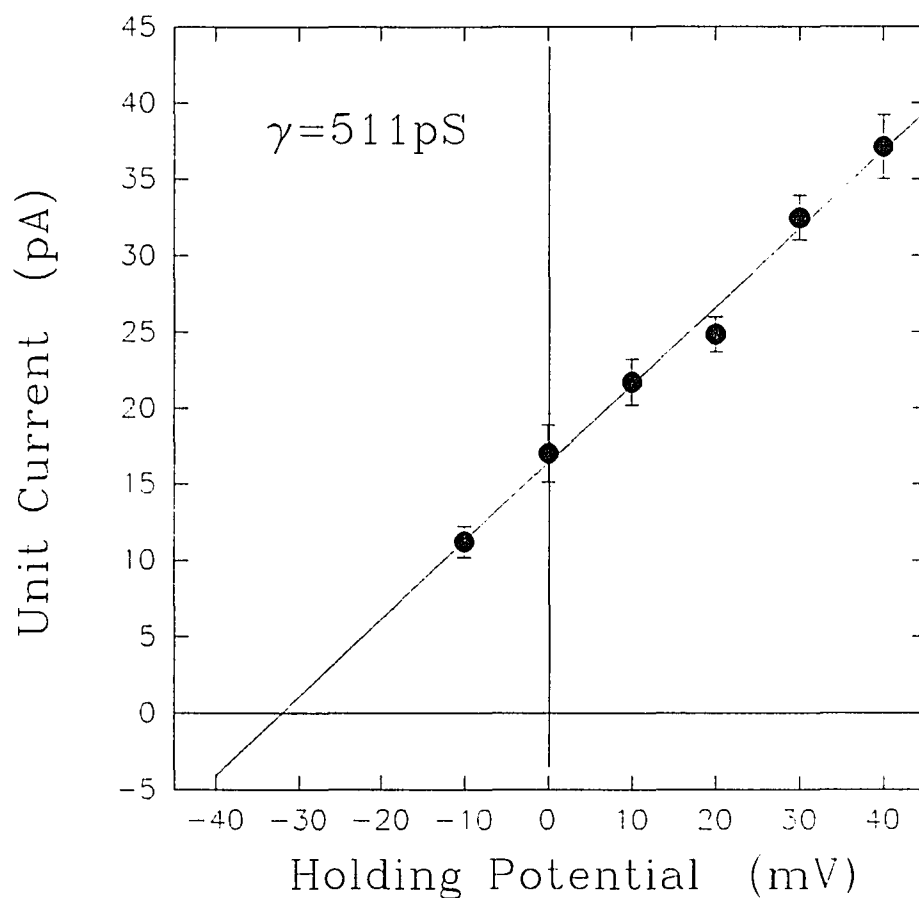


**Figure 15.** The current-voltage curve of a typical native SR  $\text{Ca}^{2+}$  channel in a 500 mM to 100 mM CsCl gradient. The data represents three independent experiments. The best fit gives single channel conductance of  $511 \pm 24$  pS, and reversal potential of  $-32 \pm 10$  mV which results in a permeability ratio of  $\text{Cs}^+$  to  $\text{Cl}^-$  of 11.



vesicles in a CsCl gradient were activated by  $\text{Ca}^{2+}$  (Figure 19b), ATP (Figure 17b), and inhibited by  $\text{Mg}^{2+}$  (Figure 16b). This method of reconstituting the native SR  $\text{Ca}^{2+}$  release channel in 5:1 CsCl gradient proved to be efficient.

Once active channels are incorporated into bilayers routinely, subsequent investigation of channel behavior can be carried out. Figure 16a shows a typical current trace of  $\text{Cs}^+$  transport through SR  $\text{Ca}^{2+}$  release channel in the presence of 5  $\mu\text{M}$  cis (the myoplasmic face of the SR)  $\text{CaCl}_2$ . The addition of 1 mM  $\text{MgCl}_2$  to the cis chamber (Figure 16b) decreased the open probability of the channel ( $P_0$ ), and the subsequent addition of 1 mM of ATP stimulated the channel activity (Figure 16c). This is the optimal condition for  $\text{Ag}^+$  to induce rapid  $\text{Ca}^{2+}$  release from isolated SR vesicles. Addition of 0.7  $\mu\text{M}$   $\text{Ag}^+$  to the cis chamber of the bilayer increased channel activity (Figure 16d).  $\text{Ag}^+$  affects the  $\text{Ca}^{2+}$  release channel of SR membrane by increasing its open probability without changing the single channel conductance. It is also concluded that the  $\text{Cl}^-$  conductance was not sensitive to  $\text{Ag}^+$  based on the fact that the background current is not affected by  $\text{Ag}^+$  (Figure 16). At submicromolar concentration,  $\text{Ag}^+$  increased the permeability of SR membrane by directly activating the  $\text{Ca}^{2+}$  release channel. One distinct feature of  $\text{Ag}^+$  modification was that the activation was transient (10-40 seconds). As demonstrated in Figure 16e, the  $\text{Ag}^+$  activation of the channel was followed by a spontaneous inactivation of

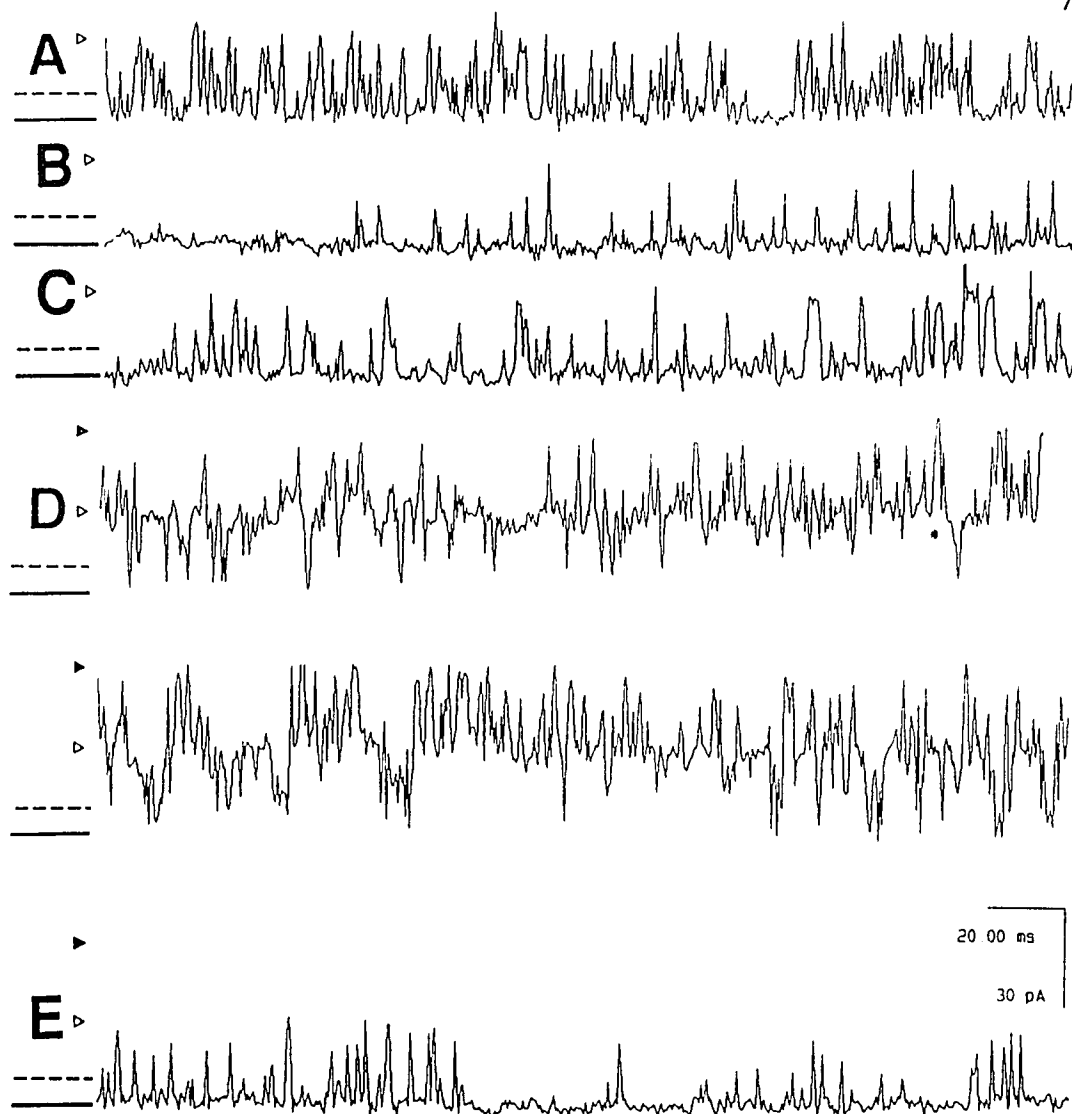


**Figure 16.**  $\text{Ag}^+$  modification of a native SR  $\text{Ca}^{2+}$  release channel under physiological conditions. Single channel current was recorded in 5:1 CsCl gradient after fusion of a SR vesicle with two channels to a bilayer. (A)  $[\text{Ca}^{2+}]_{\text{cis}} = 5 \mu\text{M}$ . (B) After addition of 1.0 mM of  $\text{Mg}^{2+}$  to the cis chamber. (C) 1.0 mM of ATP was added to the cis chamber. (D)  $0.7 \mu\text{M}$  of  $\text{Ag}^+$  was added to the cis side of the channel. (E) 20 seconds after  $\text{Ag}^+$  activation. HP = +20 mV. The dash lines indicate zero. The bars indicate the closed state of the channel. The open triangles indicate the current level of one open channel and the filled triangles indicate the current level when two channels open at the same time. (n=2)

the channel. This inactivation phase of the  $\text{Ag}^+$  effect was observed in all the experiments, and was independent of the SR preparation and experimental conditions (as shown later).

The  $\text{Ag}^+$  modification of the SR  $\text{Ca}^{2+}$  release channel also occurred in the absence of  $\text{MgCl}_2$ . The channel activity (Figure 17a,  $[\text{Ca}^{2+}]_{\text{cis}} = 5 \mu\text{M}$ ) was increased by the addition of 1 mM ATP to the cis chamber (Figure 17b). The channel activity was increased further by the addition of  $0.7 \mu\text{M}$   $\text{Ag}^+$  to the cis chamber (Figure 17c). Spontaneous inactivation was evident following the  $\text{Ag}^+$  activation. The long time scale is chosen to show the inactivation phase.

$\text{Ag}^+$  activation of the SR  $\text{Ca}^{2+}$  release channel was observed at low myoplasmic  $\text{Ca}^{2+}$  concentration. Figure 18a shows a current trace after vesicle-bilayer fusion in the presence of 160 nM free  $\text{Ca}^{2+}$ . The channel was opened by the addition of  $0.5 \mu\text{M}$   $\text{Ag}^+$  to cis chamber (Figure 18b), and then inactivated spontaneously (Figure 18c).

The SR  $\text{Ca}^{2+}$  release channel is still sensitive to ruthenium red after the interaction with  $\text{Ag}^+$ . Figure 19 shows a native SR  $\text{Ca}^{2+}$  release channel in 5:1 CsCl gradient with  $5 \mu\text{M}$  free  $\text{Ca}^{2+}$  in the cis chamber. It was activated by  $50 \mu\text{M}$  myoplasmic  $\text{Ca}^{2+}$  (Figure 19b), inhibited by 1 mM  $\text{Mg}^{2+}$  (Figure 19c), and activated by  $0.4 \mu\text{M}$   $\text{Ag}^+$  added to the cis chamber (Figure 19d). After the spontaneous deactivation (Figure 19e),  $6 \mu\text{M}$  ruthenium red added to the cis chamber completely inhibited the channel. Following a similar

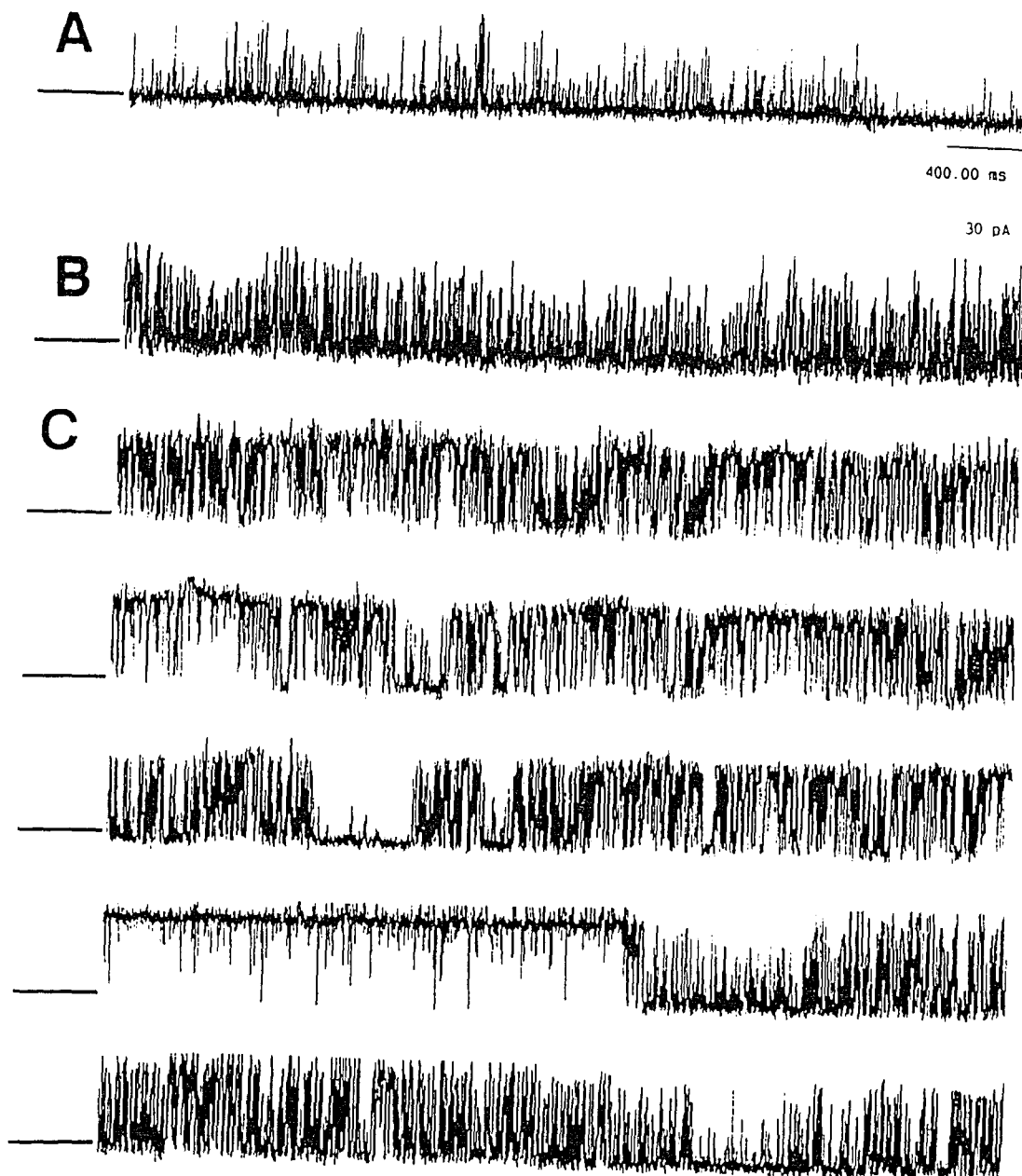


**Figure 17.**  $\text{Ag}^+$  modification of the SR  $\text{Ca}^{2+}$  channel in the absence of  $\text{MgCl}_2$ . (A)  $[\text{Ca}^{2+}]_{\text{cis}} = 5 \mu\text{M}$  (0.1 mM  $\text{CaCl}_2$ , 0.1 mM EGTA),  $P_0 = 2\%$ . (B) 1.0 mM of ATP was added to the cis chamber,  $P_0 = 16\%$ . (C) 0.7  $\mu\text{M}$  of  $\text{Ag}^+$  was added to the cis chamber,  $P_0 = 74\%$  (before inactivation). Activation lasted about 20 seconds. Long time scale is used in order to show the inactivation. HP = +20 mV. The bars indicate the closed state of the channel. (n=2)

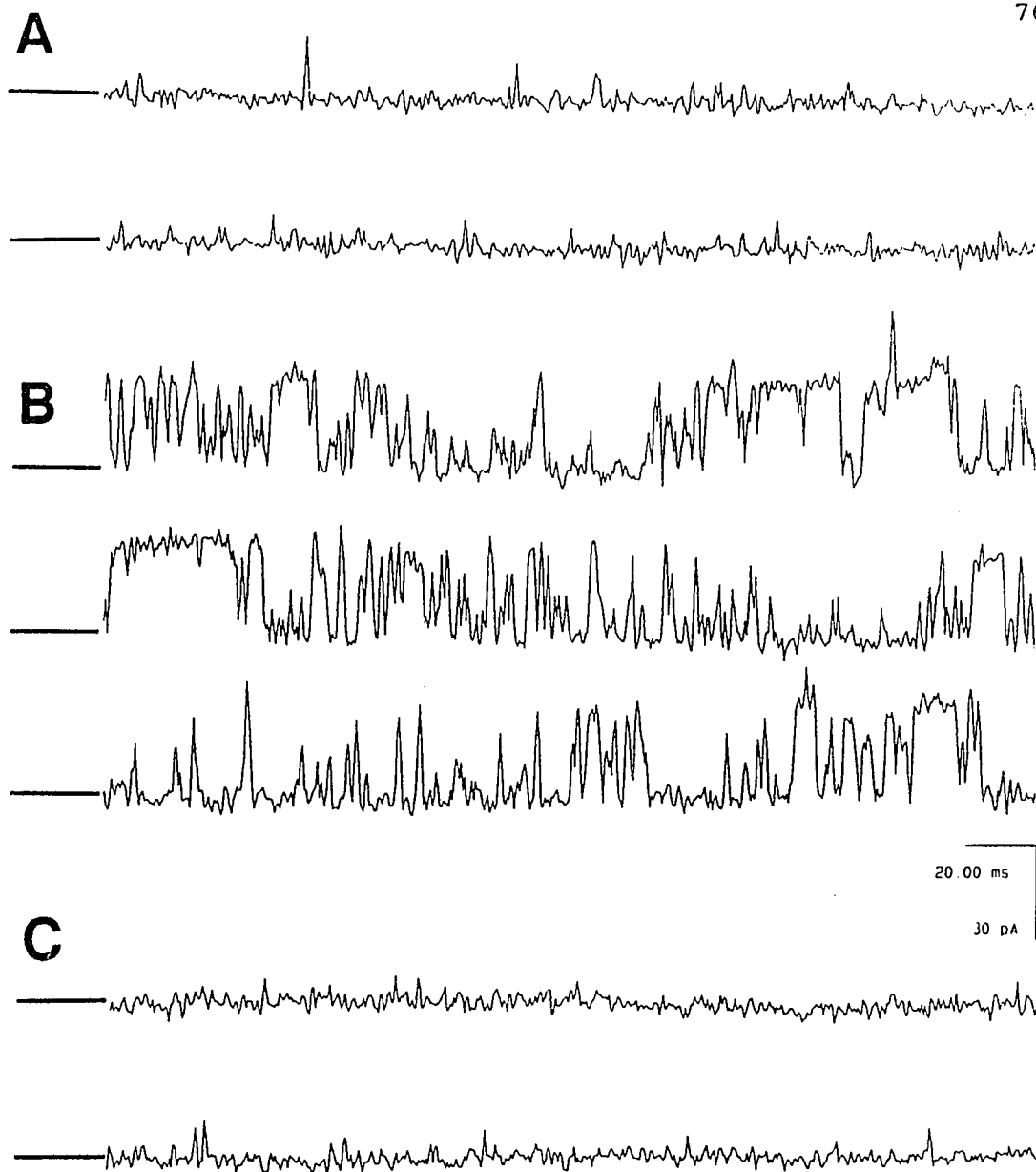


**Figure 18.**  $\text{Ag}^+$  modification of SR  $\text{Ca}^{2+}$  release channel at a low  $\text{Ca}^{2+}$  concentration. Following fusion of a SR vesicle to the bilayer with  $0.35 \text{ mM}$   $\text{cis CaCl}_2$ , a two fold excess of EGTA was added to the cis chamber to prevent further fusion events and to achieve low  $\text{Ca}^{2+}$  concentration. (A)  $[\text{Ca}^{2+}]_{\text{cis}} = 160 \text{ nM}$  ( $0.35 \text{ mM CaCl}_2$ ,  $0.70 \text{ mM EGTA}$ ),  $P_0 = 1\%$ . (B) After addition of  $0.5 \mu\text{M}$   $\text{Ag}^+$  to the cis chamber,  $P_0 = 34\%$ . (C) Spontaneous inactivation followed the  $\text{Ag}^+$  activation (10 seconds),  $P_0 = 1\%$ . The bars indicate the closed state of the channel.  $\text{HP} = +30 \text{ mV}$ . ( $n=4$ )

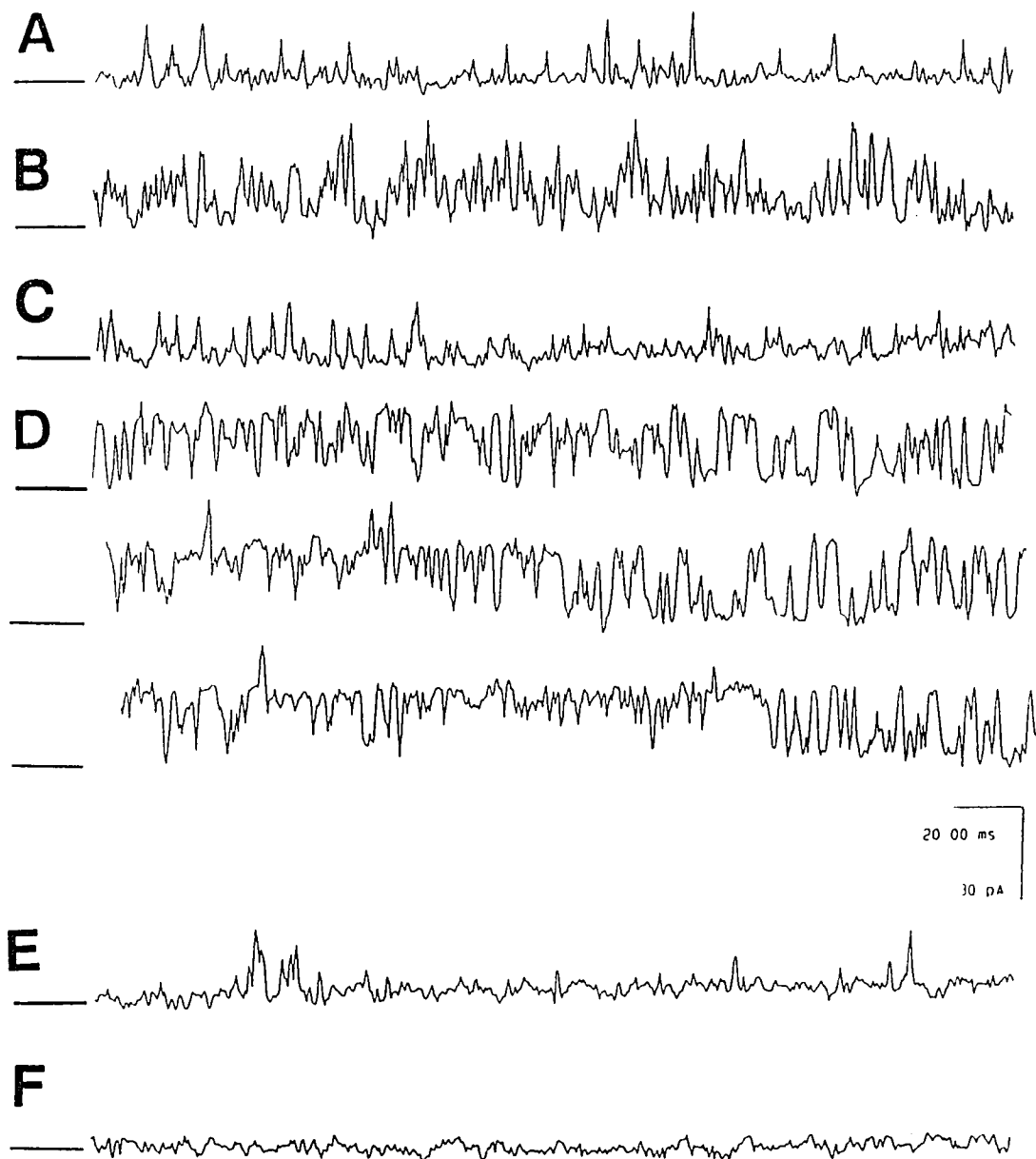


**Figure 19.** Ruthenium red inhibition of the SR Ca<sup>2+</sup> channel after Ag<sup>+</sup> modification. (A) [Ca<sup>2+</sup>]<sub>cis</sub> = 5 μM (0.1 mM CaCl<sub>2</sub>, 0.1 mM EGTA), P<sub>0</sub> = 11%. (B) After the addition of 50 μM of Ca<sup>2+</sup> to the cis chamber, P<sub>0</sub> = 23%. (C) 1.0 mM of MgCl<sub>2</sub> was added to the cis chamber, P<sub>0</sub> = 9%. (D) 0.4 μM of Ag<sup>+</sup> was added to the cis chamber, P<sub>0</sub> = 78%. (E) Spontaneous inactivation followed the Ag<sup>+</sup> activation (40 seconds), P<sub>0</sub> = 6%. (F) After cis addition of 6 μM ruthenium red, P<sub>0</sub> = 0%. The bars indicate the closed state of the channel. HP = +20 mV. (n=4)

protocol, except adding the  $0.4 \mu\text{M}$   $\text{Ag}^+$  to the trans chamber, Figure 20 shows that the  $\text{Ag}^+$  is equally effective from luminal face of the SR.

As demonstrated in Figure 21, high concentration of  $\text{Ag}^+$  ( $7 \mu\text{M}$ ) causes a large change of membrane permeability. The mean current over a given period of time is partially inhibited by ruthenium red.

The action of  $\text{Ag}^+$  on the purified 106 kDa protein was also investigated. Purified 106 kDa protein was added to both sides of a bilayer in a symmetric NaCl buffer ( $250 \text{ mM}$ ,  $[\text{Ca}^{2+}]_{\text{free}} = 100 \mu\text{M}$ ) at a final concentration of  $50\text{--}500 \text{ ng/ml}$ . As shown in Figure 22, the activity of the reconstituted 106 kDa protein is activated by addition of  $0.6 \mu\text{M}$   $\text{Ag}^+$  to both side of bilayer (Figure 22b). No spontaneous inactivation was observed.

## DISCUSSION

Heavy metals such as  $\text{Ag}^+$  and  $\text{Hg}^{2+}$  have been reported to increase the  $\text{Ca}^{2+}$  permeability of isolated SR vesicles. The increase of  $\text{Ca}^{2+}$  permeability was suggested to be caused by the inhibition of the SR  $\text{Ca}^{2+}$  pump molecules (Shamoo and MacLennan, 1975; Gould et al., 1987). However, other studies presented evidence that heavy metals inducing  $\text{Ca}^{2+}$  release by acting on the SR  $\text{Ca}^{2+}$  release pathway (Salama and Abramson, 1984; Palade, 1987; and Tatsumi et al., 1988). This issue can only be resolved indirectly with isolated vesicle system. The

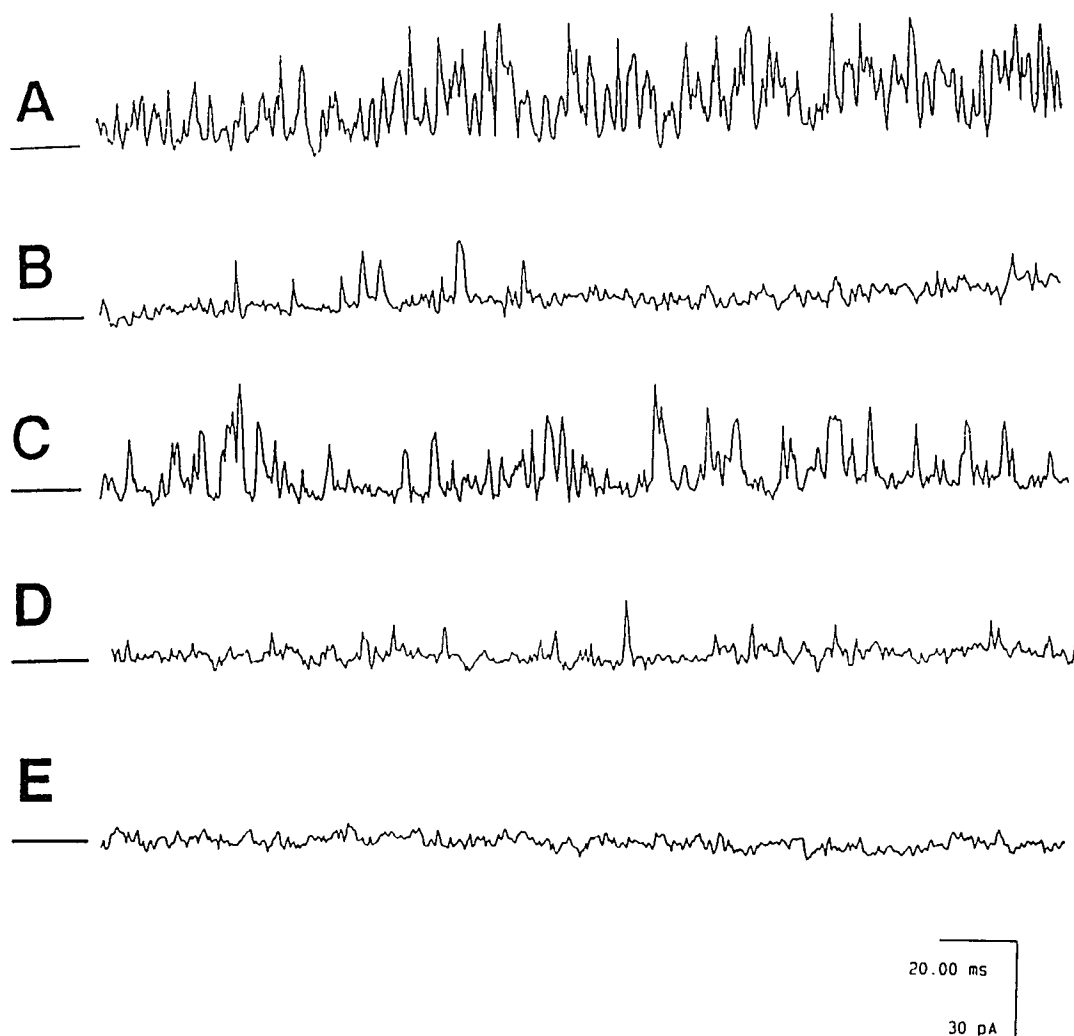


**Figure 20.**  $\text{Ag}^+$  modification of the  $\text{Ca}^{2+}$  channel from the luminal face of the SR. (A)  $[\text{Ca}^{2+}]_{\text{cis}} = 50 \mu\text{M}$ ,  $P_0 = 45\%$ . (B) 1.0 mM of  $\text{MgCl}_2$  was added to the cis chamber,  $P_0 = 1\%$ . (C)  $0.4 \mu\text{M}$  of  $\text{Ag}^+$  was added to the trans chamber,  $P_0 = 23\%$ . (D) Spontaneous inactivation followed the  $\text{Ag}^+$  activation (10 seconds),  $P_0 = 3\%$ . (E) After cis addition of  $6 \mu\text{M}$  ruthenium red,  $P_0 = 0\%$ . The bars indicate the closed state of the channel. HP = +25 mV. (n=2)



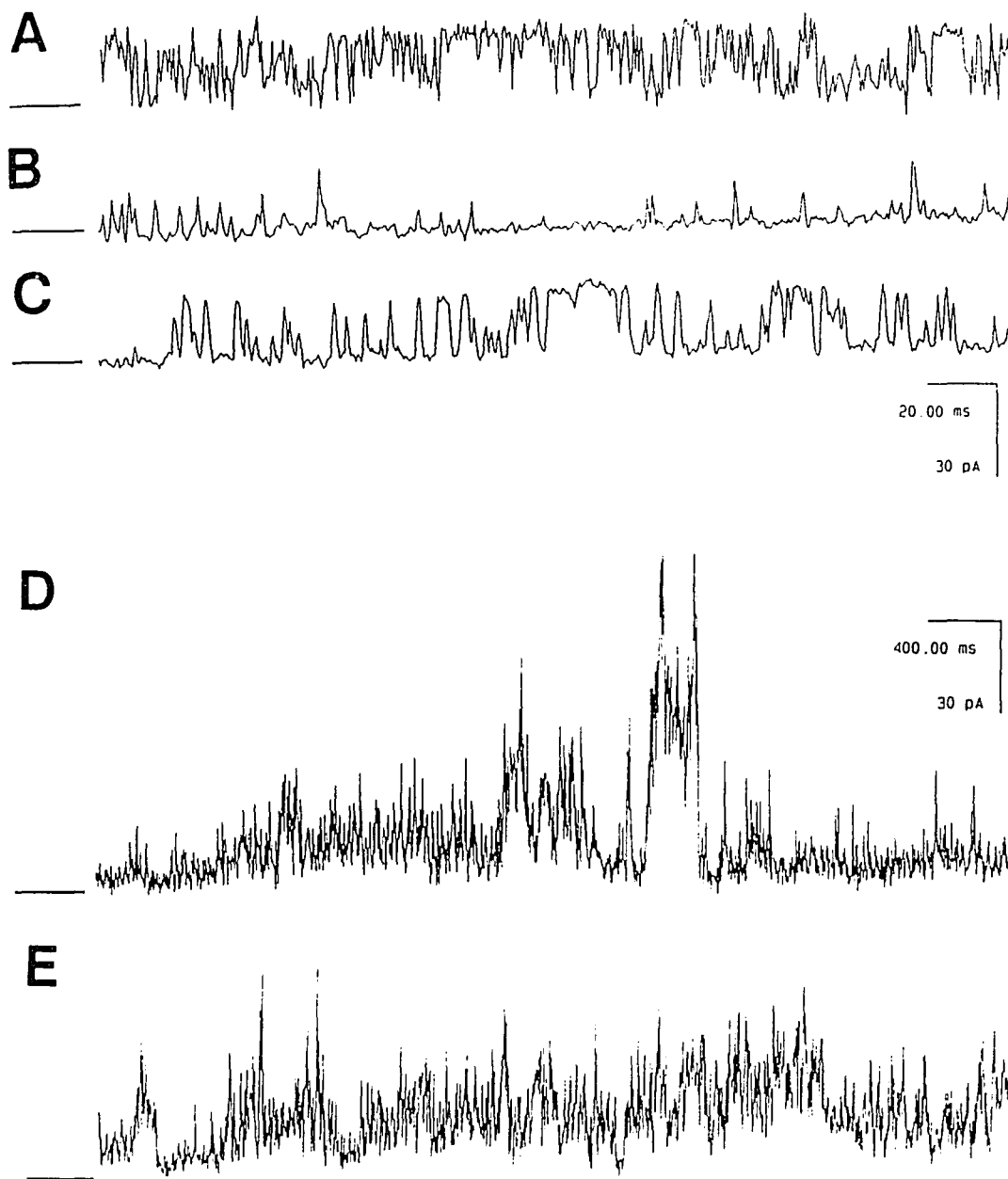


**Figure 21.** The effect of high concentration of  $\text{Ag}^+$  on the SR  $\text{Ca}^{2+}$  channel. (A)  $[\text{Ca}^{2+}]_{\text{cis}} = 50 \mu\text{M}$ ,  $P_0 = 82\%$ . (B) 1.0 mM of  $\text{MgCl}_2$  was added to the cis chamber,  $P_0 = 4\%$ . (C) 0.6  $\mu\text{M}$  of  $\text{Ag}^+$  was added to the cis chamber,  $P_0 = 23\%$ . (D) Subsequently 7  $\mu\text{M}$   $\text{Ag}^+$  was added to the cis chamber. (E) After cis addition of 6  $\mu\text{M}$  ruthenium red. The bars indicate the closed state of the channel. HP = +20 mV. (n=5)

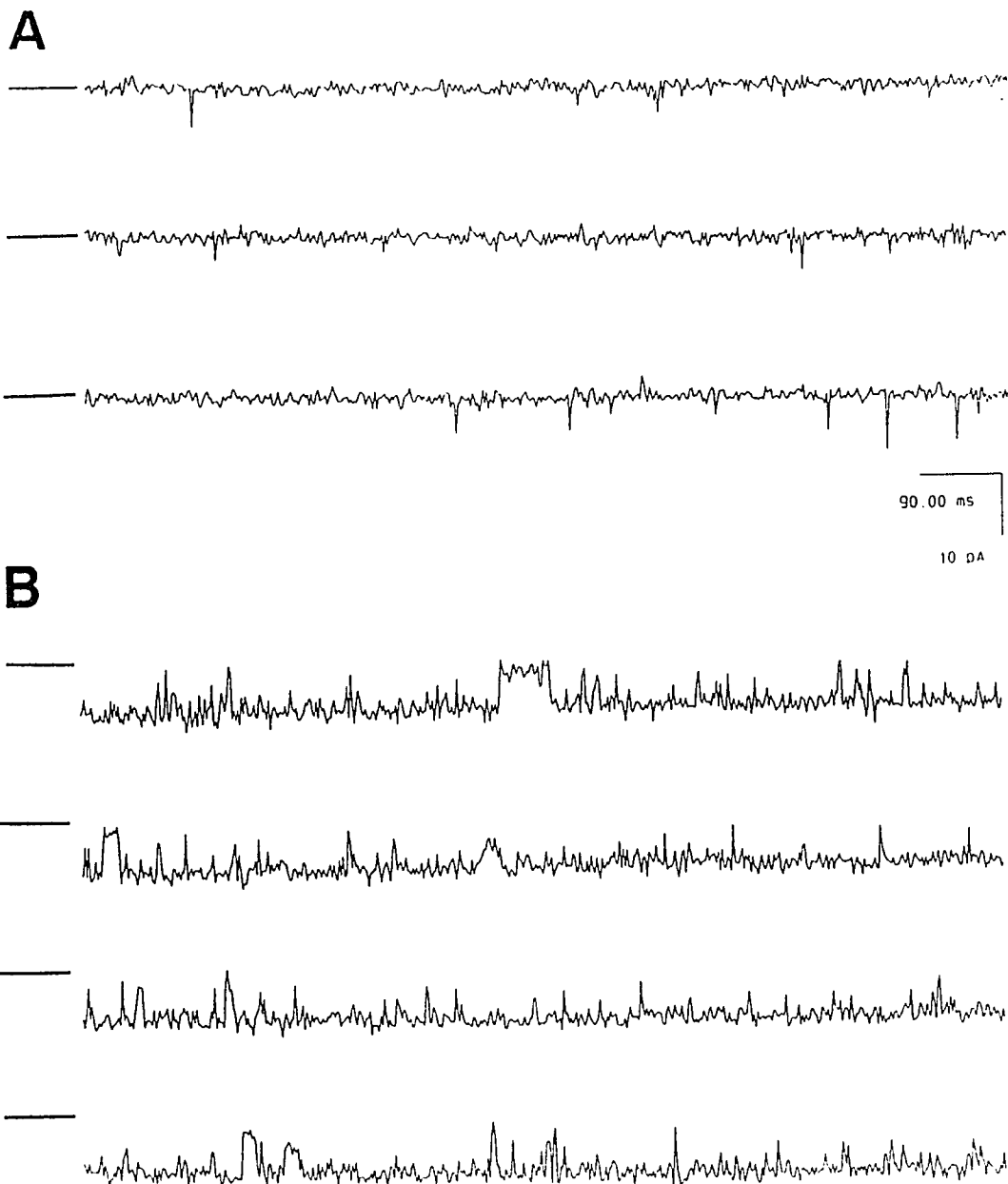


**Figure 22.** The effect of  $\text{Ag}^+$  on the purified 106 kDa SR  $\text{Ca}^{2+}$  release channel. Purified 106 kDa protein was incorporated to a bilayer in symmetric 250 mM NaCl buffer. (A) Current fluctuation in the presence of  $1 \mu\text{M}$   $\text{Ca}^{2+}$ ,  $P_0 = 1\%$ . (B) After the addition of  $0.6 \mu\text{M}$   $\text{Ag}^+$  to both sides of the channel,  $P_0 = 88\%$ . HP = -20 mV. (n=3)

general approach is to examine the distribution of  $\text{Ca}^{2+}$  release activity among different SR fraction (i.e. LSR and HSR), and to assess the ability of known SR  $\text{Ca}^{2+}$  channel modulators to modulate the release. Evidences strongly imply that  $\text{Ag}^+$  induces  $\text{Ca}^{2+}$  release by interacting directly with the  $\text{Ca}^{2+}$  release channel of SR.

The development of the single channel recording technique provides an excellent method to directly study drug action on channel activities. Using the CsCl gradient procedure described in Chapter II, active  $\text{Ca}^{2+}$  channels can be observed and characterized easily. The channels are activated by submillimolar  $\text{Ca}^{2+}$ , millimolar ATP, and inhibited by millimolar  $\text{Mg}^{2+}$ , and micromolar ruthenium red. The current-voltage curve reveals a single channel conductance of  $511 \pm 24$  pS and a reversal potential of  $-32$  mV ( $P_{\text{Cs}}/P_{\text{Cl}} = 11$ ). The effect of  $\text{Ag}^+$  on the SR  $\text{Ca}^{2+}$  release channel in the lipid bilayer was investigated. The results of this chapter clearly demonstrate the direct modulation of the SR  $\text{Ca}^{2+}$  release channel by  $\text{Ag}^+$  and explain the SR  $\text{Ca}^{2+}$  permeability increase observed in the SR vesicles experiments.  $\text{Ag}^+$  apparently did not affect the SR  $\text{Cl}^-$  channel.

The SR  $\text{Ca}^{2+}$  release channel is modified by low concentrations of  $\text{Ag}^+$  at physiological condition, and also in the absence of ATP or  $\text{Mg}^{2+}$ .  $\text{Ag}^+$  modification is equally effective from either side of the channel. There are two possible explanations for this observation. While binding

sites for  $\text{Ag}^+$  may exist at both sides of the channel, it is likely that the  $\text{Ag}^+$  ions can cross the bilayer through the  $\text{Ca}^{2+}$  channel itself to reach the binding sites from either side of the membrane.

Tatsumi et al. (1988) studied the  $\text{Ag}^+$  effect on isolated SR vesicles at different myoplasmic  $\text{Ca}^{2+}$  concentration. They reported that  $\text{Ag}^+$  only stimulated  $\text{Ca}^{2+}$  induced  $\text{Ca}^{2+}$  release and had no effect beyond the CICR range ( $[\text{Ca}^{2+}] = 1 \mu\text{M}$  to  $1 \text{ mM}$ ). Their results would predict that  $\text{Ag}^+$  binds to a site only available when  $\text{Ca}^{2+}$  is bound, and  $\text{Ag}^+$  increases the open probability of an channel already partially activated by  $\text{Ca}^{2+}$ . However, Moutin et al. (1989) suggest that  $\text{Ag}^+$  is more effective at stimulating  $\text{Ca}^{2+}$  release at low  $\text{Ca}^{2+}$  concentrations. The results presented in this Chapter indicate that  $\text{Ag}^+$  is also able to activate a channel at low  $\text{Ca}^{2+}$  concentration.

While it is difficult to generate a reproducible dose-response curve with a bilayer system, my results at different  $\text{Ag}^+$  concentrations do qualitatively agree with the results of vesicle flux experiments. At low concentration ( $< 1 \mu\text{M}$ ),  $\text{Ag}^+$  increases the permeability of SR by activating the  $\text{Ca}^{2+}$  release channel. At high concentration ( $> 5 \mu\text{M}$ ),  $\text{Ag}^+$  induces large current through bilayers and no discrete channels can be easily resolved. The current is only partially inhibited by ruthenium red. This indicates that at high concentrations  $\text{Ag}^+$  may not specifically interact with the  $\text{Ca}^{2+}$  release channel.

One of the advantages to study single channel behavior is its high time resolution. It allows us to observe the behavior of individual channels and resolve events according to the sequence in which they occur. In efflux measurements with the isolated SR vesicle system, at intermediate  $\text{Ag}^+$  concentrations, below that of causing the nonspecific interaction and above that needed to cause rapid specific  $\text{Ca}^{2+}$  release, a slower release rate was observed (Figure 14). Brunder et al (1988) made the same observation and suggested that  $\text{Ag}^+$  binds to a second activation site with a lower affinity to  $\text{Ag}^+$ . When  $\text{Ag}^+$  interacts with SR following fusion to a bilayer, a spontaneous inactivation was observed following  $\text{Ag}^+$  activation at all  $\text{Ag}^+$  concentration tested. Even at high  $\text{Ag}^+$  concentration that causing nonspecific interaction partial inactivation was always evident. Generally,  $\text{Ag}^+$  activation lasted between a few seconds to half a minute before the inactivation occurred. The fact that the inactivation was not complete and occasional gating was further inhibited by ruthenium red indicates that the inactivation was not due to denaturation of the channel. One possible interpretation of this observation is that  $\text{Ag}^+$  binds to an inhibitory site of the channel which has lower affinity to  $\text{Ag}^+$ . Thus, the spontaneous inactivation seen with  $\text{Ag}^+$  is likely due to a specific reaction between  $\text{Ag}^+$  and an endogenous SH which closes the channel. This hypothesis

readily explains the action of intermediate concentrations of  $\text{Ag}^+$  on isolated SR vesicles.

Any agent that causes  $\text{Ca}^{2+}$  release from SR could in principle yield some clues about the nature of EC coupling.  $\text{Ag}^+$  induces rapid  $\text{Ca}^{2+}$  release from isolated heavy SR vesicles, and causes contracture in skinned muscle fibers (Aoki et al., 1986; Pike et al., 1987).  $\text{Ag}^+$  is the most potent of a number of  $\text{Ca}^{2+}$ -releasing drugs (Palade, 1987). Even though  $\text{Ag}^+$  is not a physiological trigger for  $\text{Ca}^{2+}$  release from SR, the SHs to which  $\text{Ag}^+$  binds, can be oxidized, and open the  $\text{Ca}^{2+}$  release channel. It is possibly the physiological target site for opening the release channel. A large number of proteins contain SH groups that undergo oxidation-reduction reactions on a millisecond time scale (Williams, 1976). The  $\text{Ca}^{2+}$  permeability of human platelets (Adunyah and Dean, 1986), insulinoma cells (Erlichman et al., 1979), and liver microsomes (Thor et al., 1985) have all been shown to be regulated by SH interactions. SH group oxidation-reduction may play a general role in controlling the state of many membrane-bound transport proteins. Trimm et al. (1986) showed that oxidation induced  $\text{Ca}^{2+}$  release from SR vesicles (stimulated by  $\text{Cu}^{2+}$ /cysteine) could be reversed by addition of the reducing agent DTT. It is believed that DTT closed the  $\text{Ca}^{2+}$  channel by reducing the disulfide bond between cysteine and the endogenous critical SH group. Brunde et al (1988) showed that both reducing agents glutathione (GSH) and DTT

prevented the rapid  $\text{Ca}^{2+}$  release induced by  $\text{Ag}^+$  ( $1\ \mu\text{M}$ ) on HSR, while neither of the agents had an effect on  $\text{Ca}^{2+}$  release induced by caffeine, alkalization or  $\text{Cl}^-$ . They also showed that GSH and DTT at millimolar concentration prevented contracture of skinned muscle fibers. In an effort to study the physiological relevance of this observation and to evaluate the role of sulfhydryl oxidation in EC coupling, the voltage clamped cut frog skeletal muscle fibers were used to test whether depolarization fail to cause  $\text{Ca}^{2+}$  release from SR in the presence of DTT and GSH. The results was ambiguous, although it was interpreted that SH oxidation may not interfere with physiological SR  $\text{Ca}^{2+}$  release. Clearly, more careful studies need to be done regarding to the intriguing role of sulfhydryl oxidation in EC coupling.

The single channel data of this chapter shows that  $\text{Ag}^+$  interacts directly with the SR  $\text{Ca}^{2+}$  release channel of skeletal muscle.  $\text{Ag}^+$  activates the channel by increasing the open probability. The spontaneous inactivation caused by  $\text{Ag}^+$  is likely due to the binding of  $\text{Ag}^+$  to an endogenous SH group which closes the channel.

## CHAPTER V

### PHOTOOXIDATION OF THE SR CALCIUM RELEASE CHANNEL

#### SUMMARY

In this chapter, the effect of photooxidation of rose bengal on the gating characteristics of the reconstituted  $\text{Ca}^{2+}$  release channel from skeletal muscle SR is examined. To study the native SR channel, a series of experiments were performed by using the vesicle fusion technique in a 5:1 CsCl gradient. The results showed that rose bengal activated the  $\text{Ca}^{2+}$  release channel in the presence of light. The photooxidation of the channel increased the channel open probability and left the single channel conductance unchanged. This photoactivation was independent of the myoplasmic  $\text{Ca}^{2+}$  concentration, and could be achieved from either side of the membrane. In addition, the effect was inhibited by addition of 10-20  $\mu\text{M}$  ruthenium red. If the  $\text{Ca}^{2+}$  release channel was in its subconducting state induced by ryanodine, subsequent addition of rose bengal reactivated the channel to its rapidly fluctuating full conducting state. Rose bengal also stimulated the channel activity of the reconstituted 106 kDa protein. Furthermore, rose bengal could reverse the modification of the 106 kDa protein by ryanodine.



## INTRODUCTION

The lethal effect of light and oxygen on microbes in the presence of certain dyes was discovered at the turn of the century. This effect, termed photodynamic action, was later shown to result from the sensitized photooxidation of certain amino acid residues in protein molecules. The dyes act as photosensitizers in these reactions. Photosensitizers absorb light and produce chemical reactions which would not occur in their absence. A photosensitizer has two electronically excited states, the singlet and the triplet. The short-lived singlet state is the initial product of light absorption. It rapidly decays by fluorescence to the ground state or by electronic intersystem crossing to a long-lived triplet state. It is the triplet state of a photosensitizer that participates in photooxidation of protein molecules. The most effective sensitizers are therefore those that have a high quantum yield of a long-lived triplet state.

There are two major classes of reaction for the sensitizer triplet. In Type I, the sensitizer triplet state undergoes a chemical interaction with a substrate in the system. This reaction results in the formation of a free radical pair through electron or hydrogen atom transfer. Subsequently the radicals react with oxygen to form peroxy radicals or superoxide radicals. In Type II, the sensitizer triplet state transfers energy to oxygen ( $^3\text{O}_2$ ), resulting in the generation of excited singlet oxygen ( $^1\text{O}_2$ ). Photosensitized

oxidations of many biomolecules have been shown to involve the Type II pathway with the formation of singlet oxygen. High concentrations of sensitizer may switch the photooxidation process to a Type I pathway.

The xanthene dye rose bengal (Figure 23) is a well known photosensitizer, and has been used as a photosensitizer for  $^1\text{O}_2$  formation (reviewed by Neckers, 1987; 1989). In their study,

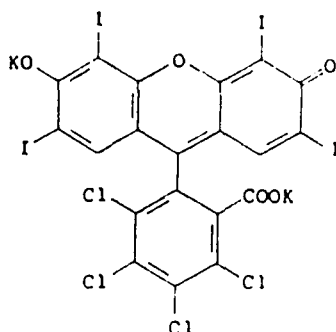


**Figure 23.** The structure of rose bengal as C-2', C-6 potassium salt. The maximum absorbance  $\lambda_{\text{max}}$  is 549.0 nm in  $\text{H}_2\text{O}$ , and the quantum yield of singlet oxygen formation in  $\text{H}_2\text{O}$  at  $20^\circ\text{C}$  is 0.75 (Neckers, 1989).

Lee and Rodgers (1987) showed that photooxidation of rose bengal in aqueous solution produces about 75%  $^1\text{O}_2$  and about 20% superoxide ( $\text{O}_2^-$ ). This study indicates the relative participation of each process in the photooxidation of rose bengal, with the Type II pathway as the dominant process. Photooxidation of rose bengal has been studied in some biological model systems. It was reported that photooxidation of SR vesicles with rose bengal resulted in inhibition of

$\text{Ca}^{2+}$ -ATPase activity and inhibition of active  $\text{Ca}^{2+}$  uptake (Yu et al., 1974). This photooxidation was proposed to involve either histidyl, or tryptophan residues (Kondo et al., 1974). Watson and Haynes (1982) reported an increase in passive  $\text{Ca}^{2+}$  permeability of SR vesicles photosensitized by rose bengal and suggested functional damage to  $\text{Ca}^{2+}$  pumps.

Photooxidation, sensitized by rose bengal, increases the  $\text{Ca}^{2+}$  permeability of the SR vesicles. While previous work has focused on the  $\text{Ca}^{2+}$  pump, investigation in our laboratory indicates that the rapid increase of the  $\text{Ca}^{2+}$  permeability is primarily due to photooxidation of the  $\text{Ca}^{2+}$  release pathway (Stuart et al., 1991). At low concentration (10 nM to 1  $\mu\text{M}$ ), rose bengal causes rapid  $\text{Ca}^{2+}$  efflux from actively loaded SR vesicles when irradiated with a light source. At concentration of 5  $\mu\text{M}$  or greater, rose bengal causes  $\text{Ca}^{2+}$  release without direct irradiation (Figure 24). Rose bengal, at nanomolar concentrations, inhibits high affinity [ $^3\text{H}$ ]ryanodine binding to its receptor on the SR in a light dependent manner. At a rose bengal concentration of 0.1  $\mu\text{M}$ ,  $\text{Ca}^{2+}$ -ATPase activity is less than 50% inhibited after 1 minute of light exposure, yet all the  $\text{Ca}^{2+}$  has exited from the SR vesicles with less than 30 seconds of exposure. These evidence suggest the involvement the of SR  $\text{Ca}^{2+}$  release channel in the process of photooxidation.

The photooxidation site on the SR appears to be a histidyl residue (Stuart et al., 1991). This suggestion is

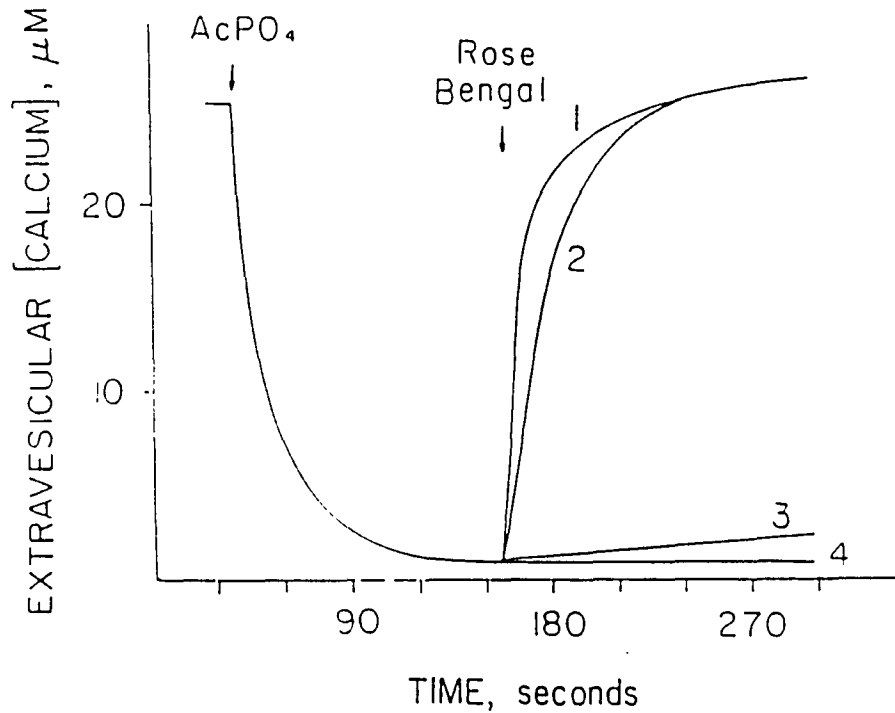


**Figure 24.** Rose bengal induced  $\text{Ca}^{2+}$  efflux from actively loaded SR vesicles. Efflux measurements were carried out in 100 mM KCl, 3 mM  $\text{MgCl}_2$ , 50 mM HEPES, pH 7.0. The  $\text{Ca}^{2+}$  was taken up in the presence of 2.0 mM  $\text{AcPO}_4$ . After accumulation of the added  $\text{Ca}^{2+}$ , efflux was initiated by the addition of (1) 5  $\mu\text{M}$  rose bengal in the dark, (2) 1  $\mu\text{M}$  rose bengal with irradiation from a 360 W light source, and (3) 1  $\mu\text{M}$  rose bengal in the dark. In (4), no reagent was added. Extravesicular  $\text{Ca}^{2+}$  concentration was monitored using a  $\text{Ca}^{2+}$  selective electrode.

supported by the observation that excess histidine in the reaction buffer decreases  $\text{Ca}^{2+}$  efflux rates induced by rose bengal by about 40%. Cysteine or lysine in the reaction buffer had no effect on the release rates. Also, when SR residues are photooxidized in the presence of rose bengal for 1 minute, a strong absorbance maximum appears at 250 nm which is attributed to the photooxidation of histidine. At longer illuminations times tryptophan residues are also modified. Since photooxidation induced  $\text{Ca}^{2+}$  efflux is essentially complete within 30 seconds, it is unlikely that the oxidation of the tryptophanyl residues is responsible for inducing rapid  $\text{Ca}^{2+}$  efflux. This is further supported by the observation that ethoxyformic anhydride (EFA), a known histidyl modifying reagent also is effective in inducing  $\text{Ca}^{2+}$  release from SR vesicles. Furthermore, EFA induced release responds to modulators of  $\text{Ca}^{2+}$  release in the same manner as that of rose bengal induced release. Therefore it is concluded that photooxidation target on the SR is likely to involve modification of histidyl residues.

While some data suggest the involvement of the  $\text{Ca}^{2+}$  release channel in the rose bengal sensitized photooxidation of the SR, rose bengal-induced  $\text{Ca}^{2+}$  release shows unexpected ligand sensitivity. Unlike  $\text{Ca}^{2+}$ -induced  $\text{Ca}^{2+}$  release or sulfhydryl oxidation-induced  $\text{Ca}^{2+}$  release, rose bengal-induced  $\text{Ca}^{2+}$  release is independent of  $\text{Ca}^{2+}$  or  $\text{Mg}^{2+}$ . It is inhibited by ATP, and only partially inhibited by ruthenium red.

Furthermore, HSR is only about 40% more sensitive to rose bengal than is LSR. The reconstituted  $\text{Ca}^{2+}$  release channel is an ideal system to verify that whether the channel is a target for rose bengal sensitized photooxidation. The effect of photooxidation was shown first on native SR  $\text{Ca}^{2+}$  channels, and then the study was carried further to the purified 106 kDa  $\text{Ca}^{2+}$  channel.

## RESULTS

The single channel recording technique was used to study the effect of photooxidation on the native SR  $\text{Ca}^{2+}$  release channel following fusion of SR vesicles to planar lipid bilayer membranes (phosphatidylethanolamine / phosphatidylserine = 5:3). SR vesicles were added to the cis chamber of an asymmetric 5:1 CsCl gradient at a final concentration of 2-10  $\mu\text{g}/\text{ml}$ . The cis chamber contained 500 mM CsCl, 10 mM Tris-HEPES, 0.1 mM  $\text{CaCl}_2$ , 0.1 mM EGTA, pH 7.2; the trans chamber contained 100 mM CsCl, 10 mM Tris-HEPES, pH 7.2. After addition of 0.35 mM  $\text{CaCl}_2$  to the cis chamber, and fusion of a SR vesicle, a two fold excess of EGTA was added, and the solution in the cis chamber was changed to prevent further fusion events. Figure 25a shows a typical current trace of  $\text{Cs}^+$  transport through a single SR  $\text{Ca}^{2+}$  channel ( $[\text{Ca}^{2+}]_{\text{free}}^{\text{cis}} = 5 \mu\text{M}$ ). As demonstrated in Figure 25b, addition of 0.5  $\mu\text{M}$  rose bengal in the presence of light increases the probability of finding the  $\text{Ca}^{2+}$  channel in its open state ( $P_0$ ). Subsequent

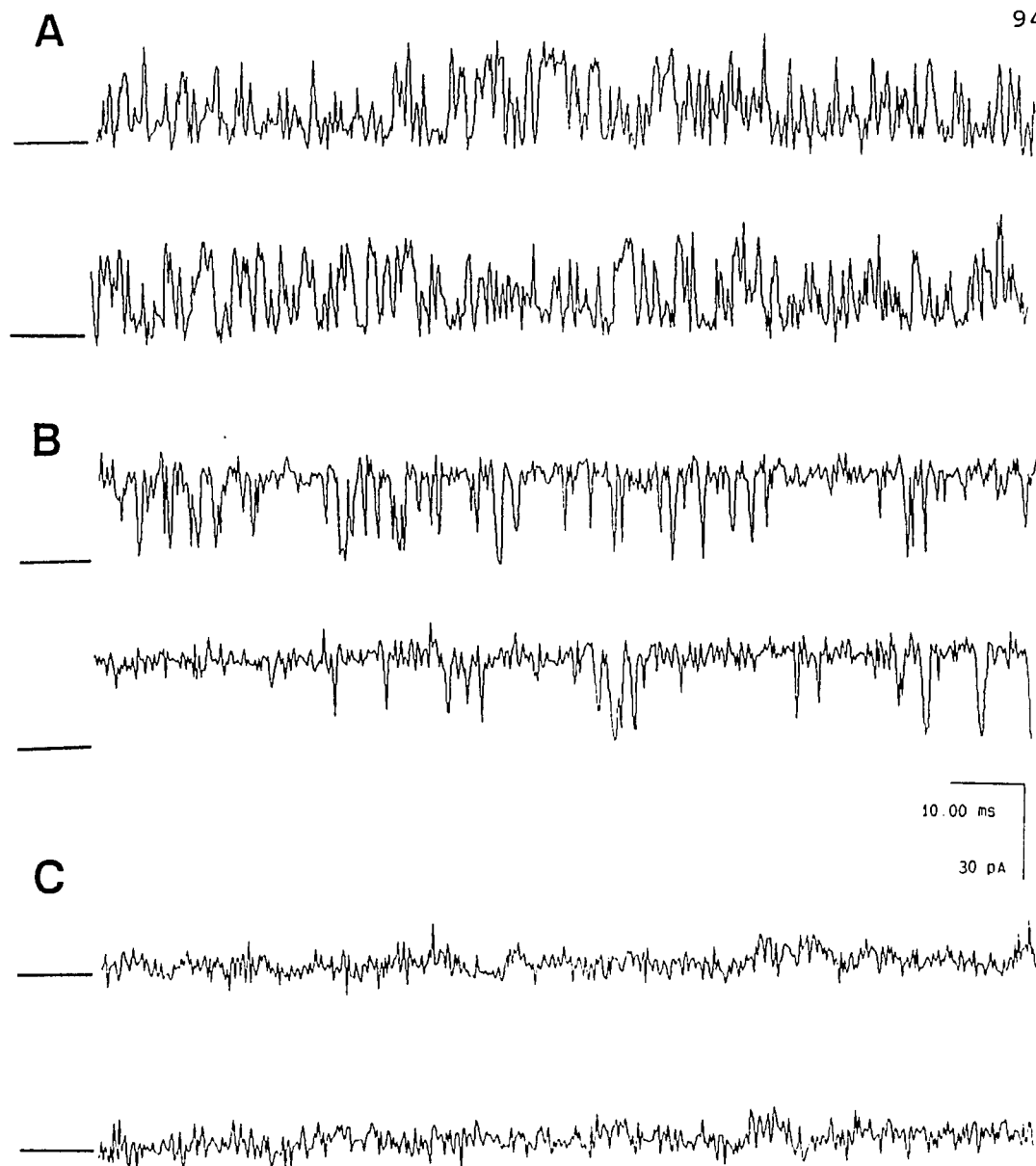


**Figure 25.** Rose bengal activation and ruthenium red inhibition of the SR  $\text{Ca}^{2+}$  release channel. Single channel current in 5:1 CsCl gradient after fusion of a SR vesicle to phospholipid bilayer. (A)  $[\text{Ca}^{2+}]_{\text{cis}} = 5 \mu\text{M}$  (0.1 mM  $\text{CaCl}_2$ , 0.1 mM EGTA),  $P_0 = 29\%$ . (B) Addition of  $0.5 \mu\text{M}$  of rose bengal to the cis chamber in the presence of light (8000 lux).  $P_0 = 88\%$ . (C) Addition of  $10 \mu\text{M}$  of ruthenium red to the cis chamber after the activation of rose bengal.  $P_0 = 2\%$ . Holding potential (HP) was +20 mV. The horizontal bars indicate the closed state of the channel. Number of independent bilayer experiments (n) is 5.

addition of 10  $\mu M$  ruthenium red to the cis chamber greatly inhibits the channel activity (Figure 25c).

Although the channel activity was stimulated by photooxidation, the single channel conductance ( $479 \pm 31$  pS) and the selectivity of the channel remains unaffected (Figure 26). The reversal potential of -33 mV yields a permeability ratio ( $P_{Cs}/P_{Cl}$ ) of 13. The relative abundance of  $Cl^-$  channels was found to vary among SR preparations. Most of the experiments described were carried out with SR preparations containing a relatively low number of  $Cl^-$  channels. The background current, including the  $Cl^-$  current, of the bilayer was not affected by photooxidation.

Figure 27 and 28 display the lifetime histogram for the recordings of channel activity from which the traces in figure 25 were taken. For the open lifetimes (Figure 27), the best fit was obtained with a single exponential. The fitting reveals open time constant (mean open lifetime) of  $1.1 \pm 0.1$  ms and  $7.3 \pm 0.8$  ms before and after photooxidation respectively. The analysis of the closed lifetime (Figure 28) reveals a time constant (mean closed time) of  $3.5 \pm 0.8$  ms for the control trace and  $0.82 \pm 0.04$  ms after addition of 0.5  $\mu M$  rose bengal and exposure to light. Thus, photooxidation causes the  $Ca^{2+}$  channel to stay open longer. The data was filtered at 1,500 Hz and digitalized at 4,000 Hz.

In a similar experiment to that shown in Figure 25, rose bengal was added in the darkness before exposure to light. As



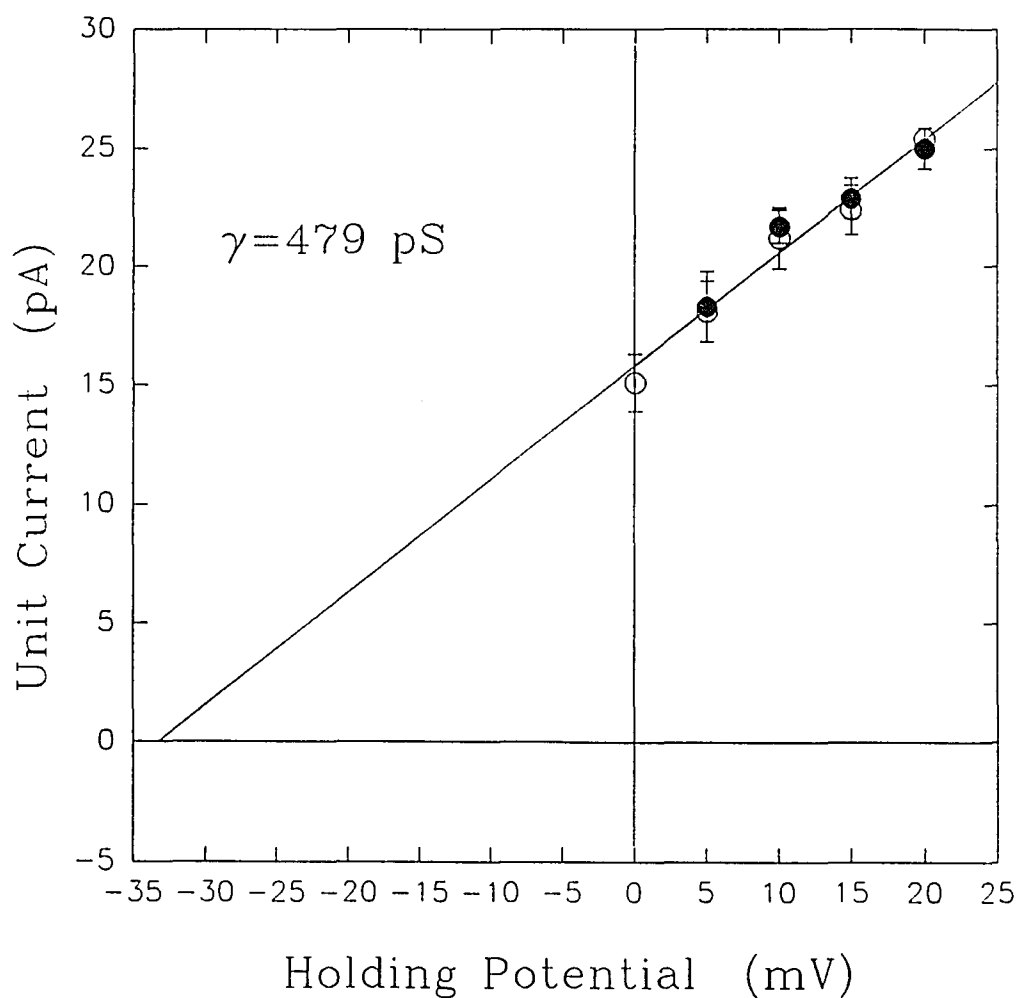


**Figure 26.** Current-voltage curve of a single  $\text{Ca}^{2+}$  channel in the absence and presence of  $0.5 \mu\text{M}$  rose bengal with illumination. The data are taken from the experiment showed in Figure 25. Current-voltage curve of a typical native  $\text{Ca}^{2+}$  release channel in the absence (o) and presence of rose bengal with illumination (●). The least-square fit of all points yields a slope of 479 pS, and an X interception of -33 mV.

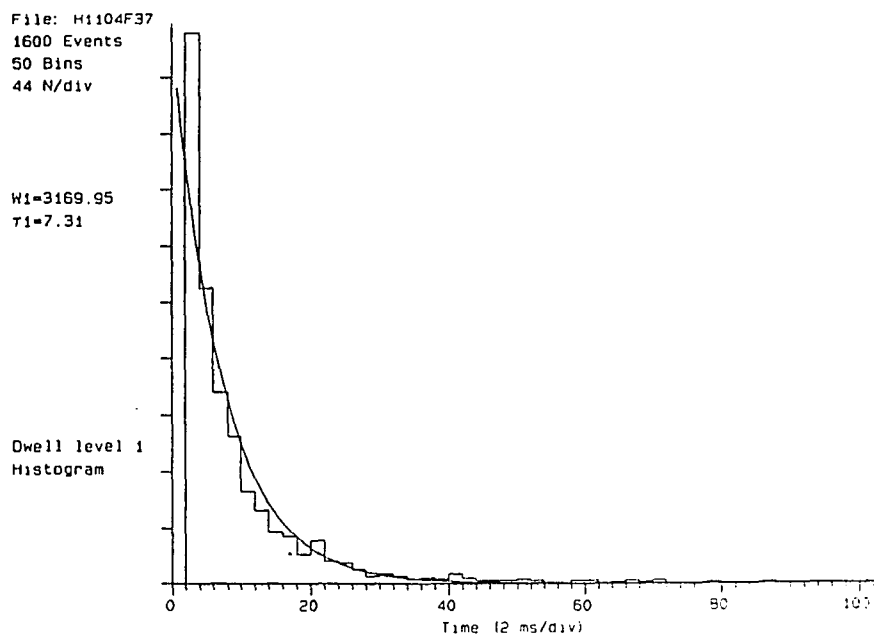
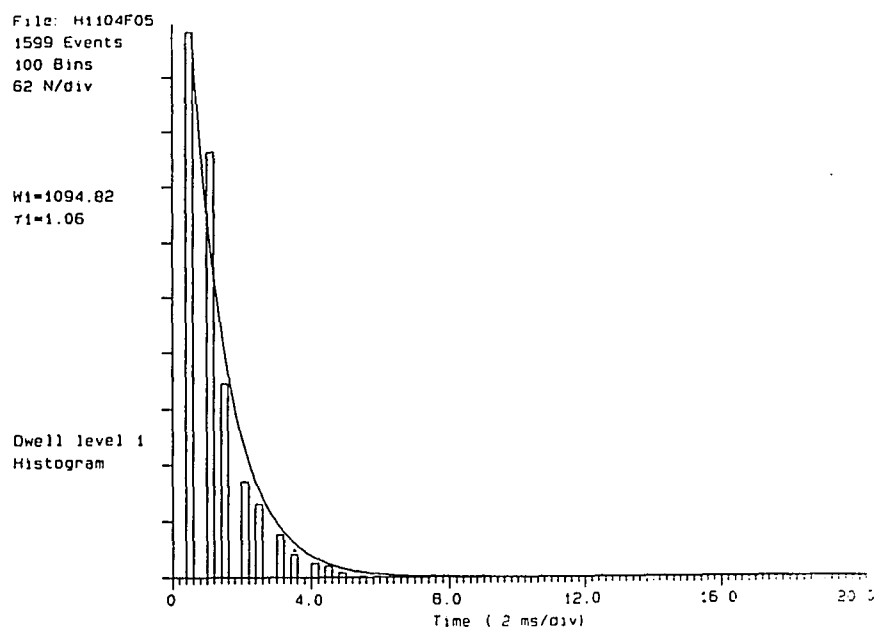
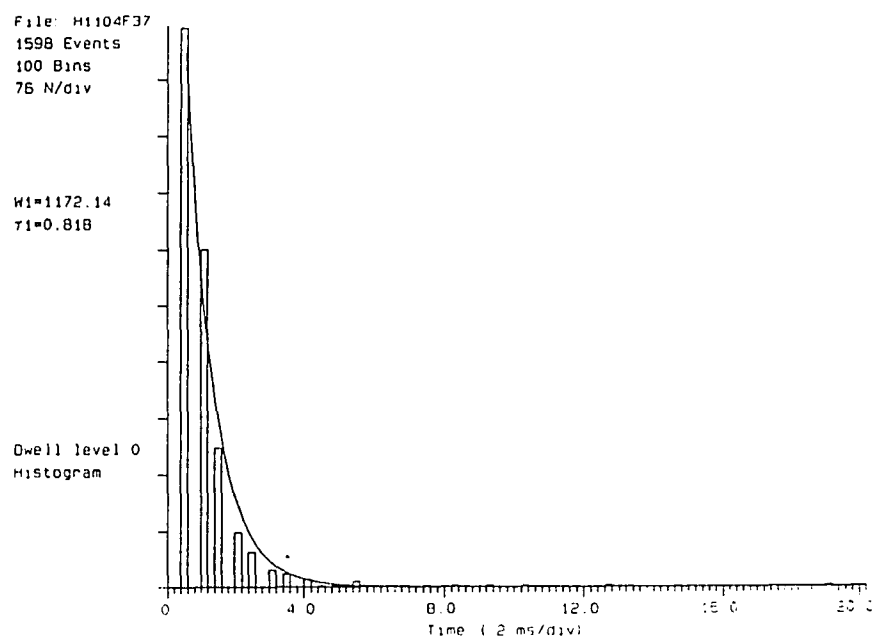
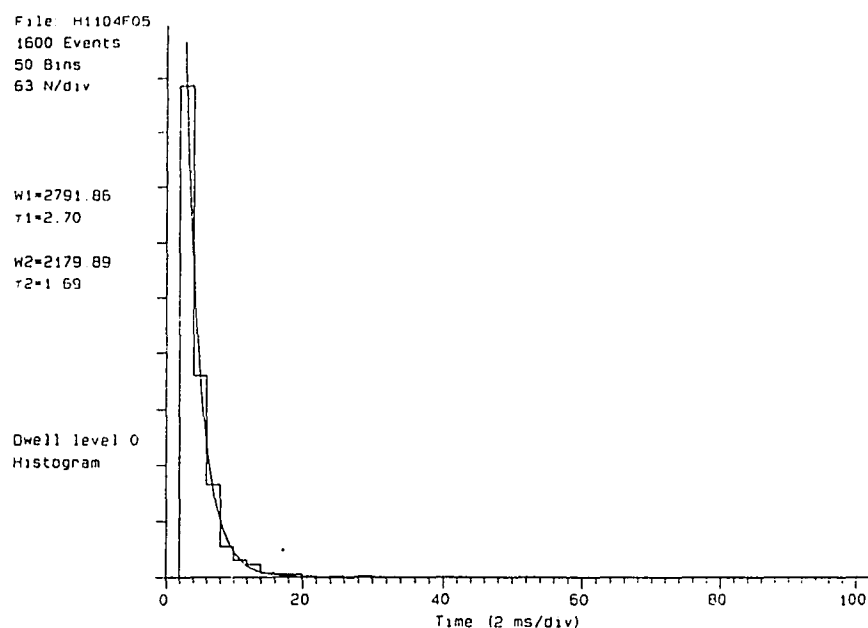


Figure 27. Open lifetime analysis of a SR  $\text{Ca}^{2+}$  release channel upon photooxidation. The analysis was done with the data from recordings of Figure 25. Open lifetime histograms before (top panel) and after (bottom panel) the addition of  $0.5 \mu\text{M}$  cis rose bengal with illumination.



**Figure 28.** Closed lifetime analysis of a SR  $\text{Ca}^{2+}$  release channel upon photooxidation. The analysis was done with the data from recordings of Figure 25. Close lifetime histograms before (top panel) and after (bottom panel) the addition of  $0.5 \mu\text{M}$  cis rose bengal with illumination.

shown in Figure 29b, 1  $\mu\text{M}$  rose bengal had no effect in the dark. Immediately after illumination for a few seconds, the  $\text{Ca}^{2+}$  channel activity was greatly increased (Figure 29c). Higher rose bengal concentrations ( $> 5 \mu\text{M}$ ) were needed to stimulate SR  $\text{Ca}^{2+}$  release channel activity in the dark.

In  $\text{Ca}^{2+}$  flux measurements, rose bengal stimulated  $\text{Ca}^{2+}$  release from SR vesicles is insensitive to extravesicular free  $\text{Ca}^{2+}$  concentration. This observation is in contrast to  $\text{Ca}^{2+}$  release induced by other activators which shows a marked dependence on myoplasmic  $\text{Ca}^{2+}$  concentration. As shown in Figure 30, channel activity was stimulated by photooxidation even at low  $\text{Ca}^{2+}$  concentration (18 nM).

As shown in Figure 31, addition of 1  $\mu\text{M}$  rose bengal to either side of the bilayer results in similar activation of channel activity upon exposure to light. Light dependent stimulation of channel activity is presumably caused by singlet oxygen production. Singlet oxygen can readily diffuse across biological membranes, and therefore one might expect  $\text{Ca}^{2+}$  channel activity to be activated by rose bengal added to either the cis or trans chamber.

It has previously been shown with the bilayer fusion technique that micromolar concentrations of ryanodine lock the native SR  $\text{Ca}^{2+}$  release channel in a half conductance state (Rousseau et al., 1987). As shown in Figure 32, addition of 0.7  $\mu\text{M}$  ryanodine to the cis chamber modified the channel (479 pS) to a long open subconducting state (about 250 pS).

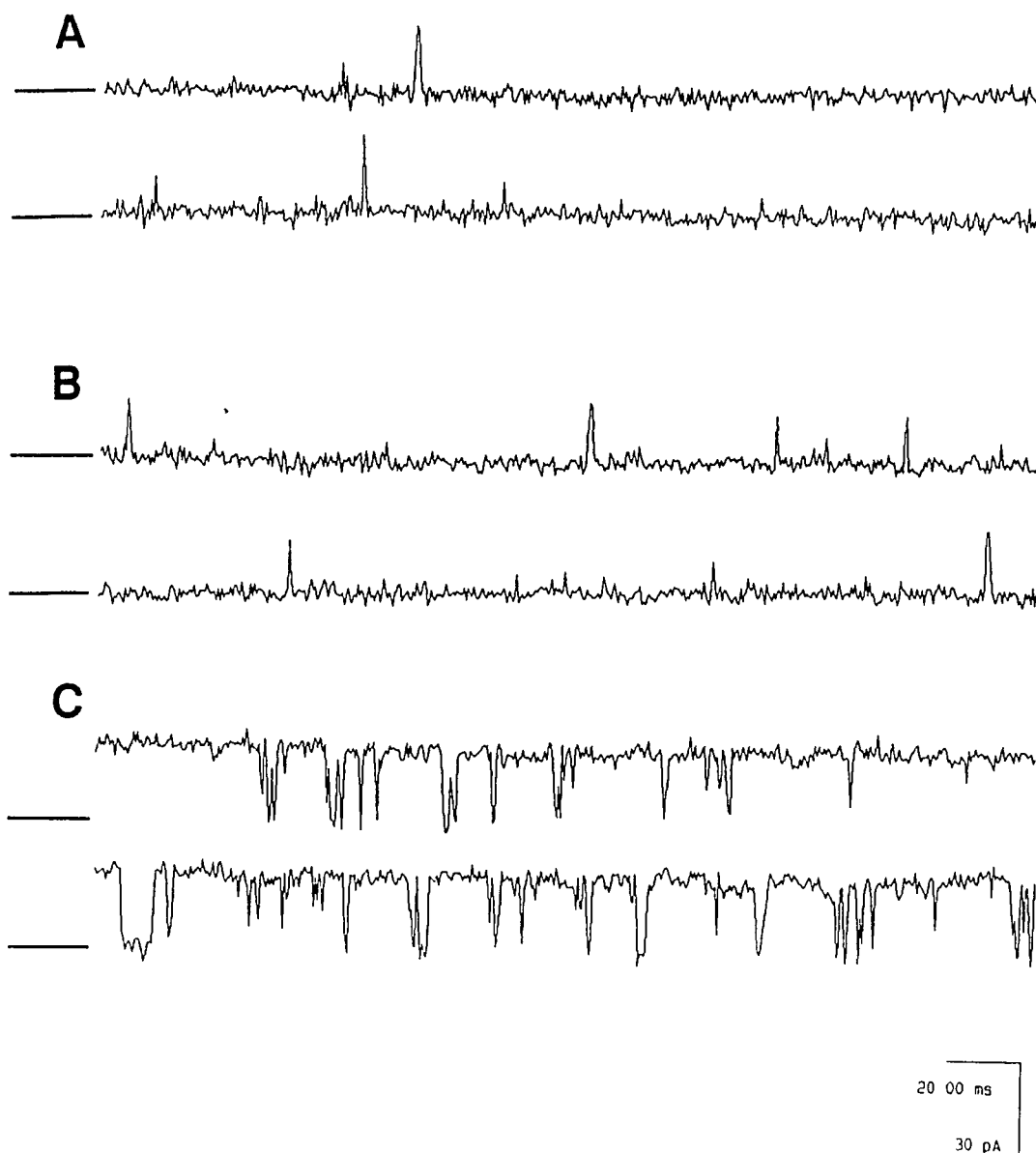


**Figure 29.** Light dependence of the rose bengal effect. Single channel current was recorded in 5:1 CsCl gradient after fusion of a SR vesicle to phospholipid bilayer. (A)  $[Ca^{2+}]_{cis} = 5 \mu M$  (0.1 mM  $CaCl_2$ , 0.1 mM EGTA),  $P_0 = 1\%$ . (B) addition of  $1.0 \mu M$  of rose bengal to the cis chamber in the absence of light.  $P_0 = 1\%$ . (C) Immediate after exposure to light.  $P_0 = 95\%$ . HP = +20 mV. (n = 5)

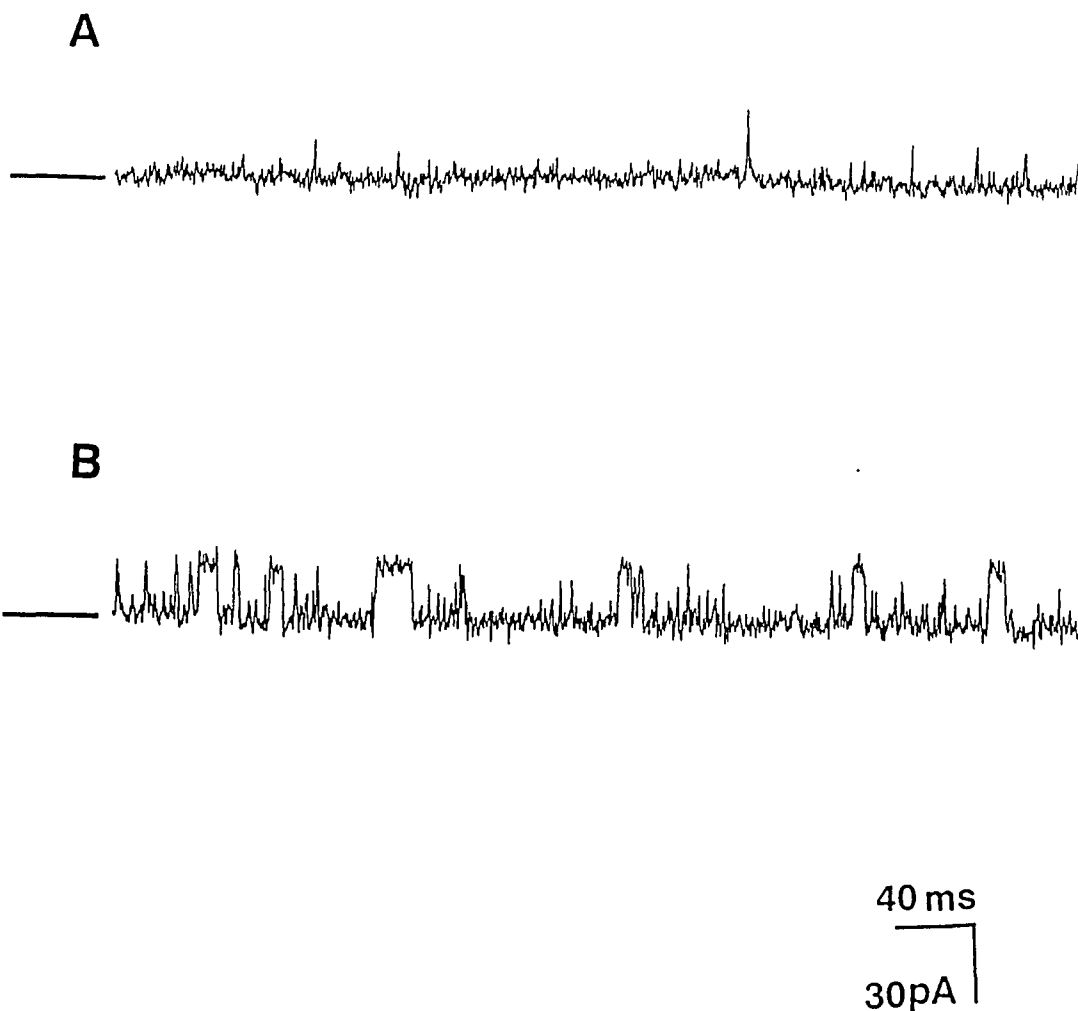


**Figure 30.** Rose bengal activation of SR  $\text{Ca}^{2+}$  release channel at low  $\text{Ca}^{2+}$  concentration. Following fusion of a SR vesicle to the bilayer with 0.35 mM cis  $\text{CaCl}_2$ , a ten fold excess of EGTA was added to the cis chamber to prevent further fusion events and to achieve low  $\text{Ca}^{2+}$  concentration. (A)  $[\text{Ca}^{2+}]_{\text{cis}} = 18 \text{ nM}$  (0.35 mM  $\text{CaCl}_2$ , 3.5 mM EGTA). (B) After addition of 0.6  $\mu\text{M}$  rose bengal to the cis chamber and activation by light. HP = +20 mV. (n = 5)

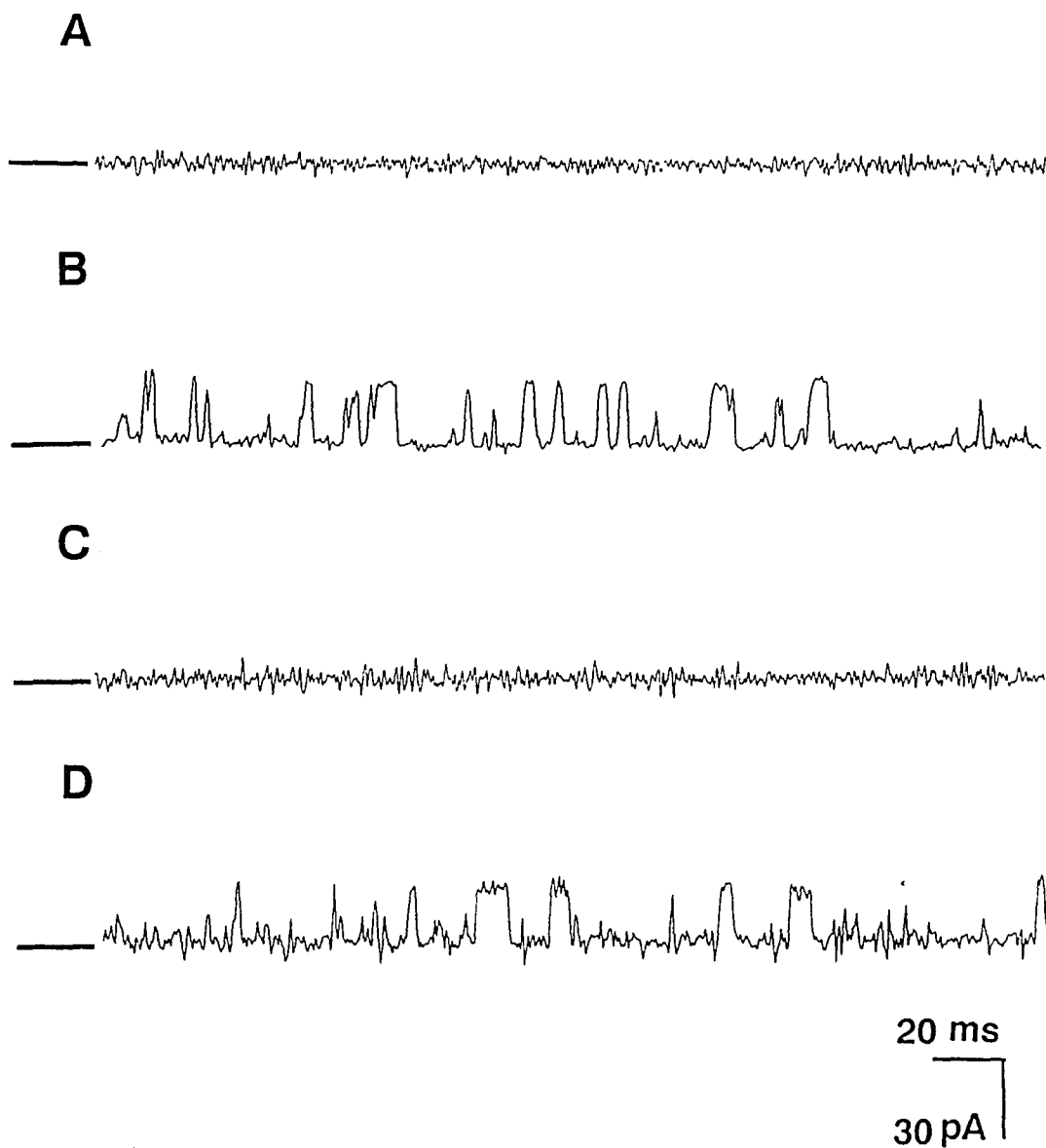


**Figure 31.** Rose bengal activation of channel activity is side independent. Following fusion of a SR vesicle to the bilayer with 0.35 mM cis  $\text{CaCl}_2$ , a two fold excess of EGTA was added to the cis chamber ( $[\text{Ca}^{2+}]_{\text{cis}} = 160 \text{ nM}$ ) to prevent further fusion events. (A) Control trace. (B) Addition of  $1.0 \mu\text{M}$  rose bengal to the trans chamber and activation by light. HP = +20 mV. ( $n = 3$ ). (C) Control cis with a new bilayer. (D) Addition of  $1.0 \mu\text{M}$  rose bengal to the trans chamber and activation by light. HP = +20 mV. ( $n = 6$ )

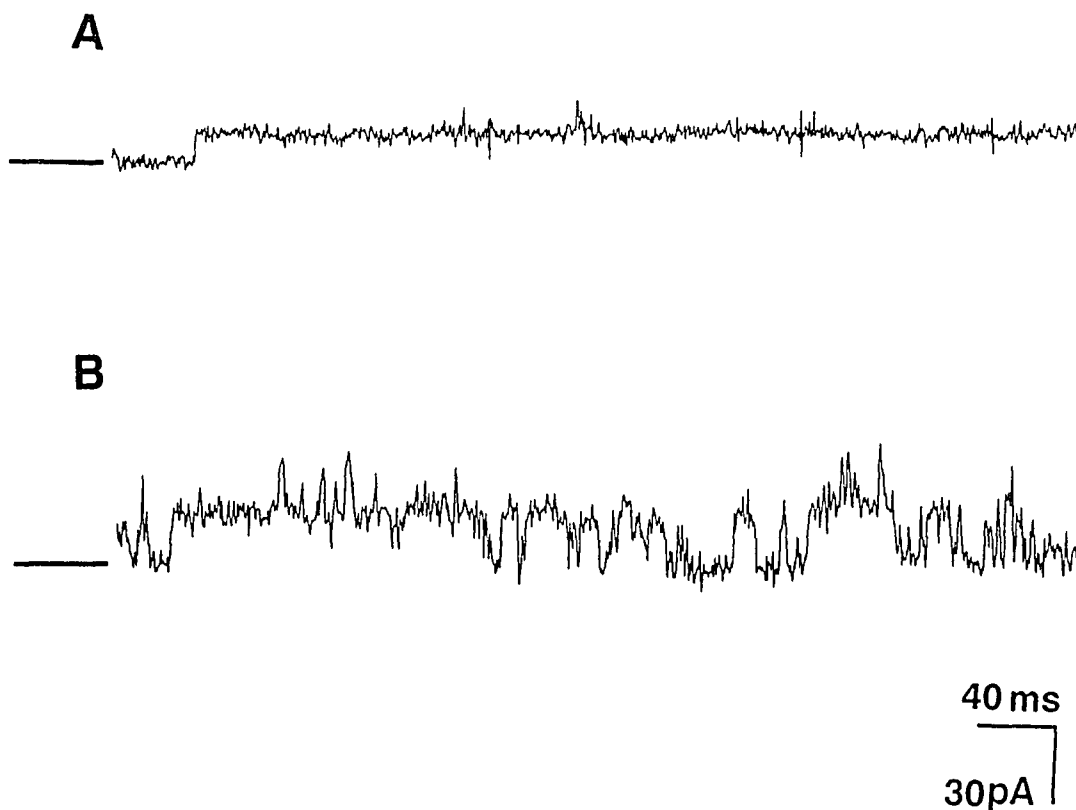


**Figure 32.** Ryanodine modification of the  $\text{Ca}^{2+}$  release channel is reversed by rose bengal. After incorporation of a SR vesicle and changing the cis solution,  $100\ \mu\text{M}$  of  $\text{Ca}^{2+}$  was added to the cis chamber. (A)  $0.7\ \mu\text{M}$  ryanodine was added to the cis chamber. (B) After addition of  $0.6\ \mu\text{M}$  rose bengal to the cis chamber and activation by light. HP = +20 mV. (n = 5)



Subsequent addition of 0.6  $\mu\text{M}$  rose bengal in the presence of light reversed the effect of ryanodine. The channel returns to a rapidly fluctuating full conductance state. This implies that rose bengal can displace bound ryanodine from its receptor. Dr. Pessah in collaboration with this laboratory examined the interaction between ryanodine and rose bengal using a ryanodine binding assay (Figure 33). His results showed that high affinity bound [ $^3\text{H}$ ]-ryanodine was rapidly displaced by addition of rose bengal. Displacement of bound [ $^3\text{H}$ ]-ryanodine is shown to be rose bengal concentration dependent and requires the presence of light (Xiong et al., 1991).

Photooxidation of the purified 106 kDa protein was also investigated. The purified 106 kDa protein was added to both sides of a bilayer in a symmetric NaCl buffer (250 mM,  $[\text{Ca}^{2+}]_{\text{free}} = 100 \mu\text{M}$ ) at a final protein concentration of 50-500 ng/ml. As shown in Figure 34, the activity of the reconstituted 106 kDa protein is also stimulated by addition of 500 nM rose bengal (Figure 34b). Channel activity is further increased by exposure to light (Figure 34c). Activation by rose bengal was partially reversed by the subsequent addition of 10 nM ryanodine (Figure 34d).

Similar to the observation on the native channel (Figure 32), photooxidation with 500 nM rose bengal reactivated the ryanodine modified channel. Figure 35 shows the modification by ryanodine of the reconstituted 106 kDa channel, and the

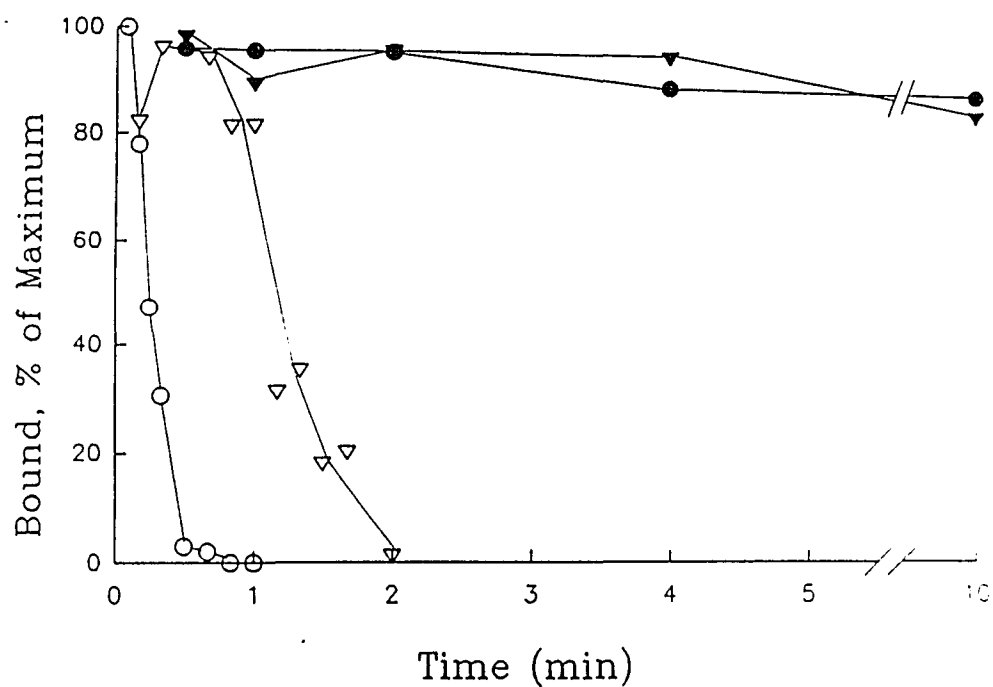


**Figure 33.** Light dependent displacement of [ $^3\text{H}$ ]-ryanodine from its binding sites by rose bengal. Junctional SR vesicles ( $30\ \mu\text{g}$ ) were equilibrated with  $1\ \text{nM}$  [ $^3\text{H}$ ]-ryanodine for 3 hours. The samples were then exposed to either  $50\ \text{nM}$  ( $\blacktriangledown, \triangledown$ ) or  $500\ \text{nM}$  ( $\bullet, \circ$ ) rose bengal in the dark ( $\bullet, \blacktriangledown$ ) or in the presence of white light of  $6500\ \text{lux}$  ( $\circ, \triangledown$ ) for various amounts of time. The assays were terminated with ice-cold wash buffer and radioactivity of the samples was measured by scintillation spectroscopy.

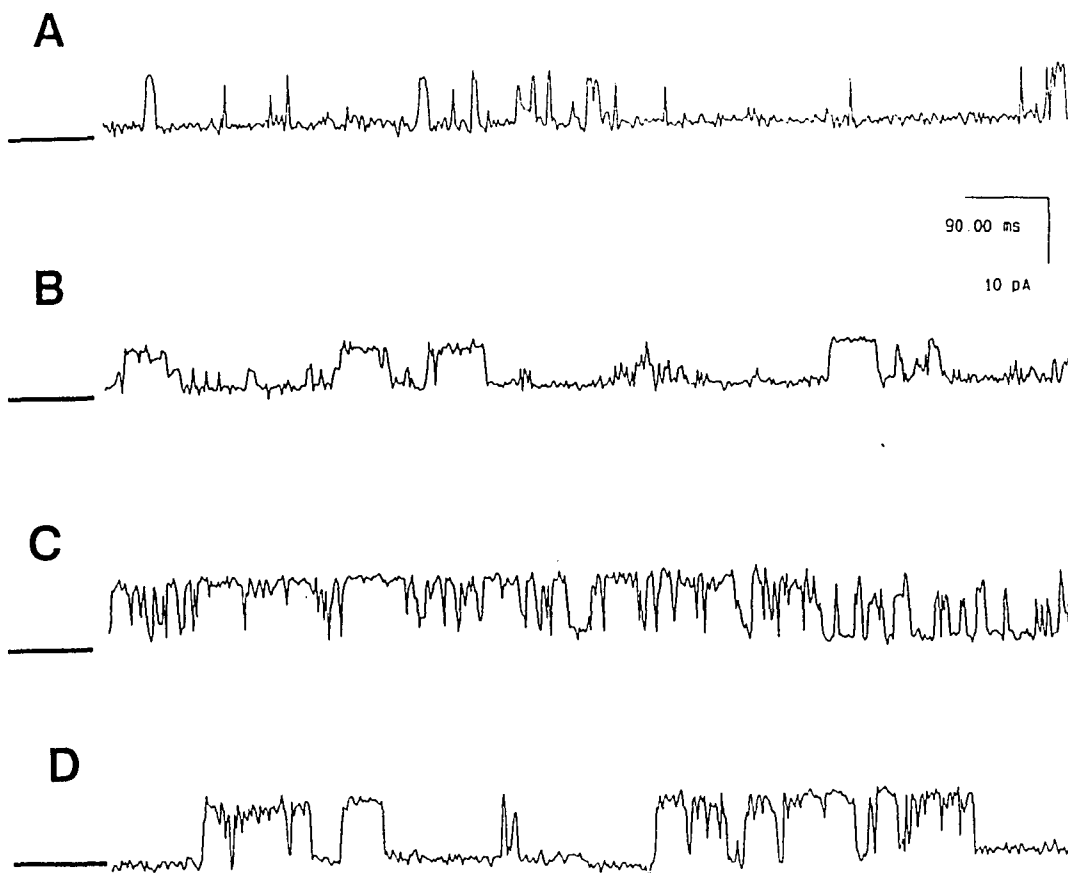


**Figure 34.** Rose bengal activation of the purified  $\text{Ca}^{2+}$  release channel and subsequent modification by ryanodine. Purified 106 kDa protein was incorporated to a bilayer in symmetric 250 mM NaCl buffer ( $[\text{Ca}^{2+}]_{\text{free}} = 100 \mu\text{M}$ ). (A) Control trace ( $[\text{Ca}^{2+}]_{\text{free}} = 100 \mu\text{M}$ ).  $P_0 = 9\%$ . (B) 0.5  $\mu\text{M}$  rose bengal was added to both chamber.  $P_0 = 20\%$ . (C) Immediately following exposure to light.  $P_0 = 71\%$ . (D) 10 nM ryanodine was added to both chamber.  $P_0 = 62\%$ . HP = +20 mV. (n = 3)

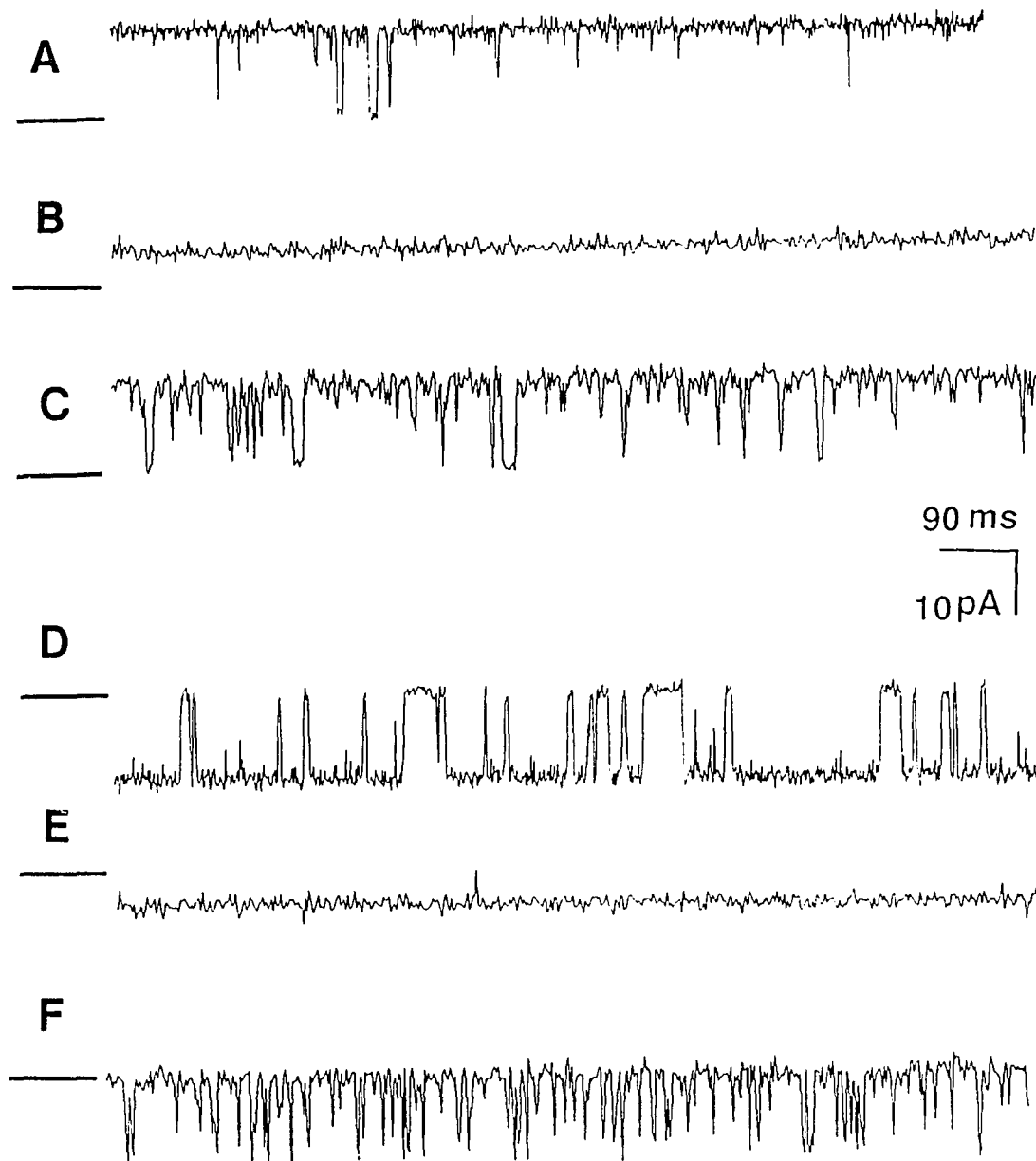


**Figure 35.** Rose bengal activation of ryanodine modified 106 kDa  $\text{Ca}^{2+}$  release channel. Purified 106 kDa protein was incorporated to a bilayer in symmetric 250 mM NaCl buffer ( $[\text{Ca}^{2+}]_{\text{free}} = 100 \mu\text{M}$ ). (A) Control trace at +40 mV.  $P_0 = 99\%$ . (B) Same as in (A), HP = -40 mV.  $P_0 = 92\%$ . (C) After addition of 10 nM ryanodine. HP = +40 mV. (D) Same as in (C), HP = -40 mV. (E) 0.5  $\mu\text{M}$  rose bengal was added to both chamber in the presence of light.  $P_0 = 93\%$ . (F) Same as in (E), HP = -40 mV.  $P_0 = 12\%$ . The bars indicate the closed state of the channel. (n = 3)

subsequent reversal of the effect by photooxidation. Also note the voltage dependence of the open channel probability ( $P_0$ ). After rose bengal activation, this voltage asymmetry is still evident.

## DISCUSSION

Exposure of the photosensitizer rose bengal to light results in the production of  $^1O_2$  and the activation of rapid  $Ca^{2+}$  release from skeletal muscle SR vesicles. Evidence presented in this chapter shows that the  $Ca^{2+}$  release channel from SR is activated by rose bengal ( $< 1 \mu M$ ) in the presence of light. Photooxidation of the SR  $Ca^{2+}$  release channel increases the open probability ( $P_0$ ) of the channel, and does not affect the single channel conductance. The selectivity of the channel ( $P_{Cs}/P_{Cl}$ ) is unaffected by photooxidation. Results indicate that the SR  $Cl^-$  channels do not respond to photooxidation. The photooxidation of SR  $K^+$  channel was also investigated with planar lipid bilayer technique. A fellow student, Ed Buck, showed that rose bengal, in the presence of light, had no effect on SR  $K^+$  channels.

Photooxidative modification of the  $Ca^{2+}$  release channel is independent of the side to which rose bengal is added. The life time of singlet oxygen in water is 2-5  $\mu sec$  (Perez, 1985). Given the high diffusion coefficient of  $O_2$  in water ( $D = 10^{-9} m^2 s^{-1}$ ), it is likely that  $^1O_2$  diffuses at least ten times the thickness of the bilayer before decaying. It is therefore

not surprising that photooxidation of the  $\text{Ca}^{2+}$  release channel is independent of the side to which rose bengal is added.

The activity of the SR  $\text{Ca}^{2+}$  release channel is  $\text{Ca}^{2+}$  dependent (Smith et al., 1986). Activation of channel activity by adenine nucleotides (Meissner, 1984), ryanodine (Rousseau et al., 1987), and doxorubicin (Abramson et al. 1988; Ondrias et al., 1990) is also  $\text{Ca}^{2+}$  dependent. Maximal channel activity activation occurs at about  $100 \mu\text{M}$   $\text{Ca}^{2+}$ . At  $\text{Ca}^{2+}$  concentrations as low as 20 nM, the channel is completely inhibited. However,  $\text{Ca}^{2+}$  release induced by rose bengal and the  $\text{Ca}^{2+}$  channel activity stimulated by rose bengal are both observed to be insensitive to  $\text{Ca}^{2+}$  (Stuart et al., 1991; Figure 27). This indicates that the molecular mechanism underlying stimulation of  $\text{Ca}^{2+}$  channel activity by photooxidation is likely different than previous observed with other activators.

The other distinguishing feature of photooxidation is the fast response time. When rose bengal is added in the dark, the SR  $\text{Ca}^{2+}$  channel is opened immediately after light illumination. Unlike the isolated SR vesicle system, a reconstituted  $\text{Ca}^{2+}$  release channel in a bilayer responds more slowly to any added reagent. This is partly due to the mixing time. In the case of photooxidation, the channel is not affected after the addition and mixing of rose bengal. It opens up as soon as a light is switching on.

The sarcoplasmic reticulum has previously been implicated as a site of action for oxygen free radical damage. However,

previous studies have focused on the  $\text{Ca}^{2+}$ ,  $\text{Mg}^{2+}$ -ATPase as the primary target. Studies in our laboratory demonstrated that the  $\text{Ca}^{2+}$  release pathway is more sensitive to photooxidation than the  $\text{Ca}^{2+}$  pump. This study indicates that photooxidation of rose bengal stimulates  $\text{Ca}^{2+}$  release from SR by directly interacting with the  $\text{Ca}^{2+}$  release protein.

Although this study has been carried out with skeletal muscle SR, it may enhance our understanding of reperfusion damage of the myocardium. It has been reported that photooxidation of rose bengal in rat heart results in the rapid development of various arrhythmias (Hearse et al., 1988). The electrophysiological changes induced in the heart by reactive oxygen intermediates are similar to those associated with severe ischemia-reperfusion injury. Free radical scavengers, such as glutathione and superoxide dismutase reduce reperfusion damage. Intracellular  $\text{Ca}^{2+}$  overload has been proposed as a general pathogenic mechanism of reperfusion damage, and two membrane systems (SR and the sarcolemma) are the principal targets of reactive oxygen intermediates. My results imply that in skeletal muscle the intracellular  $\text{Ca}^{2+}$  overload is a direct result of an interaction between reactive oxygen intermediates and the SR  $\text{Ca}^{2+}$  release channel. A recent abstract indicates that the photooxidation of rose bengal modifies the sheep cardiac SR  $\text{Ca}^{2+}$  release channel (Cumming et al., 1990). Whether or not the cardiac SR  $\text{Ca}^{2+}$  release protein is the primary site of

action of singlet oxygen during reperfusion of cardiac muscle will require further detailed studies.



## CHAPTER VI

### CONCLUSION

This research examined several aspects of the SR  $\text{Ca}^{2+}$  release channel from skeletal muscle. When this work started in the summer of 1986, the investigation of the gating characteristics of the SR  $\text{Ca}^{2+}$  release channel had just begun. The planar lipid bilayer technique had successfully been used to examine channel behavior following fusion of SR vesicles to lipid bilayers. The activity of individual channels under electrically and chemically well defined conditions could be examined. The initial phase of my research involved setting up a planar lipid bilayer system in our laboratory. The establishment of this system was a great extension of the research capability in this laboratory. Combined with three other  $\text{Ca}^{2+}$  flux measurement systems, the single channel recording system has aided us in our effort to understand the SR  $\text{Ca}^{2+}$  release mechanism.

At this same time attempts were being made to purify the  $\text{Ca}^{2+}$  channel protein. The ryanodine receptor complex was purified in 1987, and, using the bilayer technique, it was identified and characterized as a  $\text{Ca}^{2+}$  channel with similar properties to the native SR  $\text{Ca}^{2+}$  release channel. The sulfhydryl activated  $\text{Ca}^{2+}$  channel protein was purified in 1989. However, this protein appeared not to be the same

protein as the ryanodine receptor complex isolated by others. As described in Chapter III, the sulfhydryl activated 106 kDa protein also showed similar channel properties in the artificial bilayer to the native SR  $\text{Ca}^{2+}$  release channel. Further experiments will be needed to clarify the relationship between the high molecular mass ryanodine receptor and the 106 kDa sulfhydryl activated  $\text{Ca}^{2+}$  channel protein.

The work presented in Chapter IV is a continuation of our investigation into the interaction of sulfhydryl reagents and the SR  $\text{Ca}^{2+}$  release mechanism.  $\text{Ag}^+$  activation of the  $\text{Ca}^{2+}$  release channel was studied at the single channel level.  $\text{Ag}^+$  activates the channel by increasing its open probability. The spontaneous inactivation following  $\text{Ag}^+$  activation is likely due to a specific interaction between  $\text{Ag}^+$  and an endogenous sulfhydryl group which closes the channel. Single channel data helped explain the interesting multiphasic  $\text{Ag}^+$  dependence of the  $\text{Ca}^{2+}$  release rate from SR vesicles.

The work presented in Chapter V is an extension of Dr. Janice Stuart's work on modification of the SR  $\text{Ca}^{2+}$  release mechanism with the photosensitizing dye, rose bengal. The discrepancy between the pK of a free cysteine and the optimal pH of sulfhydryl oxidation-induced  $\text{Ca}^{2+}$  release led Dr. Stuart's research on the possible involvement of histidyl residues in the  $\text{Ca}^{2+}$  release process. In the presence of light, nanomolar concentrations of rose bengal induced  $\text{Ca}^{2+}$  release from isolated SR vesicles. Detailed studies could not

determine whether the target of rose bengal sensitized photooxidation was the  $\text{Ca}^{2+}$  release channel. One possible reason for the rose bengal-increased  $\text{Ca}^{2+}$  permeability of the SR membrane was that other channels present in the SR were being modified in such a way as to conduct  $\text{Ca}^{2+}$ . Assays carried out by Dr. Stuart could not rule out this possibility. Bilayer experiments described in Chapter V demonstrated that the target of rose bengal sensitized photooxidation is the SR  $\text{Ca}^{2+}$  release channel.

Data presented in this dissertation provide a new and valuable molecular description of the SR  $\text{Ca}^{2+}$  release channel from skeletal muscle.

## REFERENCES

- Abramson, J.J., Trimm, J.L., Weden, L., and Salama, G. (1983) "Heavy metal induce rapid calcium release from sarcoplasmic reticulum vesicles isolated from skeletal muscle," Proc. Natl. Acad. Sci. USA 80, 1526-1530.
- Abramson, J.J., and Salama, G. (1987) "Critical sulfhydryls regulate calcium release from sarcoplasmic reticulum," (1989) J. Bioenerg. Biomembr. 21: 283-294.
- Arreola, J., Calvo, J., Garcia, M.C., and Sanchez, J.A. (1987) "Modulation of calcium channels of twitch skeletal muscle fibers of the frog by adrenaline and cyclic adenosine monophosphate," J. Physiol. 393: 307-330.
- Baylor, S.M. (1983) "Optical studies of excitation-contraction coupling using voltage-sensitive probes," In: Handbook of Physiology. Skeletal Muscle, Bethesda, MD:Am. Physiol. Soc., vol. 10, p.355-379.
- Baylor, S.M., and Hollingworth, S. (1988) "Fura-2 calcium transients in frog skeletal muscle fibres," J. Physiol. Lond., 403:151-192.
- Beam, K.G., Knudson, C.M. (1988a) "Calcium currents in embryonic and neonatal mammalian skeletal muscle," J. Gen. Physiol. 91: 781-798.
- Beam, K.G., Knudson, C.M. (1988b) "Effect of postnatal development on calcium currents and slow charge movement on mammalian skeletal muscle," J. Gen. Physiol. 91: 799-815.
- Bean, B.P. (1989) "Classes of calcium channels in vertebrate cells," Annu. Rev. Physiol. 51: 367-384.
- Beatty, G.N., Cota, G., Nicola Siri, L., Sanchez, J.A., and Stefani, E. (1987) "Skeletal muscle  $\text{Ca}^{2+}$  channels," In: Structure and Physiology of the Slow Inward Calcium Channel, edited by Triggle, D.J., and Venter, J.C., New York: liss, 1: 123-140.
- Berridge, M.J. (1987) "Inositol trisphosphate and diacylglycerol: two interacting second messengers," Ann. Rev. Biochem. 56: 159-193.

- Blinks, J.R., Wier, W.G. and Prendergast, F.G. (1982) "Measurements of  $\text{Ca}^{2+}$  concentrations in living cells," Prog. Biophys. Mol. Biol., 40:1-114.
- Block, B.A., Imagawa, T., Campbell, K.P., Franzini-Armstrong, C. (1988) "Structural evidence for direct interaction between the molecular components of the transverse tubule/sarcoplasmic reticulum junction in skeletal muscle," J. Cell Biol. 107: 2587-2600.
- Borsotto, M., Barhanin, J., Norman, R. I., and Lazdunski, M. (1984) "Purification of the dihydropyridine receptor of the voltage-dependent  $\text{Ca}^{2+}$  channel from skeletal muscle transverse tubules," Biochem. Biophys. Res. Commun. 122: 1357-1366.
- Brandt, N.R., Caswell, A.H., Wen, S.R., and Talvenheimo, J.A. (1990) "Molecular interactions of the junctional foot protein and dihydropyridine receptor in skeletal muscle triads," J. Membr. Biol. 113: 237-251.
- Brunder, D.G., Dettbarn, C., and Palade, P. (1988) "Heavy metal-induced  $\text{Ca}^{2+}$  release from sarcoplasmic reticulum," J. Biol. Chem. 263: 18785-18792.
- Cambell, K.P., Franzini-Armstrong, C., and Shamoo, A.E. (1980) "further characterization of light and heavy sarcoplasmic reticulum vesicles: identification of the 'sarcoplasmic reticulum feet' associated with heavy sarcoplasmic reticulum vesicles," Biochim. Biophys. Acta 602: 97-116.
- Caswell, A.H., Lau, Y.H., and Brunschwig, J.P. (1976) "Ouabain binding vesicles from skeletal muscle," Arch. Biochem. Biophys. 176: 417-430.
- Caswell, A.H., Lau, Y.H., and Brunschwig, J.P. (1979) "Recognition and junction formation by isolated transverse tubules and terminal cisternae of skeletal muscle," J. Biol. Chem. 254: 202-208.
- Caswell, A.H. and Brandt N.R. (1981) "Correlation of  $\text{Ca}^{2+}$  release from terminal cisternae with integrity of triad junction," In: The Mechanism of Gated Calcium Transport Across Biological Membranes edited by S.T. Ohnishi and M. Endo. New York: Academic. p. 219-226.
- Chandler, W.K., Rakowski, F.R., Schneider, M.F. (1976) "Effects of glycerol treatment and maintained depolarization on charge movement in skeletal muscle," J. Physiol. 254: 285-316.

- Corbett, A.M., Caswell, A.H., Brandt N.R., and Brunschwig, J.P. (1985) "Determinants of triad junction reformation: Identification and isolation of an endogenous promotor for junction reformation in skeletal muscle," J. Membr. Biol. 86: 267-276.
- Coronado, R., Rosenberg, R.L., and Miller, C. (1980) "Ionic selectivity, saturation, and block in a K<sup>+</sup>-selective channel from sarcoplasmic reticulum," J. Gen. Physiol. 76: 425-446.
- Costantin, L.L., and Podolsky, R.J. (1967) "Depolarization of the internal membrane system in the activation of frog skeletal muscle," J. Gen. Physiol. 50:1101-1124.
- Cumming, D., Holmberg, S., Kusama, Y., Shattock, M. and Williams, A. (1990) "Effects of reactive oxygen species of the structure and function of the calcium release channel from isolated sheep cardiac sarcoplasmic reticulum," J Physiol. Abstr. 420: 88P.
- Curtis, B.M., Catterall, W.A. (1984) "Purification of the calcium antagonist receptor of the voltage-sensitive calcium channel from skeletal muscle transverse tubules," Biochemistry 23:2113-2118.
- Donaldson, S.K. (1985) "Peeled mammalian skeletal muscle fibers: possible stimulation of Ca<sup>2+</sup> release via a TT-SR mechanism," J. Gen. Physiol. 86:501-525.
- Ebashi, S. (1975) "Regulatory mechanism of muscle contraction with special reference to the Ca-troponin-tropomyosin system," Essays Biochem. 10: 1-36.
- Eisenberg, R.S. (1987) "Membranes, calcium and coupling," Can. J. Physiol. Pharmacol. 65: 686-690.
- Endo, M., Tanaka, M., and Ogawa, Y. (1970) "Calcium induced release of calcium from the sarcoplasmic reticulum of skinned skeletal muscle fibers," Nature 228: 34-36.
- Endo, M. (1977) "Calcium release from the sarcoplasmic reticulum," Physiol. Rev. 57: 71-108.
- Endo, M. (1985) "Calcium release from sarcoplasmic reticulum," Curr. Top. Membr. Transp. 25: 181-230.
- Endo, M. and Iino, M. (1988) " Measurement of Ca<sup>2+</sup> release in skinned fibers from skeletal muscle," In:Methods in Enzymology, Vol 157, p.12-26.

- Fill, M., Coronado, R., Mickelson, J.R., Vilven, J., and Ma, J. et al. (1990) "Abnormal ryanodine receptor channels in malignant hyperthermia muscle," J. Biophys. 50: 471-475.
- Fleischer S., Inui, M. (1989) "Biochemistry and biophysics of excitation-contraction coupling," Annu. Rev. Biophys. Biophys. Chem. 18: 333-364.
- Ford, L.E., and Podolsky, R.J. (1970) "Regenerative calcium release within muscle cells," Science 167: 58-59.
- Fox, A.P., Nowycky, M.C., and Tsien, R.W. (1987) "Kinetic and pharmacological properties distinguishing three types of calcium currents in chick sensory neurones," J. Physiol. 394: 149-172.
- Franzini-Armstrong, C. (1975) "Membrane particles and transmission at the triad," Federation Proc. 34: 1382-1389.
- Franzini-Armstrong, C. (1980) "Structure of sarcoplasmic reticulum," Federation Proc. 39: 2403-2409.
- Garcia, J., and Stefani, E. (1987) "Appropriate conditions to record activation of fast  $\text{Ca}^{2+}$  channels in frog skeletal muscle," Pflugers Arch. 408: 646-648.
- Gould, G.W., Colyer, J., East, J.M., and Lee, A.G. (1987) "Silver ions trigger  $\text{Ca}^{2+}$  release by interaction with the ( $\text{Ca}^{2+}$ - $\text{Mg}^{2+}$ -ATPase in reconstituted systems," J. Biol. Chem. 262: 7676-7679.
- Hagiwara, S. (1983) Membrane Potential-Dependent Ion Channels in Cell Membrane. New York: Raven. p. 5-47.
- Hagiwara, N., Irisawa, H., and Kameyama, M. (1988) "Contribution of two types of calcium currents to the pacemaker potentials of rabbit sino-atrial node cells," J. Physiol. 359: 233-253.
- Hearse, D.J., Kusama, Y., and Bernier, M. (1988) "Rapid electrophysiological changes leading to arrhythmias in the aerobic rat heart," Circulation Research 65: 146-153.
- Hodgkin, A.L., and Horowicz, P. (1957) "The differential action of hypertonic solution on the twitch and action potential of a muscle fibre," J. Physiol. London 153: 386-403.

- Ikemoto, N., Antoniu, B., and Kim, D.H. (1984) "Rapid calcium release from the isolated sarcoplasmic reticulum is triggered via the attached transverse tubular system," J. Biol. Chem. 259: 13151-13158.
- Ikemoto, N., Antoniu, B., and Meszaros, L.G. (1985) "Rapid flow calcium quench studies of calcium release from isolated sarcoplasmic reticulum," J. Biol. Chem. 260: 14096-14100.
- Imagawa, T., Smith, J.S., Coronado, R., and Campbell, K.P. (1987) "Purified ryanodine receptor from skeletal muscle sarcoplasmic reticulum is the  $\text{Ca}^{2+}$  permeable pore of the calcium release channel," J. Biol. Chem. 262: 16636-16643.
- Inui, M., Saito, A., and Fleischer, S. (1987) "Purification of the ryanodine receptor and identity with feet structure of junctional terminal cisternae of sarcoplasmic reticulum from fast skeletal muscle," J. Biol. Chem. 262: 1740-1747.
- Jorgensen, A.O., Shen, A.C.Y., Campbell, K.P., and MacLennan, D.H. (1983) "Ultrastructural localization of calsequestrin in rat skeletal muscle by immunoferritin labeling of ultrathin frozen sections," J. Cell Biol. 97: 1573-1581.
- Kelly, A.M. (1980) "T tubules in neonatal rat soleus and extensor digitorum longus muscles," Dev. Biol. 80: 501-505.
- Kim, D.H., Ohnishi, S.T., and Ikemoto, N. (1983) "Kinetic studies of calcium release from sarcoplasmic reticulum in vitro," J. Biol. Chem. 258: 9662-9668.
- Kometani, T., and Kasai, M. (1978) "Ion permeability of sarcoplasmic reticulum vesicles measured by light scattering method," J. Membr. Biol. 41: 295-304.
- Kondo, M., and Kasai, M. (1974) "Photodynamic inactivation of sarcoplasmic reticulum vesicle membranes by xanthene dyes," Photochem. Photobiol. 19: 35-41.
- Lee, K.S., and Tsien, R.W. (1984) "High selectivity of calcium channels in single dialysed heart cells of the guinea-pig," J. Physiol. 354: 253-272.
- Lee, P.C., and Rodgers M.A. (1987) "Laser flash photokinetic studies of rose bengal sensitized photodynamic interactions of nucleotides and DNA," Photochem. Photobiol. 45: 79-86.



- Lai, F.A., Ericksen, H.P., Rousseau E., Liu, Q.Y., and Meissner G. (1988) "Purification and reconstitution of the calcium release channel from skeletal muscle," Nature 331: 315-319.
- Luff, A.R., and Atwood, H.L. (1971) "Changes in the sarcoplasmic reticulum and transverse tubule system of fast and slow skeletal muscles of the mouse during postnatal development," J. Cell Biol. 51: 369-383.
- Liu, Q.Y., Lai, F.A., Rousseau, E. Jones, R.V. and Meissner, G (1989) "Multiple conductance states of the purified calcium release channel complex from skeletal sarcoplasmic reticulum," Biophys. J. 55: 415-424.
- Ma, J.J., Fill, M., Knudson, C.M., Campbell, K.P., and Coronado, R. (1988) "Ryanodine receptor of skeletal muscle is a gap junction type channel," Science 242: 99-102.
- MacLennan, D.H. (1970) "Purification and properties of an adenosine triphosphatase from sarcoplasmic reticulum," J. Biol. Chem. 245: 4508-4518.
- MacLennan, D.H. and Wong, P.T. (1971) "Isolation of a calcium sequestering protein from sarcoplasmic reticulum," Proc. Natl. Acad. Sci. U.S.A. 68: 1231-1235.
- MacLennan, D.H., Campbell, K.P., and Reithmeier, R.A.F. (1983) "Calsequestrin," In: Calcium and Cell Function edited by Cheung, W., Academic Press, New York, Vol 4: 151-179.
- Mathias, R.T., Levis, R. A., and Eisenberg, S. (1980) "Electrical models of excitation contraction coupling and charge movement in skeletal muscle," J. Gen. Physiol. 76: 1-13.
- Martonosi, A. and Feretos, R. (1964) "Sarcoplasmic reticulum I. The uptake of  $\text{Ca}^{2+}$  by sarcoplasmic reticulum fragments," J. Biol. Chem. 239: 648-653.
- Martonosi, A.N. (1984) "Mechanisms of  $\text{Ca}^{2+}$  release from sarcoplasmic reticulum of skeletal muscle," Physiol. Rev. 64: 1240-1320.

- McCleskey, E.W. (1985) "Calcium channels and intracellular calcium release are pharmacologically different in frog skeletal muscle," J. Physiol. 361:231-249.
- McCleskey, E.W., Fox, A.P., and Tsien, R.W. (1986) "Different types of calcium channels," J. Experim. Biol. 124: 177-190.
- McCleskey, E.W., Fox, A.P., Feldman, D.H., Cruz, L.J., Olivera, B.M., et al. (1987) "  $\omega$ - conotoxin: direct and persistent blockade of specific typos of calcium channels in neurons but not muscle," Proc. Natl. Acad. Sci. USA 84: 4327-4331.
- Meissner, G. (1975) "Isolation and characterization of two types of sarcoplasmic reticulum vesicles," Biochim. Biophys. Acta 389: 51-68.
- Meissner, G., and Mckinley, D., (1976) "Permeability of sarcoplasmic reticulum membrane- the effect of changed ionic environments on  $\text{Ca}^{2+}$  release," J. Memb. Biol. 30: 79-98.
- Meissner, G. (1984) "Adenine nucleotide stimulation of  $\text{Ca}^{2+}$ -induced  $\text{Ca}^{2+}$  release in sarcoplasmic reticulum," J. Biol. Chem. 259: 2365-2374.
- Meissner, G. (1986) "Permeability of sarcoplasmic reticulum to monovalent ions," In: Sarcoplasmic Reticulum in Muscle Physiology edited by Entman, M.L., and Barry Van Winkle, W., CRC Press, Vol 2: 21-29
- Miller, C., and Racker, E. (1976) " $\text{Ca}^{2+}$ -induced fusion of fragmented sarcoplasmic reticulum with artificial planar bilayers," J. Membr. Biol. 30: 283-300.
- Miller, C. (1978) "Voltage-gated cation conductance channel from fragmented sarcoplasmic reticulum: steady-state electrical properties," J. Membr. Biol. 40: 1-23.
- Miller, C. Bell, J.E., and Garcia, A.M. (1984) "The potassium channel of sarcoplasmic reticulum," In: Current Topics in Membranes and Transport edited by Stein, W.D., Acad. Press Inc., New York, Vol 21:99-132.
- Mitchell, R.D., Palade, P., and Fleischer, S. (1983) "Purification of morphologically intact triad structures from skeletal muscle," J. Cell Biol. 96: 1008-1016.
- Miyamoto, H., and Racker E. (1982) "Mechanism of calcium release from skeletal sarcoplasmic reticulum," J. Membr. Biol. 66: 193-201.

- Moutin, M.J., Abramson, J.J., Salama, G. and Dupont, Y. (1989) "Rapid  $\text{Ag}^+$ -induced release of  $\text{Ca}^{2+}$  from sarcoplasmic reticulum vesicles of skeletal muscle: a rapid filtration study," Biochim. Biophys. Acta. 984: 289-292.
- Nagasaki, K. and Fleischer, S. (1989) "Modulation of the calcium release channel of sarcoplasmic reticulum by adriamycin and other drugs," Cell Calcium 10: 63-70.
- Neckers, D.C. (1987) "The indian happiness wart in the development of photodynamic action," J. Chem. Educ. 64:649-656.
- Neckers, D.C. (1989) "Rose bengal," J. Photochem. Photobiol. A47: 1-29.
- Notori, R. (1954) "The role of myofibrils, sarcoplasm and sarcolemma in muscle contraction," Jikeikai Med. J., 1:18-20.
- Notori, R. (1965) "Effects of Na and Ca ions on the excitability of isolated myofibrils," In: Molecular Biology of Muscular Contraction, Elsevier, Amsterdam, p.190-196.
- Ohnishi, S.T. (1981) "Calcium induced calcium release as a gated calcium transport," In: The Mechanism of Gated calcium Transport Across Biological Membranes edited by Ohnishi, S.T., and Endo, M. New York: Academic, p. 275-293.
- Ondrias, K., Borgatta, L., Kim, D.H., and Ehrlich, B.E. (1990) "Biphasic effect of doxorubicin on the calcium release from sarcoplasmic reticulum of cardiac muscle," Circ. Res. 67: 272-283.
- Palade, P. (1987) "Drug-induced  $\text{Ca}^{2+}$  release from isolated sarcoplasmic reticulum," J. Biol. Chem. 262: 6142-6148.
- Pape, P.C., Konishi, M., Baylor, S.M., and Somlyo, A.P. (1988) "Excitation-contraction coupling in skeletal muscle fiber injected with the  $\text{InsP}_3$  blocker, heparin," FEBS Lett. 235: 57-62.
- Peachey, L.D. (1965) "The sarcoplasmic reticulum and transverse tubules of the frog sartorius," J. Cell Biol. 25: 209-231.

- Peachey, L.D., and Franzini-Armstrong, C. (1983) "Structure and function of membrane systems of skeletal muscle cells," In: Handbook of Physiology--Skeletal Muscle, edited by Peachey, L.D., and Adrian, R.H., American Physiological Society. p. 23-71.
- Perez, H.D. (1985) In: Handbook of Methods for Oxygen Radical Research, edited by Greenwald, R.A., CRC Press, Boca Raton, Fl, pp. 111-113.
- Pessah, I. N., Stambuk, R. A., and Casida, J. E. (1987) "Ca<sup>2+</sup>-activated ryanodine binding: mechanisms of sensitivity and intensity modulation by Mg<sup>2+</sup>, caffeine, and adenine nucleotides," Mol. Pharmacol. 31: 232-238.
- Rios E., Brum, G. (1987) "Involvement of dihydropyridine receptors in excitation-contraction coupling," Nature 325: 717-720.
- Rios, E., and Pizarro, G. (1991) "Voltage sensor of excitation-contraction coupling in skeletal muscle," Physiol. Rev. 71: 849-908.
- Rosseau, E., Smith, J.S. and Meissner, G. (1987) "Ryanodine modifies conductance and gating behavior of single Ca<sup>2+</sup> release channel," Am. J. Physiol. 253: C364-C368.
- Rousseau, E., Roberson, M., and Meissner, G. (1988) "Properties of single chloride selective channel from sarcoplasmic reticulum," European Biophys. J. 16: 143-151.
- Salama, G., and Abramson, J.J. (1984) "Silver ions trigger Ca<sup>2+</sup> release by acting at the apparent physiological release site in sarcoplasmic reticulum," J. Biol. Chem. 259: 13363-13366
- Schneider, M.F., and Chandler, W.K. (1973) "Voltage dependent charge movement in skeletal muscle: a possible step in excitation-contraction coupling," Nature 242:244-246.
- Schwartz, L.M., McCleskey, E.W., and Almers, W. (1985) "Dihydropyridine receptors in muscle are voltage-dependent but most are not functional calcium channels," Nature 314: 747-751.
- Selser, J.C., Yeh, Y., and Baskin, R.J. (1976) "A light-scattering measurement of membrane vesicle permeability," Biophys. J. 16: 1357-1365.

- Shamoo, A.E. and MacLennan, D.H. (1975) "Separate effects of mercurial compounds on the ionophoric and hydrolytic function of the  $\text{Ca}^{2+}+\text{Mg}^{2+}$ -ATPase of sarcoplasmic reticulum," J. Membr. Biol. 25: 67-74.
- Shamoo, A.E., and Goldstein, D.A. (1977) "Isolation of ionophores from ion transport systems and their role in energy transduction," Biochim. Biophys. Acta 427: 13-53.
- Smith, J.S., Coronado, R., and Meissner, G. (1985) "Sarcoplasmic reticulum contains adenine nucleotide-activated calcium channel," Nature 316: 446-449.
- Smith, J.S., Coronado, R., and Meissner, G. (1986) "Single channel measurements of the calcium release channel from skeletal muscle sarcoplasmic reticulum," J. Gen. Physiol. 88: 573-588.
- Smith, J.S., Imagawa, T., Ma, J.J., Fill, M., Campbell, K.P., and Coronado, R. (1988) "Purified ryanodine receptor from rabbit skeletal muscle is the calcium release channel of sarcoplasmic reticulum," J. Gen. Physiol. 92: 1-26.
- Somlyo, A.V., Gonzalez-Serratos, H. Shuman, H., McClellan, G., and Somlyo, A.P. (1981) "Calcium release and ionic changes in the sarcoplasmic reticulum of tetanized muscle," J. Cell Biol. 90: 577-594
- Somlyo, A.P., and Somlyo, A.V. (1986) "Smooth muscle structure and function," In: The Heart and Cardiovascular System, edited by Fozzard, H., Jennings, R., Haber, E., Katz, A., Morgan, H., New York: Raven, pp. 845-864.
- Stephenson, E.W. (1981) "Activation of fast skeletal muscle: contributions of studies on skinned fibers," Am. J. Physiol. 240: C1-C19.
- Stuart, J., Pessah, I. N., Favero, T.G., and Abramson, J.J. (1991) "Photooxidation of skeletal muscle sarcoplasmic reticulum induces rapid calcium release," Arch. Biochem. Biophys. In press.
- Suarez-Isla, A.B., Irribarra A.V., Oberhauser, A., Larralde, L., Bull, R., Hidalgo, C., and Jaimovich, E. (1988) "Inositol 1,4,5-trisphosphate activates a calcium channel in isolated sarcoplasmic reticulum membranes." Biophys. J. 54: 737-741.

- Takeshima, H., Nishimura, S., Matsumoto, T., Ishida, H., Kangawa, K., Minamino, N., Matsuo, H., Ueda, M., Hanaoka, M., Hirose, T. and Numa, S. (1989) "Primary structure and expression from complementary DNA of skeletal muscle ryanodine receptor," Nature 339, 439-445.
- Tanabe, T., Takeshima, H., Midami, A., Flokerzi, V. et al. (1987) "Primary structure of the receptor for calcium channel blockers from skeletal muscle," Nature 328: 313-318.
- Tanabe, T., Beam, K.G., Powell, J.A., and Numa, S. (1988) "Restoration of excitation-contraction coupling and slow calcium current in dysgenic muscle by dihydropyridine receptor complementary DNA," Nature 336: 134-139.
- Tatsumi, S., Suzuno, M., Takahias, T., and Kasai, M. (1988) "Effects of silver ion on the calcium-induced calcium release channel in isolated sarcoplasmic reticulum," J. Biochem. 104: 279-284.
- Tsien R.W. (1983) "Calcium channels in excitable cell membranes," Annu Rev. Physiol. 45: 341-358.
- Trimm, J.L., Salama, G., and Abramson, J.J. (1986) "Sulfhydryl oxidation induces rapid calcium release from sarcoplasmic reticulum vesicles," J. Biol. Chem. 261: 16092-16098.
- Vergara, J., Tsien, R.Y., and Delay, M. (1985) "Inositol 1,4,5-trisphosphate: a possible chemical link in excitation-contraction coupling in muscle," Proc. Natl. Acad. Sci. USA 82: 6352-6356.
- Volpe, P., Salviati, G., DiVirgilio, F., and Pozzan, T. (1985) "Inositol 1,4,5-trisphosphate induces calcium release from sarcoplasmic reticulum of skeletal muscle," Nature 316: 347-349.
- Walker, J.W., Somlyo, A.V., Goldmen, Y.E., Somlyo, A.P., and Trentham, D.R. (1987) "Kinetics of smooth and skeletal muscle activation by laser pulse photolysis of caged inositol 1,4,5-trisphosphate," Nature 327: 249-252.
- Watson, B.D. and Haynes, D.H. (1982) "Structural and functional degradation of  $\text{Ca}^{2+}:\text{Mg}^{2+}$ -APTase rich sarcoplasmic reticulum vesicles photosensitized by erythrosin B," Chem. Biol. Interact. 41: 313-325.
- White, S.H. (1986) "The physical nature of planar bilayer membranes," In: Ion Channel Reconstitution, edited by Miller, C. Plenum. pp.3-35.

- Winegred, S. (1968) "Intracellular calcium movements of frog skeletal muscle during recovery from tetanus," J. Gen. Physiol. 51: 65-83.
- Winegred, S. (1970) "The intracellular site of calcium activation of contraction of frog skeletal muscle," J. Gen. Physiol. 55: 77-88.
- Xiong, H., Buck, E., Stuart, J., Pessah, I.N., Salama, G. and Abramson, J. J. (1991) "Rose bengal activates the  $\text{Ca}^{2+}$  release channel from skeletal muscle sarcoplasmic reticulum," Arch. Biochem. Biophys. In press.
- Xiong, H., Salama, G. (Abst.) (1991) Biophys. J. 59:103a
- Yu, B.P. Masoro, E.J., and Bertrand, H.A. (1974) "The functioning of histidine residues of sarcoplasmic reticulum in  $\text{Ca}^{2+}$  transport and related activities," Biochem. 25: 5083-5087.
- Zaidi, N.F., Lagenaur, C.F., Abramson, J.J., Pessah, I., and Salama, G. (1989a) "Disulfide linkage of biotin identifies a 106 kDa  $\text{Ca}^{2+}$  release channel in sarcoplasmic reticulum," J. Biol. Chem. 264: 21725-21736.
- Zaidi, N.F., Lagenaur, C.F., Hilkert, R.J., Xiong, H., Abramson, J.J., and Salama, G. (1989b) "Reactive disulfides trigger  $\text{Ca}^{2+}$  release from sarcoplasmic reticulum via an oxidation reaction," J. Biol. Chem. 264: 21737-21747.

## APPENDIX

### THE CALCULATION OF PERMEABILITY RATIO

To obtain the relationship between the membrane potential and the membrane permeability in a bilayer system, we begin with the Goldman equation:

$$J_i = \frac{Z_i \theta P_i (C_{i,c} - C_{i,t} e^{Z_i \theta})}{(1 - e^{Z_i \theta})}$$

Where

$J_i$  = flux of the  $i$ th substance in  $\text{mol} \cdot \text{cm}^{-2} \text{s}^{-1}$ .  $J$  is positive when the flux is from the cis side of the membrane to the trans side.

$\theta = (FV) / (RT)$  where  $F$  is the Faraday;  $R$  is the gas constant; and  $T$  is the absolute temperature.  $V$  is the membrane potential.  $V = V_{cis} - V_{trans}$ .

$P_i$  = the permeability of the  $i$ th substance in  $\text{cm} \cdot \text{s}^{-1}$ .

$C_i$  = concentration of  $i$ th substance in  $\text{mol} \cdot \text{cm}^{-3}$ .

$Z_i$  = valence of the  $i$ th substance.

Applying the steady-state condition ( $I=0$ )  $\sum_i Z_i J_i = 0$ , we obtain

$$\alpha \xi^2 + \beta \xi - \gamma = 0$$



Where

$$\xi = e^{\frac{VF}{RT}} \quad (V = E_{rev} \text{ for the above condition})$$

$$\alpha = \sum_{i(-1)} P_i C_{i,t} + \sum_{i(+1)} P_i C_{i,c} + 4 \sum_{i(+2)} P_i C_{i,c}$$

$$\beta = - \sum_{i(-1)} P_i C_{i,c} + \sum_{i(+1)} P_i C_{i,c} - \sum_{i(+1)} P_i C_{i,t}$$

$$\gamma = \sum_{i(-1)} P_i C_{i,c} + \sum_{i(+1)} P_i C_{i,t} + 4 \sum_{i(+2)} P_i C_{i,t}$$

Solving the quadratic equation, we obtain

$$E_{rev} = \frac{RT}{F} \ln \left( \frac{\sqrt{\beta^2 + 4\alpha\gamma} - \beta}{2\alpha} \right) \quad (1)$$

A. In 5:1 CsCl Solution, from equation (1) we have:

$$E_{rev} = \frac{RT}{F} \ln \left( \frac{5 + \left( \frac{P_{Cs}}{P_{Cl}} \right)}{1 + 5 \left( \frac{P_{Cs}}{P_{Cl}} \right)} \right)$$

B. In the standard asymmetrical  $\text{Ca}^{2+}$  solution, if we assume that HEPES is impermeate, from equation (1) we have:

$$E_{rev} = \frac{RT}{F} \ln \left( \frac{\sqrt{1 + 16 \frac{P_{Ca}}{P_{Tris}} \frac{[Ca^{2+}]}{[Tris^+]} + 1}}{8 \frac{P_{Ca}}{P_{Tris}} \frac{[Ca^{2+}]}{[Tris^+]}} \right)$$